



LEHIGH
UNIVERSITY

Library &
Technology
Services

The Preserve: Lehigh Library Digital Collections

Batch And Semi-continuous Emulsion Copolymerization Of Vinylidene Chloride And N-butyl Methacrylate.

Citation

Lee, Ki-Chang. *Batch And Semi-Continuous Emulsion Copolymerization Of Vinylidene Chloride And N-Butyl Methacrylate*. 1987, <https://preserve.lehigh.edu/lehigh-scholarship/graduate-publications-theses-dissertations/theses-dissertations/batch-semi>.

Find more at <https://preserve.lehigh.edu/>

This document is brought to you for free and open access by Lehigh Preserve. It has been accepted for inclusion by an authorized administrator of Lehigh Preserve. For more information, please contact preserve@lehigh.edu.

INFORMATION TO USERS

The most advanced technology has been used to photograph and reproduce this manuscript from the microfilm master. UMI films the original text directly from the copy submitted. Thus, some dissertation copies are in typewriter face, while others may be from a computer printer.

In the unlikely event that the author did not send UMI a complete manuscript and there are missing pages, these will be noted. Also, if unauthorized copyrighted material had to be removed, a note will indicate the deletion.

Oversize materials (e.g., maps, drawings, charts) are reproduced by sectioning the original, beginning at the upper left-hand corner and continuing from left to right in equal sections with small overlaps. Each oversize page is available as one exposure on a standard 35 mm slide or as a 17" × 23" black and white photographic print for an additional charge.

Photographs included in the original manuscript have been reproduced xerographically in this copy. 35 mm slides or 6" × 9" black and white photographic prints are available for any photographs or illustrations appearing in this copy for an additional charge. Contact UMI directly to order.



Accessing the World's Information since 1938

300 North Zeeb Road, Ann Arbor, MI 48106-1346 USA

Order Number 8729537

**Batch and semi-continuous emulsion copolymerization of
vinylidene chloride and n-butyl methacrylate**

Lee, Ki-Chang, Ph.D.

Lehigh University, 1987

U·M·I

**300 N. Zeeb Rd.
Ann Arbor, MI 48106**

PLEASE NOTE:

In all cases this material has been filmed in the best possible way from the available copy.
Problems encountered with this document have been identified here with a check mark ✓.

1. Glossy photographs or pages _____
2. Colored illustrations, paper or print _____
3. Photographs with dark background _____
4. Illustrations are poor copy ✓ _____
5. Pages with black marks, not original copy _____
6. Print shows through as there is text on both sides of page _____
7. Indistinct, broken or small print on several pages ✓ _____
8. Print exceeds margin requirements _____
9. Tightly bound copy with print lost in spine _____
10. Computer printout pages with indistinct print _____
11. Page(s) _____ lacking when material received, and not available from school or author.
12. Page(s) _____ seem to be missing in numbering only as text follows.
13. Two pages numbered _____. Text follows.
14. Curling and wrinkled pages _____
15. Dissertation contains pages with print at a slant, filmed as received _____
16. Other _____

University
Microfilms
International

**Batch and Semi-continuous Emulsion Copolymerization of
Vinylidene Chloride and n-Butyl Methacrylate**

by

Ki-Chang Lee

A Dissertation to the Graduate Committee
of Lehigh University
in Candidacy for the Degree of
Doctor of Philosophy

in
Polymer Science and Engineering

Lehigh University
1987

Certificate of Approval

Approved and recommended for acceptance as a dissertation in partial fulfillment of the requirements for the degree of Doctor of Philosophy.

9/23/87
(date)

Accepted 9/23/87
(date)

John W. Vanderhoff
Professor in Charge

Special Committee directing
the doctoral work of
Ki-Chang Lee

John W. Vanderhoff
John W. Vanderhoff, Chairman and Co-Advisor

Mohamed S. El-Aasser
Mohamed S. El-Aasser, Co-Advisor

A. Klein
Andrew Klein

Ritchie A. Wessling
Ritchie A. Wessling

Hong Jun Yue
Hong Jun Yue

John A. Manson
John A. Manson

Acknowledgments

I would like to express my sincere gratitude and appreciation to:

My advisors, Professors J. W. Vanderhoff and M. S. El-Aasser for their valuable guidance and encouragement throughout this project.

Dr. R. A. Wessling for his valuable discussions and suggestions throughout this project.

Drs. J. A. Manson, A. Klein, and H. Yue for their generous help and service on the dissertation committee.

Dr. J. Roberts and Mr. W. Anderson for the generous help in the solid and liquid state NMR, and FTIR work. Dr. D. Nagy and Mr. B. Hook in T_g and MFFT measurements.

Dr. J. Delgado for his kind help in correcting this manuscript. Special thanks to Kenneth Earhart for his generosity in helping with material matters. The staff and colleagues of the Emulsion Polymers Institute for the valuable help and friendship.

The Dow Chemical Co. and the Emulsion Polymers Institute for the financial support during the course of this project.

Mr. and Mrs. C. Goettler for their love, encouragement and unforgettable friendship.

Drs. Jeoung-Yup Kim and Kwang-Ung Kim for their generosity.

My parents for their endless love and support.

My wife for love, patience and encouragement.

Table of Contents

1. GENERAL INTRODUCTION	4
2. BACKGROUND	13
2.1 General Consideration of Emulsion Polymerization	13
2.2 Emulsion Polymerization of Vinylidene Chloride	22
2.3 Polymerization Processes	27
2.4 Literature Review on Semi-continuous Emulsion Polymerization	30
3. EXPERIMENTAL	44
3.1 Experimental Apparatus	44
3.2 Experimental Recipes	45
3.2.1 Reagents	45
3.2.2 Recipes	47
3.2.2.1 Batch Polymerizations	47
3.2.2.2 Seeded Semi-continuous Polymerizations	49
3.2.3 Experimental Procedure	52
3.2.3.1 Batch Polymerizations	52
3.2.3.2 Semi-continuous Polymerizations	53
3.3 Conversion Measurement	54
3.3.1 Instantaneous Conversion, X_i Measurement	55
3.3.2 Conversion X_t at time t , Measurement	55
3.3.3 Monomer Concentration, $[M_p]$ in the Latex Particles	56
3.4 Characterization of the Latexes and Latex Films	56
3.4.1 Particle Size Measurements	56
3.4.2 Infrared Spectroscopy	57
3.4.3 Minimum Film Forming Temperature (MFFT)	59
3.4.4 T_g and T_m Measurements	61
3.4.5 Determination of Percent Crystallinity (62)	61
3.4.6 X-ray Powder Diffraction	62
3.4.7 Solubility (66)	63
3.4.8 Dynamic Mechanical Spectroscopy (68)	64
3.4.9 Tensile Properties	64
3.4.10 Water Vapor Transmission Rate Measurements (WVTR)	65
3.4.11 Molecular Weight Determination	67
3.4.12 Latex Cleaning and Surface Characterization (72-74)	68
3.4.13 Determination of Copolymerization Reactivity Ratios in VDC-BMA Emulsion Polymerization (75, 76)	69
3.4.14 Nuclear Magnetic Resonance Spectroscopy	71
3.4.14.1 Carbon-13 NMR Spectroscopy	71
3.4.14.2 Solid-State NMR Spectroscopy	71
4. RESULTS AND DISCUSSION	72
4.1 Reactivity Ratios of VDC-BMA in Emulsion Copolymerization	72
4.2 Syntheses of 83:17 VDC-BMA Emulsion Copolymers by Batch and Semi-Continuous Polymerization	75
4.2.1 Kinetics	75

4.2.2 Characterization of 83:17 VDC-BMA Latex Copolymers	83
4.2.2.1 Particle Size and Particle Size Distribution	83
4.2.2.2 Infrared Spectra of 83:17 VDC-BMA Latex Films	86
4.2.2.3 X-ray Powder Diffraction of 83:17 VDC-BMA Latex Copolymers	93
4.2.2.4 T_g , T_m , and Minimum Film Forming Temperature (MFFT).	96
4.2.2.5 Dynamic Mechanical Properties	106
4.2.2.6 Tensile Properties of 83:17 VDC-BMA Copolymer Latex Films	115
4.2.2.7 Solubility Behavior of 83:17 VDC-BMA Copolymer Latex Films	116
4.2.2.8 Water Vapor Transmission Rates (WVTR) of 83:17 VDC-BMA Copolymer Latex Films	120
4.2.2.9 Determination of the Aspect Ratio of the Crystallites, L/W	121
4.3 Syntheses of 60:40 and 33:67 VDC-BMA Copolymer Latexes by Batch and Semi-continuous (R_a 0.27 wt%/minute) Polymerization, as well as Poly(vinylidene chloride) and Poly(butyl methacrylate) Latexes by Batch Polymerization	122
4.3.1 Particle Size and Particle Size Distribution	122
4.3.2 Characterization of VDC-BMA Latex Copolymers	130
4.3.2.1 Molecular Weight and Molecular Weight Distribution	130
4.3.2.2 Infrared Spectra of VDC-BMA Latex Films	131
4.3.2.3 X-ray Powder Diffraction of VDC-BMA Copolymer Latex Films	131
4.3.2.4 T_g , T_m , and MFFT Values	135
4.3.2.5 Tensile Properties of VDC-BMA Copolymer Latex Films	138
4.3.2.6 Solubility of Latex Films in THF	139
4.3.2.7 WVTR Values of VDC-BMA Copolymer Latex Films	139
4.3.2.8 Surface Characterization of VDC-BMA Copolymer Latexes	143
4.3.2.9 Determination of Copolymer Composition	148
4.3.2.10 Nuclear Magnetic Resonance Spectroscopy	148
5. CONCLUSIONS	157
6. RECOMMENDATIONS FOR FUTURE WORK	162
7. VITA	169

List of Figures

Figure 1-1:	Q - e map of various monomers.	9
Figure 1-2:	VDC-BMA copolymerizations of 83:17, 60:40, 33:67 (in mol%) by batch process.	11
Figure 2-1:	Diagram of emulsion polymerization.	16
Figure 2-2:	Paths for water-initiated free radicals.	17
Figure 2-3:	Typical conversion-time curve in emulsion polymerizations.	18
Figure 2-4:	Representation of the stages of an emulsion polymerization.	19
Figure 2-5:	Conversion-time curve showing 3 stages.	25
Figure 2-6:	Flow diagram of stirred-tank reactor for emulsion polymerization; (a) Batch reactor; (b) Continuous stirred-tank reactor; (c) Semi-continuous reactor-monomer addition; (d) Semi-continuous reactor-emulsion addition.	28
Figure 3-1:	Schematic diagram of experimental apparatus.	46
Figure 3-2:	Infrared spectrum of poly(vinylidene chloride).	58
Figure 3-3:	Infrared spectrum of molten VDC-VC (vinyl chloride) copolymer containing high amount of VDC; (--)160°C, (—)Room temperature.	60
Figure 3-4:	Conductometric titration of cleaned 83:17 VDC-BMA latex prepared by batch polymerization.	70
Figure 4-1:	Reactivity ratios determined by Lewis and Mayo equation.	73
Figure 4-2:	Overall conversion versus time curves of 83:17 VDC-BMA emulsion copolymerizations.	76
Figure 4-3:	Reaction temperature versus time curves of 83:17 VDC-BMA emulsion copolymerizations.	78
Figure 4-4:	Instantaneous conversion versus time curves of 83:17 VDC-BMA emulsion copolymerizations.	79
Figure 4-5:	Conversion at time t versus time curves of 83:17 VDC-BMA emulsion copolymerizations.	80
Figure 4-6:	Monomer concentration in latex particles versus % conversion curves of 83:17 VDC-BMA emulsion copolymerizations.	82
Figure 4-7:	Transmission electron micrographs of 83:17 VDC-BMA copolymer latexes.	84
Figure 4-8:	Infrared spectra of 83:17 VDC-BMA copolymer latex films A to G without heat-treatment (see Table 3.1 for identification).	87
Figure 4-9:	Infrared spectra of 83:17 VDC-BMA copolymer latex films A to G with heat-treatment for 30 minutes at 70°C (see Table 3.1 for identification).	88
Figure 4-10:	Infrared spectra of 83:17 VDC-BMA copolymer latex	89

	film A aged for 6 months at room temperature.	
Figure 4-11:	Infrared spectra of 83:17 VDC-BMA copolymer latex film F aged for 6 months at room temperature.	90
Figure 4-12:	Infrared spectra of 83:17 VDC-BMA copolymer latex film G aged for 6 months at room temperature.	91
Figure 4-13:	X-ray diffraction patterns of the 83:17 VDC-BMA copolymer latex films heated for 30 minutes at 70°C.	94
Figure 4-14:	Debye-Scherrer ring patterns of the 83:17 VDC-BMA copolymer latex films heated for 30 minutes at 70°C.	95
Figure 4-15:	Differential scanning calorimetry curve of the 83:17 VDC-BMA copolymer A latex film.	97
Figure 4-16:	Differential scanning calorimetry curve of the 83:17 VDC-BMA copolymer B latex film.	98
Figure 4-17:	Differential scanning calorimetry curve of the 83:17 VDC-BMA copolymer C latex film.	99
Figure 4-18:	Differential scanning calorimetry curve of the 83:17 VDC-BMA copolymer D latex film.	100
Figure 4-19:	Differential scanning calorimetry curve of the 83:17 VDC-BMA copolymer E latex film.	101
Figure 4-20:	Differential scanning calorimetry curve of the 83:17 VDC-BMA copolymer F latex film.	102
Figure 4-21:	Differential scanning calorimetry curve of the 83:17 VDC-BMA copolymer G latex film.	103
Figure 4-22:	Dynamic mechanical spectrum of 83:17 VDC-BMA copolymer A.	107
Figure 4-23:	Dynamic mechanical spectrum of 83:17 VDC-BMA copolymer B.	108
Figure 4-24:	Dynamic mechanical spectrum of 83:17 VDC-BMA copolymer C.	109
Figure 4-25:	Dynamic mechanical spectrum of 83:17 VDC-BMA copolymer D.	110
Figure 4-26:	Dynamic mechanical spectrum of 83:17 VDC-BMA copolymer E.	111
Figure 4-27:	Dynamic mechanical spectrum of 83:17 VDC-BMA copolymer F.	112
Figure 4-28:	Dynamic mechanical spectrum of 83:17 VDC-BMA copolymer G.	113
Figure 4-29:	Solubility of 83:17 VDC-BMA copolymer latex films in tetrahydrofuran.	118
Figure 4-30:	Water vapor transmission rates of 83:17 VDC-BMA latex films A and G.	120
Figure 4-31:	Transmission electron micrographs of VDC-BMA copolymer latexes prepared by batch polymerization.	124
Figure 4-32:	Transmission electron micrograph of poly(vinylidene chloride) latex particles.	125
Figure 4-33:	Conversion-time curves for VDC-BMA batch copolymerizations.	126

Figure 4-34:	Infrared spectra of VDC-BMA copolymer latex films: (B) batch; (S) semi-continuous polymerization.	132
Figure 4-35:	X-ray diffraction patterns of VDC-BMA copolymer latex films: (B) batch; (S) semi-continuous polymerization.	133
Figure 4-36:	Debye-Scherrer ring patterns of VDC-BMA copolymer latex films.	134
Figure 4-37:	Variation of T_g with composition for VDC-BMA batch copolymers.	137
Figure 4-38:	Solubility in THF of VDC-BMA copolymer latex films prepared by batch polymerization: (1) PVDC; (2) 83:17; (3) 60:40; (4) 33:67; (5) PBMA.	140
Figure 4-39:	Solubility in THF of VDC-BMA copolymer latex films prepared by (b) batch and (s) semi-continuous polymerization : (2) 83:17; (3) 60:40; (4) 33:67 VDC-BMA.	141
Figure 4-40:	^{13}C solid-state NMR spectra: (A) PVDC; 83:17 VDC-BMA copolymers prepared by (B) batch and (C) semi-continuous polymerization.	150
Figure 4-41:	^{13}C liquid NMR spectrum of the 83:17 VDC-BMA copolymer prepared by semi-continuous polymerization.	151
Figure 4-42:	^{13}C Liquid NMR spectra of the 83:17 VDC-BMA copolymers prepared by (A) batch and (B) semi-continuous polymerization, obtained using solid-state NMR parameters.	152
Figure 4-43:	^{13}C liquid NMR spectra of the 60:40 VDC-BMA copolymers prepared by (A) batch and (B) semi-continuous polymerization, obtained using solid-state NMR parameters.	153
Figure 4-44:	^{13}C solid-state NMR spectra of deuterated benzene-swollen or dissolved 83:17 VDC-BMA copolymers prepared by (A) batch and (B) semi-continuous polymerization, using the cross-polarization technique	155

List of Tables

Table 1-1:	Physical properties of VDC and BMA*.	11
Table 3-1:	83:17 VDC-BMA emulsion polymerizations.	50
Table 3-2:	Assignment of infrared spectrum bands in poly(vinylidene chloride).	59
Table 3-3:	d-Spacings of VDC-VC copolymers.	62
Table 3-4:	Common solvents of saran copolymers (67).	63
Table 3-5:	Water transmission rates of polymer films.	66
Table 4-1:	Emulsion copolymerization of VDC (M_1) and BMA (M_2).	72
Table 4-2:	Reactivity ratios in VDC-BMA copolymerizations.	73
Table 4-3:	Particle sizes of 83:17 VDC-BMA copolymer latexes.	83
Table 4-4:	T_g , T_m , and MFFT for heat-treated 83:17 VDC-BMA copolymer latex films.	96
Table 4-5:	Tensile properties of 83:17 VDC-BMA copolymer latex films.	115
Table 4-6:	Solubility of 83:17 VDC-BMA copolymer latex films.	117
Table 4-7:	Particle sizes of VDC-BMA latexes.	122
Table 4-8:	Rates of polymerization in VDC-BMA batch copolymerizations.	127
Table 4-9:	Average molecular weight and molecular weight distribution.	130
Table 4-10:	T_g , T_m , and MFFT of VDC-BMA copolymer latex films.	135
Table 4-11:	Tensile properties of VDC-BMA copolymer latex films.	138
Table 4-12:	WVTR values of VDC-BMA copolymer latex films.	142
Table 4-13:	Surface characterization of cleaned VDC-BMA copolymer latexes.	143
Table 4-14:	Surface characterization of cleaned VDC-BMA copolymer latexes heated for 24 hours at 85°C.	145
Table 4-15:	Surface characterization of cleaned VDC-BMA copolymer latexes aged for four months.	146
Table 4-16:	Composition of VDC-BMA copolymers.	148
Table 4-17:	Concentrations of VDC- and BMA-centered triads in the VDC-BMA copolymers.	154

ABSTRACT

The reactivity ratios determined in vinylidene chloride (VDC, M_1)-butyl methacrylate (BMA, M_2) emulsion copolymerization system were $r_1 = 0.22$ and $r_2 = 2.41$. Seven 35%-solids (83:17 mol%) VDC-BMA copolymer latexes were prepared: one batch (G), one seeded batch (F), and 5 seeded semi-continuous polymerizations of 5 different monomer feed rates ranging from 0.27 (A) to 1.10 wt%/min (E) at 25°C using Aerosol MA emulsifier and a persulfate-bisulfite- Fe^{++} redox initiator. The seeded latexes A-F had number-average particle diameters of 120-125 nm with narrow particle size distributions; the unseeded batch latex (G) had an number-average particle diameter of 113 nm with a narrow particle size distribution.

The kinetic studies of seeded semi-continuous polymerizations A-E showed that the rates of polymerizations (R_p) were controlled by the monomer addition rates (R_a), and polymerizations A to D (0.27-0.79 wt%/min) were under monomer-starved conditions; however, polymerization E (1.10 wt%/min) was in near-flooded condition.

Significant differences were found in the physical and mechanical properties of the latex films depending on the mode of monomer addition of the polymerization; in batch polymerizations F and G, the instantaneous copolymer composition drifted with increasing conversion, resulting in copolymers of heterogeneous composition and crystalline character. In contrast, in seeded semi-continuous polymerizations A-E, the polymerizing particles were starved for monomer during the polymerization, resulting in copolymers of more uniform composition and amorphous character.

The conversion-time curves for the polymerizations of 0:100-100:0 VDC-

BMA mixtures by the batch polymerization showed that the rate of polymerization (R_p) was a function of the number of particles, and that the rate of polymerization in a latex particle (R_{pp}) increased with increasing proportions of butyl methacrylate in the monomer mixture.

The number-average particle diameters of the latexes prepared by both batch and semi-continuous polymerization increased with increasing proportion of butyl methacrylate in the monomer mixture. All of the latexes had narrow particle size distributions. The greater particle number density in VDC polymerization and the greater water solubility of VDC suggest that the homogeneous nucleation mechanism is operative in VDC-BMA emulsion copolymerizations.

The latex copolymers prepared by semi-continuous polymerization had lower number-average and weight-average molecular weights than those of the corresponding batch copolymers, resulting from the monomer starvation occurring during the semi-continuous polymerization. The broader molecular weight distributions found in batch copolymers might be explained by the occurrence of the composition drifts.

The T_g differences between copolymers prepared by batch and semi-continuous polymerization decreased with increasing amount of butyl methacrylate in the monomer mixture, indicating differences in sequence distributions. A maximum T_g was found at 39°C for the 30:70 mol% VDC-BMA monomer mixture. Only the PVDC, and 83:17 VDC-BMA copolymers prepared by batch (G) and seeded batch (F) polymerization, showed crystalline melting temperatures of 199, 187, and 184°C, respectively; all other copolymers prepared by both polymerizations showed none.

The VDC-BMA copolymers prepared by semi-continuous polymerizations were all amorphous, independent of monomer composition. In contrast, the copolymers prepared by batch polymerizations showed different degrees of crystallinity depending on the ratio of VDC to BMA in the monomer composition.

The surface characterization study of the cleaned latexes showed that, for the latexes prepared by batch polymerization, the surface charge density derived from strong-acid groups decreased with increasing proportion of VDC in the monomer mixture. This may be due to the catalytic effect of hydrochloric acid on the hydrolysis of strong-acid sulfate groups. On the other hand, for the latexes prepared by semi-continuous polymerization, the surface charge density derived from strong-acid groups did not depend on the monomer composition of the copolymers.

Chapter 1

GENERAL INTRODUCTION

Broadly speaking, the production of addition polymers can be carried out in either a homogeneous or heterogeneous environment. In homogeneous polymerizations such as bulk or solution polymerization systems, all the reactants are mutually soluble and compatible with the polymer product. In contrast, in heterogeneous polymerizations such as suspension or emulsion polymerization systems, all the reactants are not mutually miscible. In this process, the polymer exists as a separate discrete phase, dispersed in droplet or globular form in an inert suspending medium.

Bulk polymerizations are those in which only monomers, initiators, and a small amount of additives (if necessary) are charged to the reactor. This process can yield highly pure product using simple equipment. The disadvantage of this process is the difficulty in controlling the exothermic reaction so that it is restricted to materials with low reactivities and heats of reaction, such as styrene. In batch processing, the reaction is carried out in thin sections, such as sheets, slabs, or rods, under cool water. However, in large samples with low surface area to volume ratios, adequate temperature control is impossible to achieve, and localized overheating can often lead to runaway reactions or degradation and discoloration of the polymer. Another disadvantage of this polymerization is the difficulty of removal from the highly viscous medium of the unreacted monomer which can also serve as a plasticizer, thereby altering the mechanical properties of the product with toxic and giving highly objectionable odors.

In solution polymerization, a solvent is used as medium which is capable

of dissolving the monomer, the polymer, and the polymerization initiator. Diluting the monomer with solvent causes a direct reduction in the rate of polymerization and in the viscosity of the product mixture at a given degree of conversion. This polymerization can virtually eliminate the serious heat dissipation problems characteristic of bulk polymerizations. However, high molecular weight polymers are difficult to obtain by this polymerization process because of the chain transfer reaction with medium (solvent). Therefore, selection of the solvent is important in this polymerization. The major problem associated with the process is the difficulty of removal of solvent and unreacted monomer from the product.

Suspension polymerization, sometimes called pearl or bead polymerization, is carried out by suspending the monomer as droplets (0.001-1 cm in diameter) in water. The basic polymerization mixture consists of monomer, monomer-soluble initiator, suspending agent, and suspending medium (water). The low viscosity of the mixture and the diluting effect of the suspending medium allow good heat removal and temperature control. The size of the particles is determined by the rate of agitation as well as the amount and nature of the suspending agent used. Styrene, methyl methacrylate, vinyl chloride, and vinylidene chloride are polymerized by this polymerization process. The products can be isolated easily by filtration of the beads, which are then cleaned and dried to form molding powders. Suspension polymerization can be considered as bulk polymerization of small monomer droplets and can be well described by the solution kinetics. The suspension method is not used with monomers which are highly water-soluble or whose polymer has too low a glass transition temperature. For appreciably water-soluble monomers, polymerization take place

in solution as well as in the monomer droplets, with the former yielding appreciably lower molecular weights. Coagulation of the monomer droplets may occur at low conversion if the polymer T_g is lower than the polymerization temperature. The control of the particle size of products is generally difficult in suspension polymerization.

Suspension and emulsion polymerizations are alike in that the monomer is dispersed in the water medium before polymerization. However, they differ considerably in the degree of dispersion attained and in the manner by which initiation takes place in each.

The basic polymerization mixture in emulsion polymerization consists of monomer, water-soluble initiator, emulsifier, buffer, medium (water) and other additives (if necessary). The initiator radical is formed in the aqueous phase, not directly in the monomer droplets, and the major part of the polymerization generally takes place in the polymer particles. The sizes of the polymer particles produced are much smaller than in suspension polymerization. Typical latex particle dimensions are in the range of 100 to 400 nm in diameter. Emulsion polymerization is a unique process because high molecular weight polymers can be obtained at considerably enhanced polymerization rates, and most of the polymerization occurs away from the bulk of the monomer phase. Heat and viscosity control in emulsion polymerization is relatively easy compared to homogeneous polymerizations. This polymerization is of special value in producing stable latexes and dispersions, which can be used directly as coatings, water-based latex paints, adhesives, and other products, but is not as useful for producing high-purity products free of the dispersant and other additives. This process is of special importance in the production of many synthetic polymers as

well as synthetic rubber.

Emulsion polymerizations can be carried out by three different processes (batch, semi-continuous and continuous processes). It is well known (1-6) that the nature of the polymerization process can affect the kinetic behavior, microstructure, molecular weight, and homogeneity of the polymer, and thus its physical, mechanical, surface and colloidal properties.

When a batch process is used to produce copolymers, where the monomer pairs having different reactivity ratios ($r_1 \neq r_2 \neq 1$), the composition of the copolymers will change with conversion. This composition drift with conversion occurs in most of the addition polymerizations except in very special cases such as $r_1 = r_2 = 1$ or azeotropic copolymerization. The greater the difference in the values of the copolymerization reactivity ratios r_1 and r_2 , the greater the difference in the copolymer composition.

In contrast, when a semi-continuous process is used to produce copolymers, where the rate of polymerization (R_p) is controlled by the rate of monomer addition (R_a), more uniform composition copolymers can be obtained. Many studies have been done on the starved semi-continuous copolymerizations (1) for a variety of monomer systems, in which the rate of monomer feed (R_a) is carefully controlled and the rate of polymerization (R_p) is less than the maximum rate of batch polymerization ($R_{p,max}$). Under this condition, R_p is dependent on R_a , and at a sufficiently slow monomer feed rate, R_p will approach R_a , and the copolymer composition will be almost equal to the ratio of monomers in the feed. This process shows more flexibility in controlling the polymerization rates, the polymer morphology, the polymer compositions, the polymer molecular weight, and the polymerization reaction heat. Therefore, the semi-continuous

polymerization process is of considerable interest in producing industrial synthetic copolymers.

In a continuous emulsion copolymerization, intermediate addition of the more reactive monomer will also help maintain compositional uniformity of the copolymer product. However, this process is more complex than the semi-continuous process, and usually cannot be operated economically unless steady runs of rather long duration can be made with a single product.

Vinylidene chloride (VDC) monomer is one of the oldest of the commercially available vinyl monomers. VDC monomer polymerizes by both free radical and ionic mechanisms. In practice, polymerization by the free radical mechanism is the more common. VDC monomer is known to be of average reactivity when compared to other unsaturated monomers on the Q-e map shown in Figure 1.1 (7, 8). Monomers such as VDC and the acrylate esters, which fall in the middle of the Q-e map, tend to react reasonably well with a wide variety of monomers. The free radical polymerization of VDC can be carried out by bulk, suspension, and emulsion polymerization processes.

Poly(vinylidene chloride) is insoluble in its own monomer and all common solvents at room temperature, and separates from the liquid phase as a crystalline powder. Consequently, the heterogeneous polymerization reaction can have a remarkable influence on the kinetics of the reaction. Poly(vinylidene chloride) has a number of outstanding characteristics (9); since it is highly crystalline in the normal-use temperature range (0-100°C), it can be oriented into high strength fibers and films. It has outstanding resistance to solvents and chemical reagents other than bases, and flame. Of the organic coating materials, it has the lowest permeability to a wide variety of gases and vapors.

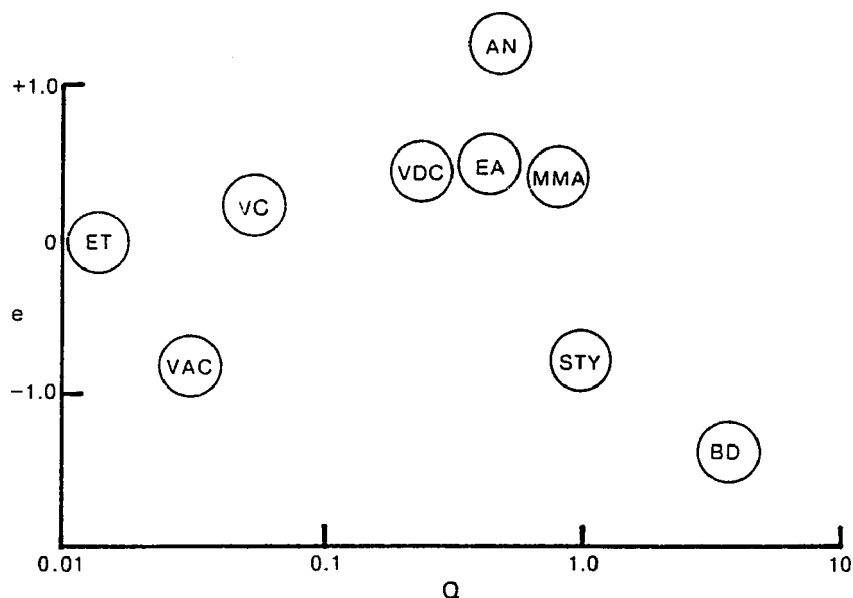


Figure 1-1: Q - e map of various monomers.

It also has a high refractive index. However, although it has many valuable properties, the homopolymer of VDC has not been used to any extent because of its difficult fabrication. It cannot be heated to the molten state for longer than a few seconds without being severely degraded. In the process of decomposition, it eliminates large quantities of hydrochloric acid, further complicating any potential fabricating process (9).

The techniques used to overcome the instability of poly(vinylidene chloride), which include copolymerization, plasticization, and stabilization, were developed at the Dow Chemical Company during the 1930's. VDC monomer is a fairly reactive monomer to copolymerize with other vinyl monomers, especially, acrylates or methacrylates. Many commercially important VDC copolymers, Saran, have been prepared and widely used in coatings (10-14), multilayer packaging films (15), and molding resins. Saran is a generic name for high

VDC-content polymers. The commercially important copolymers include those with vinyl chloride, acrylonitrile, or various alkyl acrylates, but many commercial Saran polymers contain three or more components. Usually, one component is introduced to improve the processability or the solubility of the polymer. Others are added to modify specific end-use properties. Most of these compositions have been described in the patent literature (9, 15).

Emulsion polymerization is used commercially to make vinylidene chloride copolymers, which are utilized in two ways. In some applications, the latex is used directly as a coating vehicle; in others, the polymer is first isolated from the latex as a dry powder before use. The principal advantages of emulsion polymerization as a process for preparing vinylidene chloride polymers are: (1) high molecular weight polymers can be produced with reasonable reaction rates; (2) the monomers can be added during the polymerization to maintain copolymer composition control.

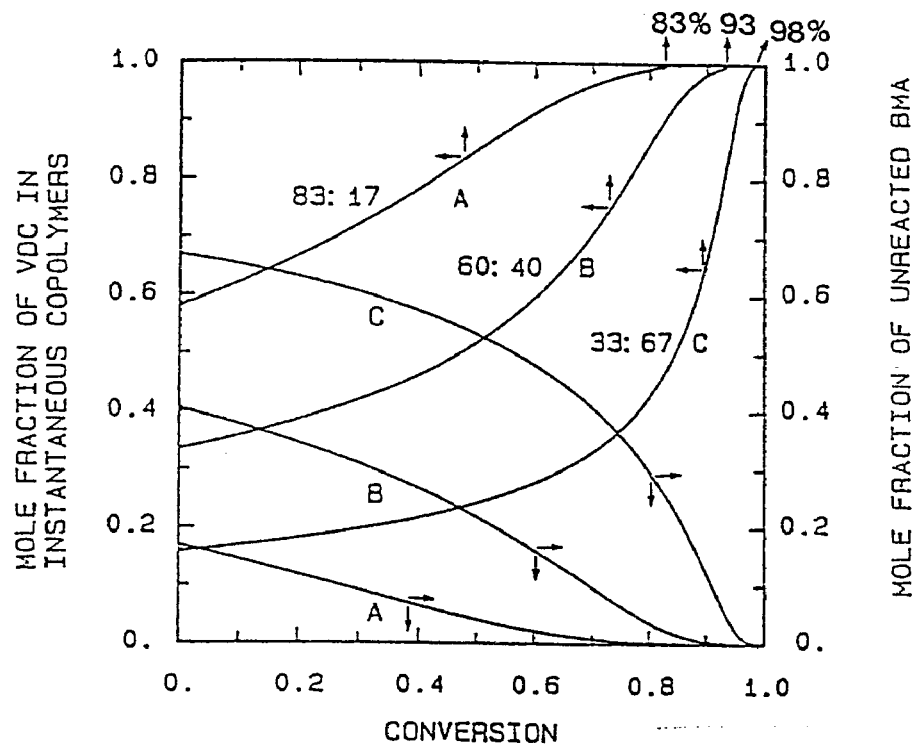
The purpose of the present study is twofold: (1) the preparation of VDC copolymer latexes with a comonomer using batch and semi-continuous processes, which give good film-forming properties, (2) the characterization of the resulting latexes and their copolymers with respect to bulk, surface, and colloidal properties. For the present study, n-butyl methacrylate (BMA) was used as a comonomer in the copolymerization of VDC. Table 1.1 shows some of the physical properties of these monomers and polymers. Both BMA and VDC monomers belong to a group of monomers which are relatively hydrophobic. However, VDC is more water-soluble than BMA. The T_g of VDC and BMA homopolymers are -17, and 20°C, respectively, so that the resulting VDC copolymer latexes with a variety of monomer compositions are expected to be

Table 1-1: Physical properties of VDC and BMA*.

PROPERTY	VDC	BMA
<u>MONOMER</u>		
molecular wt.	97.0	143.0
density, g/cm ³	1.214	0.889
solubility, g/100 ml H ₂ O	0.25	less than 0.01
<u>POLYMER</u>		
T _g , °C	-17	20
density, g/cm ³	1.7-1.9	1.05

* source references in (15, 16)

Figure 1-2: VDC-BMA copolymerizations of 83:17, 60:40, 33:67 (in mol%) by batch process.



able to form good films near room temperature.

The present work determined the reactivity ratios in VDC (M_1)-BMA (M_2) emulsion polymerizations, whose values are $r_1 = 0.22$, and $r_2 = 2.41$. Therefore, in batch copolymerizations of VDC-BMA, the instantaneous copolymer compositions will change with conversion as shown in Figure 1.2, and the homopolymer of VDC will start to appear at 83, 93, and 98% conversion for the copolymerizations of 83:17, 60:40, and 33:67 (mol%) VDC-BMA, respectively.

Composition drifts in VDC copolymerization should be controlled, because copolymer fractions containing long VDC sequences have a tendency to crystallize easily, resulting in poor solubility in solvent-based coatings, loss of film-forming ability in latexes, poor thermal stability, and poor color stability. Composition drift can be eliminated by keeping the condition of starved semi-continuous process, in which the monomer added is consumed as fast as it enters the reactor, resulting in copolymers of uniform composition.

In the present study, 83:17, 60:40, and 33:67 (mol%) VDC-BMA copolymer latexes were prepared by batch and seeded semi-continuous polymerization processes, and VDC and BMA homopolymer latexes by batch polymerization at 25°C, using Aerosol MA emulsifier and persulfate-bisulfite- Fe^{++} redox catalyst system, and characterized with respect to bulk, mechanical, colloidal, and surface properties.

Chapter 2

BACKGROUND

2.1 General Consideration of Emulsion Polymerization

Emulsion polymerization is a heterogeneous reaction in which monomers are dispersed in water with the aid of an emulsifier and polymerized with water-soluble initiators. The product is a colloidal dispersion of the polymer, which is called a latex. The emulsion polymerization process is one of the most important techniques for preparing synthetic polymers. The first synthesized latex, styrene-butadiene rubber, was produced on a large scale in the United States during the 1940's when the supplies of natural rubber were cut off during World War II. A wide range of monomers was polymerized by emulsion process to provide commercial products. These include styrene, butadiene, acrylates or methacrylates, chloroprene, vinyl chloride, vinylidene chloride, acrylonitrile, acrylamide, and ethylene.

The emulsion polymerization process has some distinct advantages. This polymerization proceeds at a high rate at relatively low temperature, making it possible to obtain high molecular weight polymers, while at the same time permitting efficient control over the exothermic polymerization reaction. The viscosity of the latex product is low and independent of molecular weight. The latex in some cases can be employed directly in final uses such as coatings, finishes, floor polishes, and paints without causing a fire hazard or air pollution.

Emulsion polymerization is carried out in a system which is comprised of a monomer and a dispersion medium (usually water) in which the monomer is insoluble. A micelle-generating substance is usually present, which includes a

number of anionic, cationic, and nonionic surfactants. A water-soluble initiator such as potassium or ammonium persulfate is generally used. Often, the emulsion polymerization is carried out by a redox initiator system, which gives higher polymerization rates at low reaction temperatures and which is especially effective in aqueous solutions for the monomers which have lower polymerization rates such as a vinylidene chloride. Various other components such as chain transfer agents, buffers, and shortstoppers may be used in the emulsion polymerization systems.

At the beginning of a batch emulsion polymerization, prior to initiation, the monomer is mixed with water and emulsifier, and emulsified under adequate agitation. When the concentration of a surfactant exceeds its critical micelle concentration (CMC), the excess surfactant molecules aggregate together to form small colloidal clusters referred to as a micelle. The transformation of a solution to the colloidal state is accompanied by a sharp drop in the surface tension of the solution. The surfactant concentrations in most emulsion polymerizations exceed the CMC, and the most of the surfactant is located in the micelles whose size is usually 50-100 Å. The surfactant molecules are arranged in a micelle with their hydrocarbon ends pointed toward the interior of the micelles and their ionic ends outward toward the water. The number of micelles and their size depends on the amount of emulsifier used compared to the amount of monomer. A larger amount of emulsifier yields a larger number of smaller-size particles.

When a water-insoluble or only sparingly water-soluble monomer is added, a very small portion dissolves. A small portion of the monomer enters the interior of hydrocarbon part of the micelles. The largest portion of the monomer

is dispersed as monomer droplets whose size is usually not less than 1 μ m (10,000 \AA). In a typical emulsion polymerization, the monomer droplets are much larger than the monomer-containing micelles. Generally, the concentration of micelles is 10^{17} - 10^{18} per milliliter, while there are at most 10^{10} - 10^{11} monomer droplets per milliliter. Therefore, it is clear that the micelles have a much greater total surface area than that of monomer droplets.

The polymerization starts with the initiation reaction of the initiator with monomer. The initiator is present in the water phase and this is where the initiating radicals are produced. The site of the polymerization is not the monomer droplets since the initiators employed are insoluble in organic monomer. This situation distinguishes emulsion polymerization from suspension polymerization. Emulsion polymerization takes place almost exclusively in the interior of the micelles. The micelles act as a meeting place for the oil-soluble monomer and the water-soluble radicals. The micelles are also found as the reaction site because of their high monomer concentration compared to the monomer in aqueous phase and their high surface-to-volume ratio compared to the monomer droplets. As polymerization proceeds, the micelles grow by the addition of monomer from the aqueous solution whose concentration is replenished by dissolution of monomer from the monomer droplets. A simplified schematic representation of an emulsion polymerization system is shown in Figure 2.1. The system consists of three types of particles: monomer droplets, inactive micelles in which polymerization is not occurring, and active micelles in which polymerization is occurring. From this point, active micelles are no longer considered as micelles but are referred to as polymer particles.

There are two basic mechanisms for particle nucleation (17, 18) in

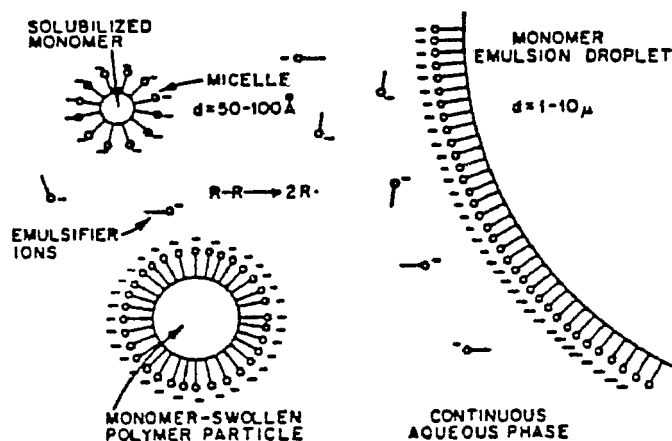


Figure 2-1: Diagram of emulsion polymerization.

emulsion polymerization as shown in Figure 2.2. One is the entry of radicals from the aqueous phase into the micelles, so called micellar nucleation, as described above. The other mechanism, homogeneous nucleation, is the initiation in the aqueous phase, in which radicals generated in the aqueous phase meet monomer units until the oligomeric radicals exceed their water solubility and precipitate. The precipitated oligomeric radicals form spherical particles which adsorb emulsifier and absorb monomer to become primary particles. These primary particles persist or flocculate with already-existing primary particles. In this system, the function of the emulsifier is to stabilize the particles precipitating from the aqueous phase. The relative extents of micellar and homogeneous nucleation would vary with the water solubility of the monomer and the surfactant concentration. Higher water solubility and low surfactant concentration generally favor homogeneous nucleation. On the other hand,

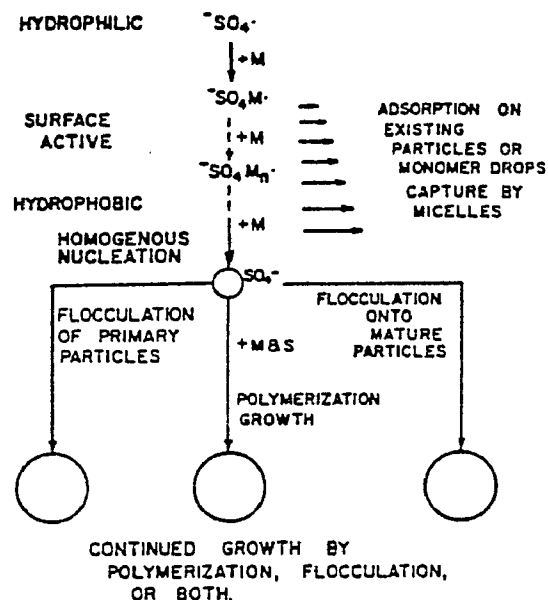


Figure 2-2: Paths for water-initiated free radicals.

micellar nucleation is favored by low water solubility and high surfactant concentration.

Typically, a batch emulsion polymerization consists of three intervals based on the particle number and the existence of a separate monomer phase, which is illustrated as a conversion versus time curve shown in Figure 2.3 and a schematic diagram of the three stages of an emulsion polymerization as shown in Figure 2.4.

The particle number increases with time in interval I and then remains constant during interval II and III. Particle nucleation occurs in interval I with the polymerization rate increasing with time as the particle number builds up.

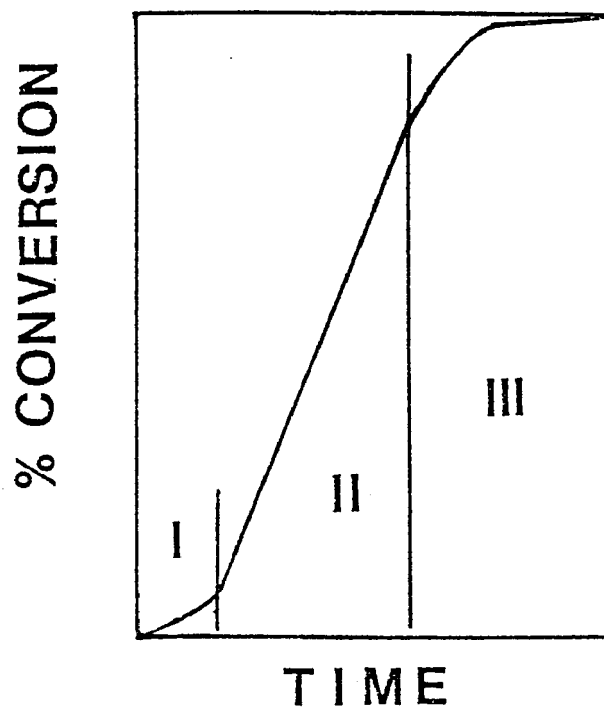
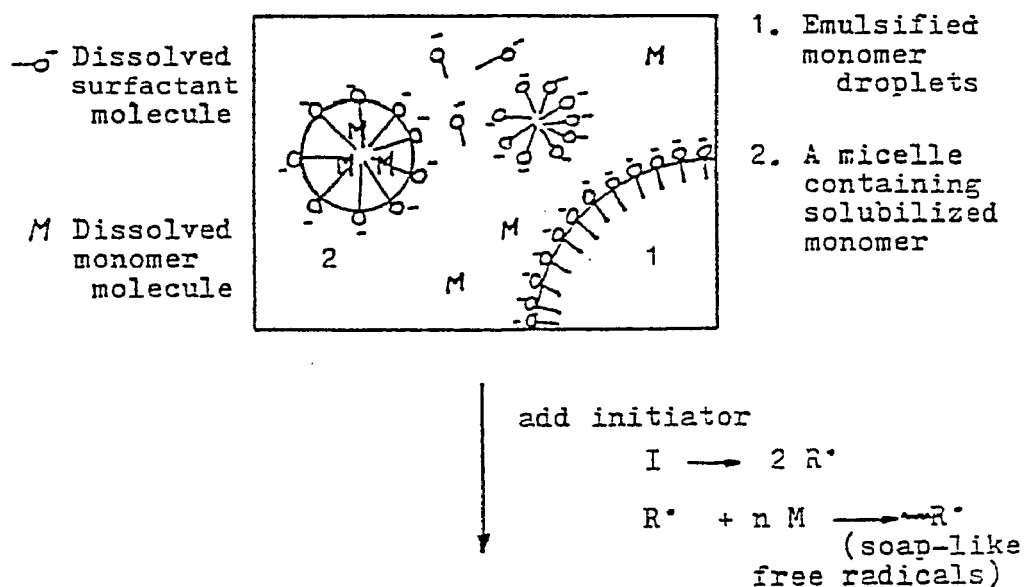


Figure 2-3: Typical conversion-time curve in emulsion polymerizations.

As the polymer particles grow in size, they adsorb more and more surfactant from the aqueous solution to stabilize them. The point is reached at which the surfactant concentration in solution falls below its CMC, the inactive micelles become unstable and disappear with dissolution of micellar surfactant. By the end of interval I, all the inactive micelles have disappeared, and their surfactant has been adsorbed on the monomer-swollen polymer particles. At this point, interval I is completed. This stage is characterized by simultaneous particle nucleation and particle growth, and the rate of polymerization increases continuously. Interval I is generally the shortest of the three intervals.

In interval II, polymerization proceeds in a fixed number of polymer

(a) Before initiation, surfactant and monomer in water



(b) Polymerization stage I (shortly after initiation)
Simultaneous particle nucleation and growth

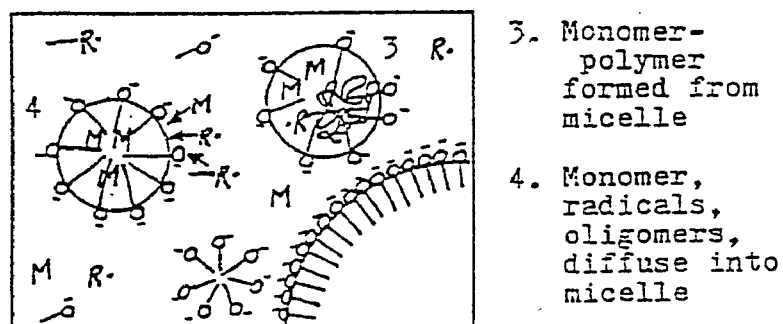
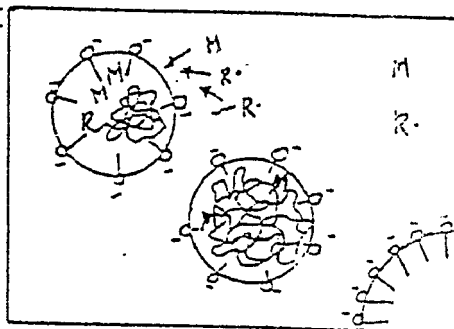
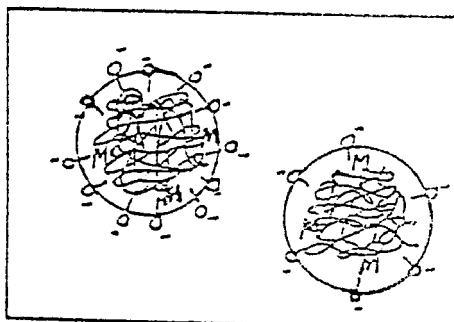


Figure 2-4: Representation of the stages of an emulsion polymerization.

- (c) Polymerization stage II
All emulsifier micelles disappear.



- (d) Polymerization
stage III.
All emulsified monomer
droplets disappear.



- (e) End of polymerization.
Particle phase.

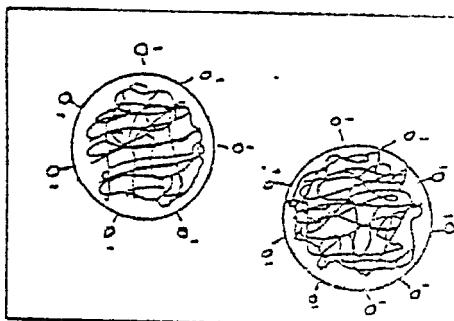


Figure 2-4, concluded

particles with constant overall rate of polymerization as the monomer concentration in the particle is maintained at the equilibrium level (saturation) by dissolution of monomer from the monomer droplets. The particles are continuously supplied with free radicals from the aqueous phase and with monomer until the emulsified monomer droplets disappear. In the system under consideration, the rate of generation of free radicals is about 10^{13} per second per milliliter and the number of active sites is between 10^{14} to 10^{15} per milliliter. Therefore, each site will capture a free radical every 10 to 100 seconds, which means that the free radicals will generally enter the particles singly. The point is that a free radical polymer chain within a monomer-polymer particle will react in an isolated state for a period of time (0-100 seconds) until another free radical enters to terminate the reaction. The particle remains inactive until another free radical enters to reinitiate polymerization. The polymerization within a monomer-polymer particle can thus be characterized by alternating periods of activity and inactivity. Since a large number of these sites are available for polymerization, and since polymerization within each site proceeds unhindered for a time, the emulsion polymerization system is featured by a rapid rate of reaction with a simultaneous generation of very high molecular weight polymer. Interval II ends when all monomer droplets disappear.

In interval III, the monomer droplets are no longer present, and the monomer concentration in latex particles decreases with time. Therefore, the overall rate of polymerization begins to deviate from linearity, and also a gel effect may present in this period.

The rate of the polymerization, R_p at any instant is given by the product of the concentration of active particles $[P\cdot]$, the monomer concentration in a

particle $[M]$, and the rate of propagation in a particle.

$$R_p = k_p[M][P\bullet] \quad (2.1)$$

$[P\bullet]$ is conveniently expressed by

$$[P\bullet] = 10^3 N' \bar{n} / N_A \quad (2.2)$$

Where N' is the concentration of micelles plus particles, \bar{n} is the average number of radicals per particle, and N_A is Avogadro's number. Combination of equations 1 and 2 yields the polymerization rate.

$$R_p = 10^3 N' \bar{n} k_p [M] / N_A \quad (2.3)$$

As N' decreases, \bar{n} increases and the product $N'\bar{n}$ increases with time during interval I. At the start of interval II, N' reaches its steady-state value N . \bar{n} may or may not reach a constant value depending on the monomer systems. \bar{n} will remain approximately constant or increase in interval III. The value of \bar{n} during interval II and III is important in determining R_p .

Three cases (19-21) can be distinguished based on the work of Smith and Ewart. The major differences between the three cases are the occurrence of radical diffusion out of the polymer particles (desorption), the particle size, modes of termination, and the rates of the initiation and termination processes relative to each other and to the other reaction parameters.

Case 2: $\bar{n} = 0.5$. This is the case usually described as applicable to most emulsion polymerizations. It occurs when the desorption of radicals does not occur or is negligible compared to the rate of radicals entering particles (absorption). Under these conditions, a radical entering a polymer particle is trapped within the particle and undergoes propagation until another radical enters, at which there is instantaneous termination. Any polymer particle will be

active half of the time and dormant the other half of the time. The number of radicals per particle \bar{n} averaged over all the particles is 0.5.

Case 1: $\bar{n} < 0.5$. The average number of radicals per particle can drop below 0.5 if radical desorption from particles and termination in the aqueous phase are not negligible. The decrease in \bar{n} is larger for small particle sizes and low initiation rates.

Case 3: $\bar{n} > 0.5$. Some fraction of the polymer particles contains two or more radicals per particle in order for \bar{n} to be larger than 0.5. This case occurs if the particle size is larger or the termination rate constant is low, while termination in the aqueous phase and desorption are not important, and the initiation rate is not too low.

The number average degree of polymerization in an emulsion polymerization can be expressed by equation.

$$\bar{X}_n = R_p/R_i = Nk_p[M]/R_i \quad (2.4)$$

In homogeneous polymerization, one can increase the polymerization rate by increasing the rate of initiation, but the result is a simultaneous lowering of the polymer molecular weight. The situation is quite different in emulsion polymerization. One can simultaneously increase R_p and \bar{X}_n by increasing N .

2.2 Emulsion Polymerization of Vinylidene Chloride

Emulsion polymerization of vinylidene chloride differs from those of usual monomers such as styrene and methyl methacrylate, which are solvents for them. Poly(vinylidene chloride) is insoluble in its own monomer and is barely swollen by it. Vinylidene chloride behaves in a particular way on homopolymerization in aqueous emulsion.

Wiener (22) studied the polymerization of vinylidene chloride in potassium laurate solutions using potassium persulfate as initiator. The polymerizations were carried out both in solution and in emulsion. The polymerization rates were determined from the vapor pressure for the solution polymerizations and by gravimetric or dilatometric methods for the emulsion polymerizations. For the emulsion polymerizations, the polymerization rate varied as the 0.6 power of the emulsifier concentration and approximately as the 0.5 power of the initiator concentration. The values for the intrinsic viscosities of the polymers were relatively independent of initiator concentration, indicating that chain transfer reaction predominates as a chain termination mechanism.

An extensive investigation of the vinylidene chloride system was described in a series of papers by Sweeting and co-workers. Hay et al. (23) described emulsion polymerizations using ammonium persulfate and sodium metabisulfite as the redox initiator system and sodium lauryl sulfate as the emulsifier, which were carried out at 36°C using a monomer/water phase ratio of 0.83, and the polymerization rates were determined by gravimetric methods. They observed at intermediate concentrations of emulsifier (1.0-5.0% based on monomer weight, 0.15% initiator) and initiator (0.075-0.30%, 2.0% emulsifier), an unusual conversion-time curve which can be divided into three stages as shown in Figure 2.5. In the first stage, a normal emulsion polymerization occurred at a rate proportional to the 0.6 power of both catalyst and emulsifier concentrations, respectively. In the second stage, the rate dropped to less than half that of the first. In the third stage, the rate increased again and exceeded that of the first. At lower or higher concentrations of emulsifier (0.5 or 10.0%) or initiator (0.0375, 0.45, 0.60%), there was no decrease in polymerization rate in stage II.

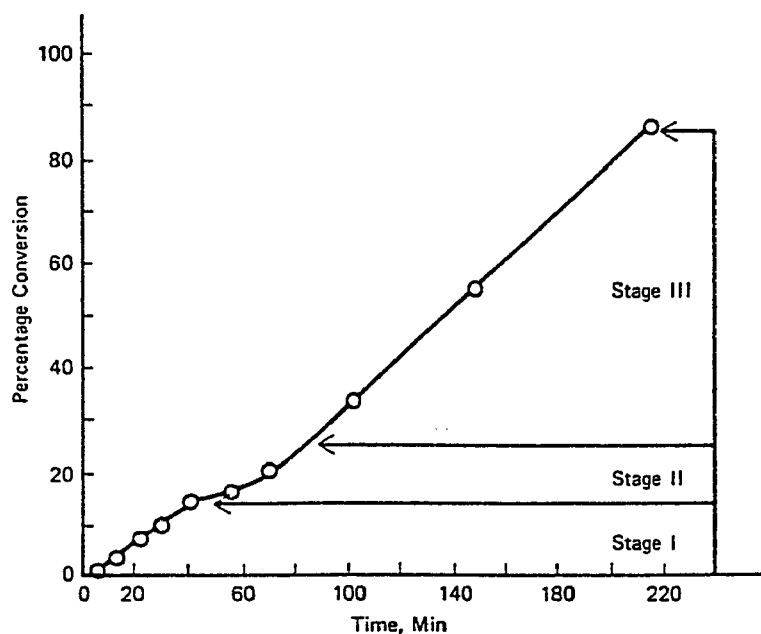


Figure 2-5: Conversion-time curve showing 3 stages.

Additional emulsifier just before the end of stage I had no effect on the polymerization rate in stage I and II but caused an increase in that of stage III. Additional emulsifier (0.5% compared to 2.0% in the initial charge) added during the early part of stage II had no effect on the polymerization rate in stages II and III.

To explain the decrease in polymerization rate in stage II and its subsequent increase in stage III, Light et al. (24, 25) proposed the following mechanism. The slowdown in polymerization rate in stage II results from monomer starvation caused by slow diffusion from coalesced monomer droplets. As the polymer particles grow in size, they compete for the available emulsifier. The instability resulting from the reduced concentration of emulsifier leads to the coalescence of polymer particles with monomer droplets. The polymerization

rate decreases because the coalescence of the monomer droplets decreases the diffusion of monomer to the particles, and the amount held in the particles is limited by the insolubility of the polymer in the monomer. The rate increases again in stage III because collisions between polymer particles and monomer droplets are effective in transferring monomer to the polymerizing particles. They also developed a theoretical expression for the overall rate of polymerization in a system in which the particles are coalescing, assuming that the coalescence begins shortly after the disappearance of the micelles and proceeds as a second order process with an invariant rate constant, and that the rate of polymerization per particle increases linearly with particle volume. They derived an equation for the variation of the amount of polymer formed with the time elapsed from the disappearance of the micelles as a function of the parameters B , denoting the rate of coalescence, and A , denoting the relative rates of radical generation and termination. This equation predicts a minimum in the polymerization rate at some time after the coalescence starts. Their polymerization data were used to test this theory. The theory was successful in accounting for the polymerization rates in stage III, but the extent of slowdown in stage II greatly exceeds that predicted by theory.

In their third paper (26), the effect of stirring rate on the polymerization rate was also studied. Evans et al. observed a decrease of polymerization rate in stage I as speed of stirring was increased, while the polymerization of stage II increased as stirring speed was increased. The polymerization rate in stage III was unaffected by speed of stirring. They explained that the slowdown of the polymerization rate in stage II results from monomer starvation, described in their first paper, caused by slow diffusion from coalesced droplets, and that

recovery is caused by transfer of monomer at the time of collision between a polymer particle and a monomer droplet, and that these collisions are allowed when the repulsive forces between monomer droplets and polymer particles are reduced because of surfactant deficiency.

Extension of this study to copolymers of vinylidene chloride and acrylonitrile by Marker et al. (27) showed a similar kinetic effect for high vinylidene chloride content polymerizations. The rate of polymerization for a system containing 90% vinylidene chloride decreases sharply after 15% conversion. A polymerization containing 70% vinylidene chloride did not show a slowdown in the rate of polymerization in stage II.

2.3 Polymerization Processes

Emulsion copolymerizations can be carried out using batch, semi-continuous, or continuous processes. It is also well known that the modes of polymerization processes can affect the kinetic behavior and many properties of the resulting copolymers (18, 28).

Batch polymerization system is a stirred tank reactor in which all the ingredients are introduced at the beginning of the polymerization. The contents are heated to polymerization temperature to initiate. The reaction mixture is brought to a specific conversion, the polymerization is stopped, and the contents discharged for further processing (Figure 2.6.a). This process is the simplest process, but the polymerization exotherm is difficult to control for monomer systems which polymerize rapidly. In general, in copolymerizations carried out by batch process in which $r_1 \neq r_2 \neq 1$, the instantaneous copolymer composition changes with increasing conversion, leading to copolymers of heterogeneous compositions.

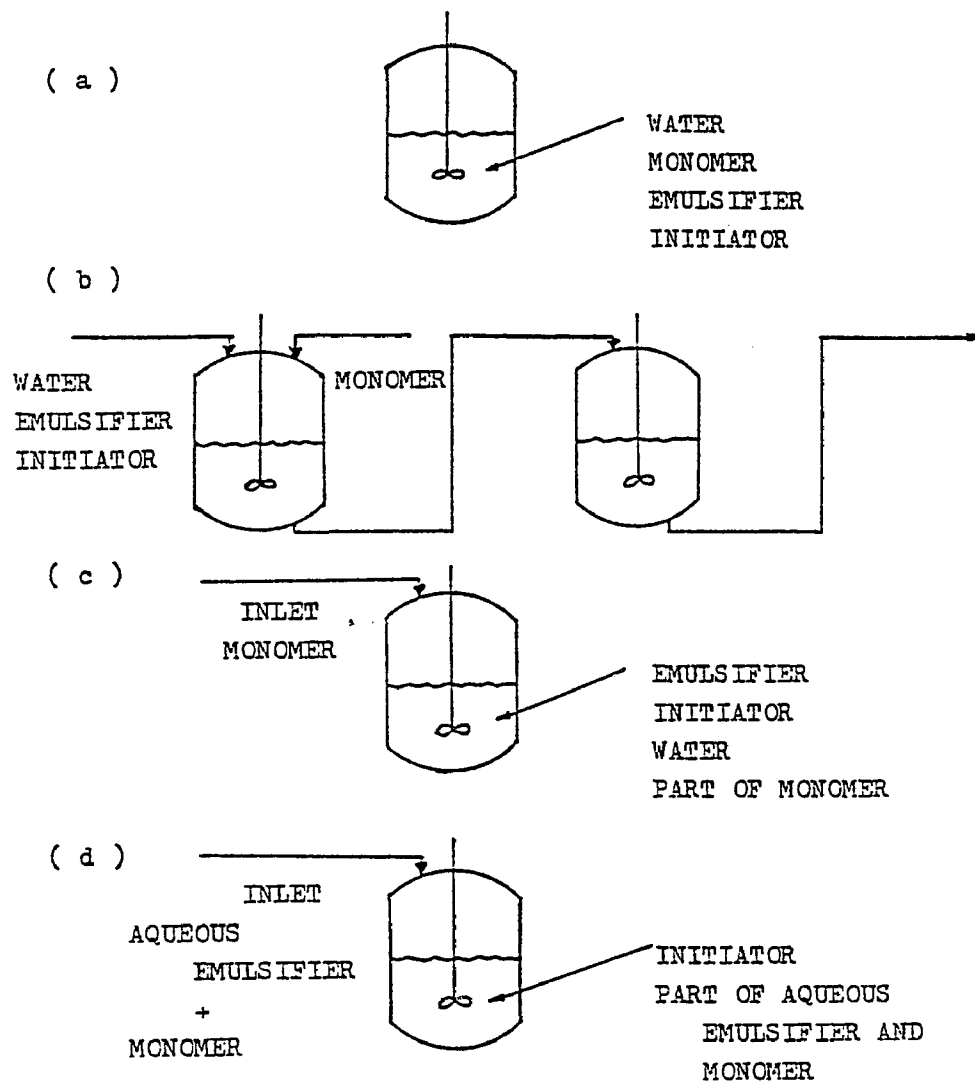


Figure 2-6: Flow diagram of stirred-tank reactor for emulsion polymerization; (a) Batch reactor; (b) Continuous stirred-tank reactor; (c) Semi-continuous reactor-monomer addition; (d) Semi-continuous reactor-emulsion addition.

The continuous polymerization system (in large scale polymer production) usually consists of several stirred tanks connected in series, with all the recipe ingredients fed into the first reactor and the product removed from the last reactor; this process is less flexible than the semi-continuous polymerization system, and usually cannot be operated economically unless steady runs of rather long duration can be made with a single product or with several closely related products (Figure 2.6.b). The particle nucleation occurs throughout the reaction so that the number of particles varies continuously and thus the particle size distribution is difficult to control; complex equipment is required in this process.

The semi-continuous polymerization process is the technique most commonly used in industry, in which the rate of polymerization is controlled by the rate of monomer addition. This process is extremely versatile in that layered or core-shell particles of complex morphology (29) can be prepared with minimum coagulum. There are two kinds of techniques used in the semi-continuous process. The first is called monomer addition, in which water, emulsifier and part of the monomer are charged into the reactor, then the polymerization is started by adding the initiator. After a certain time, the remaining monomer is fed into the reactor at a constant feed rate (Figure 2.6.c). The second method is called emulsion addition, in which a portion of aqueous emulsifier and monomer are initially charged to the reactor, the reaction is started by adding all the initiator (or part of the initiator) and usually is allowed to proceed for a certain time before the rest of the aqueous emulsified monomer (or the rest of the initiator in a different stream) is added continuously to the reactor at a constant rate (Figure 2.6.d). Semi-continuous

processes are extremely flexible, and they permit the production of a wide variety of copolymer latex products in a single reactor.

These techniques can control the:

1. polymerization rate
2. polymerization reaction heat
3. polymer microstructure
4. polymer morphology
5. polymer molecular weight and its distribution
6. latex particle size and its distribution
7. amount of surface end groups on the latex particles

2.4 Literature Review on Semi-continuous Emulsion

Polymerization

The semi-continuous process is particularly effective in emulsion copolymerization for the monomer pairs which do not form alternating copolymers in batch process. The effect of monomer and emulsion feed rates on the rate of polymerization, the degree of polymerization, and the number of particles for a variety of monomer systems have been extensively studied.

In the early literature, Naidus (30) reviewed the fundamental principles of polymerization and the role of such emulsion polymerization variable such as pH, agitation, and recipe ingredients in the preparation of emulsion polymers for paints, and also the important factors which can influence the properties such as chemical stability, mechanical stability and viscosity. Both the monomer and emulsion addition techniques of semi-continuous polymerization were used for the preparation of latexes for paints. Both techniques generally yielded the most stable latexes with the least coagulum and more uniform composition in

copolymers.

Fram et al. (31) presented the scientific investigation of semi-continuous emulsion polymerization. They prepared and characterized high-solids latexes of butyl acrylate and acrylonitrile using both semi-continuous and batch techniques. The experimental technique used in semi-continuous polymerization was the continuous addition of the monomer and catalyst solution into the reactor. When compared to the batch technique, they found that the semi-continuous technique offered easier reaction temperature control, more homogeneous copolymer composition, and special application for the preparation of high-solids latexes.

Wall et al. (32) fractionated copolymers of styrene with methyl methacrylate prepared by batch and semi-continuous processes and found that the polymerizations by batch polymerization gave a copolymer possessing much greater compositional heterogeneity than the semi-continuous type copolymers.

Elgood et al. (33) studied the emulsion polymerization of vinyl acetate by seeded semi-continuous processes. 10 wt% of the whole recipe was polymerized before the semi-continuous polymerization was started. Monomer, emulsifier, and initiator were all added continuously to the reactor over two hours. They calculated the particle volume, numbers and surface areas based on the measured solid contents, weight-average particle diameters, and densities, and found that the particle surface area is an important factor in controlling the rate of polymerization.

Vandegaer (34) presented a method of preparing a poly(vinyl toluene) latex with a particle size larger than can be obtained by direct emulsion polymerization by means of seeding technique, by feeding monomer to the seed

latex and adjusting the emulsifier concentration in a manner which prevents both coagulum and the formation of new micelles.

Woodford (35) reviewed some important aspects of the emulsion polymerization of vinylidene chloride and the properties of its copolymers. He described the use of semi-continuous monomer addition technique as a means of avoiding composition drift, in which the system is starved of monomer and any monomer added is consumed immediately. The resulting latexes showed better film-forming properties and better color stability.

Eliseeva et al. (36, 37) have prepared acrylate latexes including poly(butyl methacrylate), 45:55 mol% methyl methacrylate-butyl methacrylate copolymer, and 40:55:5 mol% methyl methacrylate-butyl methacrylate-methacrylic acid copolymer by three different polymerization methods of batch process, semi-continuous process by monomer addition, and semi-continuous process by emulsion addition, and compared the experimental % conversion, particle diameter, and molecular weight. They found that the ratio of emulsifier to monomer was the main factor in determining particle growth for a latex of the given composition, which can influence the molecular weight, particle diameter, number of polymer particles, and colloidal stability of latexes. Gradual addition of the butyl methacrylate to the emulsifier solution brought about the formation of the latex particles without seeding as a result of flocculation in this system. The effect of the emulsifier on the polymerization rate and latex formation was found to be less pronounced in the case of the more soluble (polar) monomers.

Wessling (38) studied the kinetics of emulsion polymerization by continuous process quantitatively. In the monomer addition system, when the rate of monomer addition was slow, the saturation concentration was not

reached, and the rate remained below the maximum rate of the batch polymerization. Under this condition, the rate of polymerization R_p (under starved conditions) depended on the rate of addition R_a according to a reciprocal relation: $1/R_p = 1/K + 1/R_a$, where $K = k_p N n / N_A$; R_p also depended on the number of particles per liter of the system (N), propagation rate constant (k_p), average number of free radicals per particle (n) and Avogadro's number (N_A). Above a critical value of R_a (flooded system), the particles became saturated with monomer and R_p was constant and independent of R_a .

Krackeler and Naidus (39) presented a comparison of emulsion polymerizations of styrene by batch process, semi-continuous process by monomer addition, and semi-continuous process by emulsion addition on the number of particles, particle size, particle size distribution and molecular weight. They introduced the monomer starvation concept which was related to the lower monomer concentration in the latex particles in monomer addition and emulsion addition systems as compared to the batch system. In starved emulsion polymerizations of styrene, they observed:

1) The rate of polymerization in either monomer addition or emulsion addition by semi-continuous process was much slower than in the batch system.

2) Lower molecular weight polymers were produced for monomer addition and emulsion addition by semi-continuous process compared to batch system. No significant differences in molecular weight distribution were observed.

3) The results of comparison of the number of particles, particle size and particle size distribution can be summarized as follows:

$$N_{\text{monomer addition}} > N_{\text{batch}} > N_{\text{emulsion addition}}$$

$$D_{\text{emulsion addition}} > D_{\text{batch}} > D_{\text{monomer addition}}$$

$$\text{PSD}_{\text{emulsion addition}} > \text{PSD}_{\text{monomer addition}} > \text{PSD}_{\text{batch}}$$

4) They also postulated that, in the monomer starvation system, there is a concentration gradient of monomer throughout the particles with a greater monomer concentration in the outer zone of the particles.

Gerrens (40) has also studied extensively the semi-continuous emulsion polymerization of water-insoluble styrene and relatively water-soluble methyl acrylate to determine the effect of the rate of monomer addition and emulsion addition on the rate of polymerization, the degree of polymerization, the number of particles, the particle size and the particle size distribution. The monomer concentration in the latex particles during polymerization was adjusted by controlling the rate of addition. When the monomer concentration in the latex particles fell below the saturation value (i.e., when no excess monomer phase was present), he found that:

1) When a steady state was obtained, in either the monomer addition or emulsion addition techniques, the rate of polymerization (R_p) became equal to the rate of addition (R_a), according to the following equation:

$$d[M]/dt = R_a - R_p = 0 \quad (2.5)$$

2) For the methyl acrylate system, the rate of polymerization was linearly proportional to the rate of addition for both the monomer and emulsion addition, but in the styrene system, the rate of polymerization was linearly dependent on the rate of monomer addition and almost independent of the rate of emulsion addition.

3) For both styrene and methyl acrylate, the rate of polymerization was linearly proportional to the average monomer concentration in the latex particles

for both monomer and emulsion addition systems., i.e.,

$$R_p = A[M]; R_a = A[M_p]; \quad (2.6)$$

where $A = k_p n[M_p]/N_A$

4) The degree of polymerization increased with an increase in the rate of addition for methyl acrylate in the emulsion addition system. For styrene, the degree of polymerization was almost independent of the rate of emulsion addition. When the rate of addition was fast enough to maintain the saturation point of the monomer concentration in the latex particles, the rate of polymerization and the degree of polymerization by both monomer addition and emulsion addition methods were independent of the rate of addition. Emulsion addition polymerization gave a narrower particle size distribution, if formation of new latex particles during the emulsion feed could be avoided. If not, particle size distribution was broadened and could become even broader than the other two methods.

Chujo et al. (41) studied the emulsion polymerization of vinyl acetate and butyl acrylate with various monomer addition methods. They obtained a copolymer with different physical properties by changing only the monomer addition method. Homogeneous copolymers were obtained by semi-continuous polymerization. Heterogeneous copolymers were obtained by batch polymerization or stepwise monomer addition methods. The homogeneity of the polymer had a great influence on various properties such as hardness and adhesive properties.

Wessling and Gibbs (42) studied the kinetics of the continuous monomer addition method on non-swelling (vinylidene chloride) and swellable (vinylidene chloride-butyl acrylate copolymer) latex particles ranging from 100% vinylidene chloride to 80:20 vinylidene chloride-butyl acrylate. Their primary objective was

to investigate how the kinetics can be influenced by the locus of polymerization, whether in the particle or on its surface. A poly(vinylidene chloride) seed was prepared, which was then grown to larger size by feeding the monomer to the reactor at a constant rate so that the concentration of monomer could be controlled throughout the reaction. They observed that two kinds of phenomena occur in both swelling and non-swelling systems:

A. At low feed rate:

1) The conversion-time curve was linear and the rate of polymerization R_p was controlled by the rate of monomer addition R_a .

2) In the reaction of this controlled region, all the data fitted the equation $R_p = KR_a$, where K was not dependent on monomer composition and was a constant characteristic of the monomer addition process and had an average value of 0.91.

3) In the starved regime, the monomer was consumed as fast as it entered the reactor.

4) The rate of the polymerization R_p was slightly less than the rate of addition R_a indicating that the level of unreacted monomer in the reactor built up during the run.

5) At steady state, a 25 Å-thick monomer layer could be accommodated on the particle surface. The polymerization took place at the particle-water interface or in a surface layer on the polymer particle.

B. At high feed rate:

1) The conversion-time curves were non-linear and the rate of polymerization was independent of the rate of addition, R_a , but depended on monomer composition.

2) The reaction flooded and excess monomer in the form of droplets in the reactor was detected.

They also pointed out that the kinetic behavior of the non-swelling and swelling particle systems were identical but neither followed the kinetics of the Smith-Ewart theory. They studied the morphology of poly(vinylidene chloride) particles during the polymerization to determine if crystallization takes place during or after polymerization using various techniques including electron microscopy, electron diffraction, and X-ray diffraction. The poly(vinylidene chloride) seed freshly made and cooled at 0°C turned out to be crystalline, and poly(vinylidene chloride) latexes isolated at higher conversion characterized by electron microscopy were spheroidal and showed crystalline diffraction pattern. They concluded that the crystallization takes place in the colloidal state during the polymerization process.

Snuparek (43) studied the semi-continuous emulsion copolymerization of butyl methacrylate and butyl acrylate with a monomer emulsion feed and without the preparation of seed latex. The influence of the polymerization variables on the rate of polymerization was studied by measuring the temperature changes in a thermally insulated reactor during the initial period of polymerization. The maximum polymerization rate was limited by the feeding rate of the monomer emulsion. The polymerization rate was controlled by the amount of emulsifier and its distribution between the initial reactor charge and the monomer emulsion.

Snuparek (44) also found that the overall polymerization rate and the amount of unreacted monomer in the polymerization system were proportional to the feeding rate. At a sufficiently slow feed rate, a steady state was reached.

The composition of the copolymer was equal to the ratio of monomers in the emulsion feed.

Snuparek (45) varied the distribution of a constant amount of anionic emulsifier between the initial reactor charge and the emulsion of monomer and found that the polymerization rate at the early stages is strongly affected by the amount of surfactant in the initial reactor charge. Also, the distribution of the emulsifier between the initial charge and the monomer emulsion affected the mechanism of particle growth and final particle size in the polymerization system. At high emulsifier content in the initial reactor charge, a large number of small particles were formed and were flocculated during the later stages of polymerization. At low emulsifier content in the initial reactor charge, no flocculation occurred, but new particle nucleation was observed in the latter stages of the monomer emulsion feeding.

Snuparek et al. (46) studied the emulsion polymerization of styrene and butyl acrylate in the semi-continuous emulsion addition system without the preparation of seed latex. They found that the composition of the copolymer was different from the feed composition, and the difference was proportional to the monomer emulsion feed rate. The sensitivity to the feed rate decreased as the feed composition become closer to the composition at the azeotropic point. In the case of low feeding rate (rate of addition was much smaller than the maximum rate of polymerization, $R_a \ll R_{p,max}$), the steady state was approached. The value of the differential copolymer composition was equal to the monomer feed composition; the instantaneous conversions were about 90-95%.

They (47) also studied the semi-continuous emulsion copolymerization of

acrylonitrile with butyl acrylate, and acrylonitrile with styrene and the terpolymerization of the ternary system acrylonitrile-butyl acrylate-styrene. The copolymerization of acrylonitrile-butyl acrylate and acrylonitrile-styrene reached a high degree of instantaneous conversion at the investigated feed rate range. Under this condition, the instantaneous conversion was near 100%, and the copolymer composition was equal to the monomer feed composition.

Snuparek (48, 49) also reported that, in the semi-continuous emulsion polymerization of acrylates by the emulsion addition method, the stability of the polymerization system was greatly affected by the emulsifier distribution between the initial reactor charge and the monomer addition; the amount of coagulum formed was also dependent on the polarity of monomers, and increasing the surface group concentration via copolymerization of butyl acrylate with acrylic acid or sulfoethyl methacrylate increased colloidal stability and resulted in a rapid decrease in coagulum formation.

Bataille et al. (50) studied the semi-continuous polymerization of vinyl acetate. The latexes were produced by the emulsion addition method without the preparation of a seed latex. Polymerizations were run at different feed rates, with all other variables being held constant. The monomer conversion, polymerization rate, particle size and its distribution, and molecular weight and its distribution were determined from the samples taken at regular intervals. In the starved region, the amount of polymer formed versus time curves were linear and dependent on the feed rates. The total surface area of particles was an important factor in controlling the rate of polymerization. Due to the high solubility of vinyl acetate in water, the locus of polymerization was both in the aqueous phase and in the micelles. The average number of radicals per particle

was much greater than one and the ideal Smith-Ewart case 2 model was inapplicable. Due to the chain branching which occurred in the system, an increase in the molecular weight distribution with conversion was observed.

Min et al. (51) used different experimental techniques in the studies of semi-continuous emulsion polymerization of vinyl chloride. The reactor was charged with a poly(vinyl chloride) seed latex (which was prepared in a separate polymerization), water, all of the monomer, part of the initiator and other additives. Then, both the emulsifier and initiator solutions were metered into the reactor during the polymerization. They derived a mathematical model of the particle size distribution of the poly(vinyl chloride) latex system with conversion using the following characters and assumptions: (1) The polymer particles were homogeneous with no internal structure, (2) New particles were formed from micelles, (3) The polymer particles were stabilized both by emulsifier and by polymer chain ends on the particle surface, (4) Polymer particle agglomeration was important and has been accounted for in the model, (5) The Trommsdorf effect was present from the very early stages of the reaction, (6) The shrinkage of reaction volume due to polymerization was significant, (7) The reactor was well-mixed to give spatially homogeneous conditions with regard to temperature and reaction ingredients. This model was shown to predict the bimodal particle size distribution in seeded emulsion polymerization, in good agreement with pilot plant data.

Hoy (52) studied the polymerization of acrylic monomers in the semi-continuous system. He presented the dynamic mechanical properties of three latexes made by uniform feed (continuous addition of monomer mixture with same monomer composition during the course of the polymerization), a staged

feed (stepwise addition of monomer for the formation of core-shell latex), and a linear power feed (a method of gradually changing the composition of the entering monomer during the course of the polymerization). The results from dynamic mechanical spectra showed that the uniformly-fed materials have a rather narrow peak and the power-fed materials have a single broad peak. The stage-fed latex had two peaks and became heterogeneous.

El-Aasser et al. (2-4) prepared the vinyl acetate-butyl acrylate copolymer latexes with various monomer compositions by batch and starved semi-continuous emulsion polymerization processes, and characterized those with respect to bulk, mechanical, surface, and colloidal properties. They found from dynamic mechanical spectra that batch polymerizations gave a two-peaked distribution of copolymer compositions, and semi-continuous polymerization, a single-peaked distribution of copolymer compositions. They also found that the comonomer composition and the method of monomer addition had a remarkable effect on the particle size, size distribution, surface properties and colloidal stability of the copolymer latexes. The latexes prepared by semi-continuous polymerization had broader molecular weight distributions, better colloidal stability, and greater extents of surfactant adsorption than those prepared by batch polymerization. Pichot et al. (5) investigated differences in the monomer sequence distributions between the two series of these copolymers quantitatively using ^{13}C nuclear magnetic resonance spectroscopy, and found that higher proportions of long butyl acrylate and long vinyl acetate sequences (higher concentrations of BBB, VVV triads and BB, VV dyads) in the batch copolymers as compared to the semi-continuous copolymers which contained more alternating structures such as BVB, VBV triads, and AB dyads.

Makgawinata (1) studied the kinetics of semi-continuous emulsion polymerization of 80:20 vinyl acetate-butyl acrylate and 40:60 methyl methacrylate-butyl acrylate mixtures using different monomer addition rates under the same recipes and isothermal conditions. In the starved region, the overall rates of polymerization were a function of time and were controlled by the rate of monomer addition. For the semi-continuous techniques, the average copolymer compositions were maintained at nearly the same composition as the original monomer ratios. He developed a mathematical model for the copolymerization systems based on the mass balances of the system and the assumption that the overall rates of monomer addition were slower than the overall rates of polymerization in the corresponding batch polymerization; the overall conversion was based on a curve-fitting method; the instantaneous conversion and conversion at time t were based on the mass balances of the system. A comparison was made between the theoretical results and the experimental data. The values predicted from the derived equations agreed well with the experimental data.

Jayasuriya (6) prepared various copolymer latexes of vinyl acetate (M_1)-methyl acrylate (M_2) by batch and semi-continuous processes, and measured the sequence distributions of these copolymers quantitatively using ^{13}C nuclear magnetic resonance spectroscopy. He found that the chemical shifts in the MM (methyl acrylate) and VV (vinyl acetate) dyads were more intense in the batch copolymers, indicating that the monomer sequences in the copolymers were more blocky. This blockiness is expected from the wide disparity in the copolymerization reactivity ratios ($r_1 = 0.02$; $r_2 = 6.54$). In the semi-continuous copolymers, however, the most intense chemical shift was for the MV dyad

characteristic of the linkage between the two different monomers, which indicates that the distribution of the monomer units was more random than in the batch copolymers.

Xue (53) studied the polymerization kinetics for both batch and semi-continuous copolymerizations of vinyl acetate and methyl acrylate, and characterized the properties of the latex films. In batch copolymerizations, a two-stage polymerization was detectable at the conversion-time curve, the first stage being the fast polymerization mainly of methyl acrylate followed by the polymerization of vinyl acetate due to the large difference in the polymerization rate between two monomers. However, in the seeded semi-continuous monomer addition polymerization process, the large difference in the reactivity between these two monomers was greatly restricted by the slow monomer feed rate technique. There was not much difference in the conversion-time curves, even when the comonomer ratio was varied from MA 100%:VAC 0% to MA 0%:VAC 100%. The conversion-time curves for the semi-continuous polymerizations with the higher VAC proportions in the monomer composition deviated from a linearity, indicating that excess monomer, mainly VAC, was accumulated because of the slower polymerization rate of VAC. In these curves, the unreacted monomer increased at the beginning, reached a maximum value, and then began to fall owing to the increasing rate of polymerization, and finally exceeded the feed rate; these polymerizations were neither completely flooded condition nor a typical starved condition. The copolymers with a more highly branched structure prepared by the semi-continuous process showed 2-4°C higher T_g than those with less branching prepared by the batch process.

Chapter 3

EXPERIMENTAL

3.1 Experimental Apparatus

Figure 3.1 is a schematic diagram of the experimental apparatus used in making the latexes by both batch and semi-continuous polymerization.

The polymerization reactor used in these experiments was a standard 500-ml four-necked round-bottom flask. The reactor was placed in the constant temperature water bath maintained at 25°C and then adjusted and clamped in a convenient position. A lune-type Teflon blade and glass stirrer fitted with a Teflon trubore adapter, which can prevent vinylidene chloride monomer from escaping during the polymerization, was placed in the center neck of the flask.

Inserted in the side neck of the flask was a spiral reflux condenser, in which -15°C ethylene glycol coolant was circulated to condense the vinylidene chloride vapor during the polymerization. A hose connector adapter was inserted into the top of the condenser. Poly(vinyl chloride) Tygon tubing was used to connect the adapter to a one-piece test tube, which was filled with water so as to act as a nitrogen gas pressure regulator.

A precise thermometer of 0.1°C scale was inserted into the smallest neck of the flask to monitor the reaction temperature throughout the polymerization. A rubber stopcock with three holes, in which one piece of Teflon tubing in one hole for nitrogen flushing, one for addition of monomer mixture in semi-continuous process, one for withdrawing a sample which was connected with a disposable plastic syringe, was inserted into the last neck of the flask.

For the semi-continuous polymerization, the seed formation was completed,

and the monomer mixture was fed into the reactor at the constant feed rate using the compact syringe pump (Harvard apparatus company) throughout the polymerization. The 100-ml glass syringe containing the monomer mixture was placed on the syringe holder of the compact syringe pump. The flow rate table attached on the pump shows flow rates depending on the volume of syringe expressed in ml/minute.

All batch and semi-continuous polymerizations were carried out at 25°C and 250 rpm.

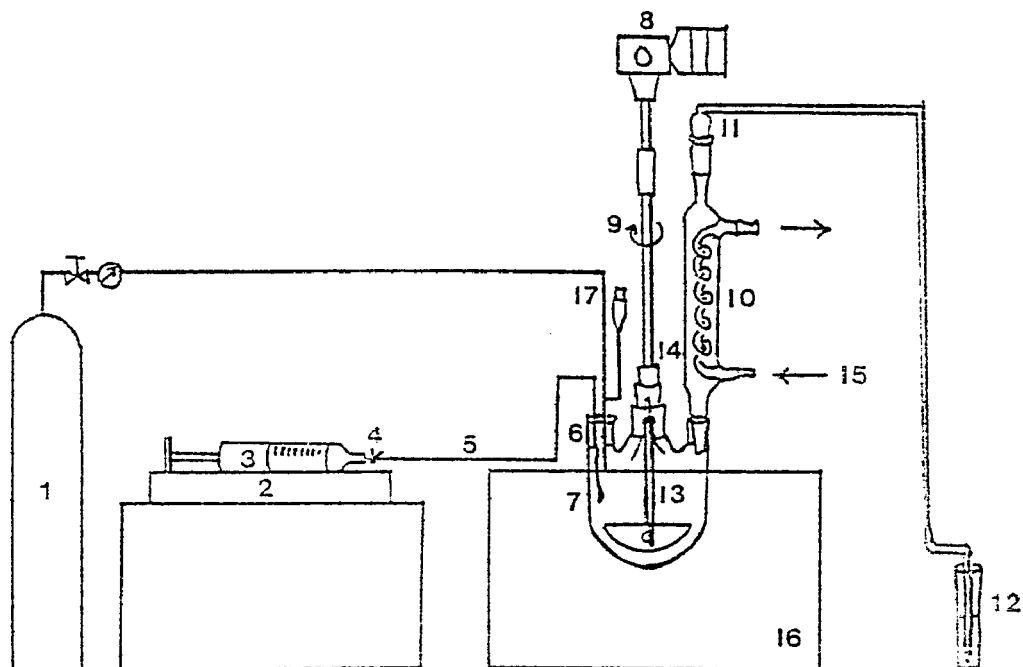
3.2 Experimental Recipes

3.2.1 Reagents

Vinylidene chloride (Dow Chemical Co.) was washed several times with 20 wt% aqueous NaOH solution to remove the inhibitor (200 ppm of methyl ether of hydroquinone) and fractionally distilled under nitrogen. The fraction distilled at 31.2°C was used immediately.

n-Butyl methacrylate (Rohm and Haas Co.) was washed several times with 10 wt% aqueous NaOH solution and deionized water, dried with anhydrous Na_2SO_4 , and finally distilled under vacuum at 57 mm Hg and nitrogen. The fraction distilled at 66°C was stored in a refrigerator prior to use.

Ammonium persulfate, sodium metabisulfite, and ferrous sulfate (Fisher Scientific Reagent Grades) were used as the oxidant, reductant, and activator, respectively, without further purification. Aerosol MA-80 (sodium dihexyl sulfosuccinate; American Cyanamid Co.) was used as emulsifier without further purification. Deionized water and nitrogen gas of zero grade (Union Carbide Co.) were used. The monomethyl ether of hydroquinone (Fisher Scientific



- | | |
|--------------------------------|----------------------------|
| 1. Nitrogen Cylinder | 10. Spiral Condenser |
| 2. Compact Syringe Pump | 11. Hose-Connector Adapter |
| 3. 100-ml Glass Syringe | 12. Test Tube |
| 4. 3-Way Stopcock | 13. Thermometer |
| 5. Teflon Tube | 14. Teflon Bearing Trubore |
| 6. Rubber Cock (3 Holes) | 15. -15°C of Coolant |
| 7. 4-necked Round-bottom Flask | 16. Water Bath (25°C) |
| 8. Variable Speed Motor | 17. Sampling Device |
| 9. Glass Stirrer | |

Figure 3-1: Schematic diagram of experimental apparatus.

Reagent Grade) was used as a shortstopper for the gravimetric determination of conversion during the polymerization.

Tetrahydrofuran (Fisher Scientific Reagent Grade) was used as the solvent in the determination of the molecular weight using gel permeation chromatography. All of the solvents used to test the solubility of VDC-BMA copolymer latex films were Reagent-Grade and were used without further purification.

For the surface characterizations of the latexes, standardized 0.02 N NaOH and HCl (Fisher Scientific Co.) were used as received.

3.2.2 Recipes

3.2.2.1 Batch Polymerizations

1) Poly(vinylidene chloride)

- Monomer: 80 g; VDC = 80 g; BMA = 0 g
- Emulsifier: 1.6%^{*}; Aerosol MA (80%) = 1.6 g
- Catalyst:

Activator: $\text{FeSO}_4 \cdot 7\text{H}_2\text{O} = 2.20 \times 10^{-3} \text{ g (0.0027\%}^*)$

Oxidant: $(\text{NH}_4)_2\text{S}_2\text{O}_8 = 0.28 \text{ g (0.35\%}^*)$

Reductant: $\text{Na}_2\text{S}_2\text{O}_5 = 0.28 \text{ g (0.35\%}^*)$

- H_2O : 152.0 g

* Based on total monomer weight (80 g)

Theoretical solids content: 35 wt%

Reaction temperature: 25°C

2) 83:17 molar ratio VDC-BMA emulsion polymerization (sample G)

- Monomer: 80 g; VDC = 61.6 g; BMA = 18.4 g

- Emulsifier: 1.6%^{*}; Aerosol MA (80%) = 1.6 g

- Catalyst:

Activator: $\text{FeSO}_4 \cdot 7\text{H}_2\text{O} = 2.20 \times 10^{-3} \text{ g (0.0027\%}^*)$

Oxidant: $(\text{NH}_4)_2\text{S}_2\text{O}_8 = 0.28 \text{ g (0.35\%}^*)$

Reductant: $\text{Na}_2\text{S}_2\text{O}_5 = 0.28 \text{ g (0.35\%}^*)$

- H_2O : 152.0 g

* Based on total monomer weight (80 g)

Theoretical solids content: 35 wt%

Reaction temperature: 25°C

3) 60:40 molar ratio VDC-BMA emulsion polymerization

- Monomer: 80 g; VDC = 40.0 g; BMA = 40.0 g

- Emulsifier: 1.6%^{*}; Aerosol MA (80%) = 1.6 g

- Catalyst:

Activator: $\text{FeSO}_4 \cdot 7\text{H}_2\text{O} = 2.20 \times 10^{-3} \text{ g (0.0027\%}^*)$

Oxidant: $(\text{NH}_4)_2\text{S}_2\text{O}_8 = 0.28 \text{ g (0.35\%}^*)$

Reductant: $\text{Na}_2\text{S}_2\text{O}_5 = 0.28 \text{ g (0.35\%}^*)$

- H_2O : 152.0 g

* Based on total monomer weight (80 g)

Theoretical solids content: 35 wt%

Reaction temperature: 25°C

4) 33:67 molar ratio VDC-BMA emulsion polymerization

- Monomer: 80 g; VDC = 20.0 g; BMA = 60.0 g

- Emulsifier: 1.6%^{*}; Aerosol MA (80%) = 1.6 g

- Catalyst:

Activator: $\text{FeSO}_4 \cdot 7\text{H}_2\text{O} = 2.20 \times 10^{-3} \text{ g (0.0027\%}^*)$

Oxidant: $(\text{NH}_4)_2\text{S}_2\text{O}_5 = 0.28 \text{ g (0.35\%*)}$

Reductant: $\text{Na}_2\text{S}_2\text{O}_5 = 0.28 \text{ g (0.35\%*)}$

▪ H_2O : 152.0 g

* Based on total monomer weight (80 g)

Theoretical solids content: 35 wt%

Reaction temperature: 25°C

5) Poly(butyl methacrylate)

▪ Monomer: 80 g; VDC = 0.0 g; BMA = 80.0 g

▪ Emulsifier: 1.6%*; Aerosol MA (80%) = 1.6 g

▪ Catalyst:

Activator: $\text{FeSO}_4 \cdot 7\text{H}_2\text{O} = 2.20 \times 10^{-3} \text{ g (0.0027\%*)}$

Oxidant: $(\text{NH}_4)_2\text{S}_2\text{O}_5 = 0.28 \text{ g (0.35\%*)}$

Reductant: $\text{Na}_2\text{S}_2\text{O}_5 = 0.28 \text{ g (0.35\%*)}$

▪ H_2O : 152.0 g

* Based on total monomer weight (80 g)

Theoretical solids content: 35 wt%

Reaction temperature: 25°C

3.2.2.2 Seeded Semi-continuous Polymerizations

1) 83:17 molar ratio VDC-BMA emulsion polymerization

▪ Monomer: 80 g; VDC = 61.6 g; BMA = 18.4 g

Monomer for seeding: 10.0 wt%* = 8.0 g; VDC = 4.0 g; BMA = 4.0 g

Monomer for addition: 90.0 wt%* = 72.0 g; VDC = 57.6 g; BMA = 14.4

g

▪ Emulsifier: 1.6 wt%*; Aerosol MA (80%) = 1.6 g

▪ Catalyst:

Activator: $\text{FeSO}_4 \cdot 7\text{H}_2\text{O} = 2.20 \times 10^{-3} \text{ g (0.0027\%*)}$

Oxidant: $(\text{NH}_4)_2\text{S}_2\text{O}_5 = 0.28 \text{ g (0.35\%*)}$

Reductant: $\text{Na}_2\text{S}_2\text{O}_5 = 0.28 \text{ g (0.35\%*)}$

▪ H_2O : 152.0 g

* Based on total monomer weight (80 g)

Theoretical solids content: 35 wt%

Reaction temperature: 25°C

The monomer feed rates used in the 83:17 VDC-BMA semi-continuous polymerizations were varied in the range of 0.27 - 1.10 wt%/minute as shown in Table 3.1.

Table 3-1: 83:17 VDC-BMA emulsion polymerizations.

SAMPLES	MONOMER FEED RATE	
	Wt%/Min	$\text{mol} \cdot \text{l}^{-1} \cdot \text{sec}^{-1} (\times 10^4)$
A	0.27	1.40
B	0.39	2.06
C	0.55	2.89
D	0.79	4.12
E	1.10	5.77
F	SEEDED BATCH	

2) 60:40 molar ratio VDC-BMA emulsion polymerization

▪ Monomer: 80 g; VDC = 40.0 g; BMA = 40.0 g

Monomer for seeding: 10.0 wt%* = 8.0 g; VDC = 4.0 g; BMA = 4.0 g

Monomer for addition: 90.0 wt%* = 72.0 g; VDC = 36.0 g; BMA = 36.0

- Emulsifier: 1.6 wt%^{*}; Aerosol MA (80%) = 1.6 g

- Catalyst:

Activator: $\text{FeSO}_4 \cdot 7\text{H}_2\text{O} = 2.20 \times 10^{-3} \text{ g (0.0027\%}^*)$

Oxidant: $(\text{NH}_4)_2\text{S}_2\text{O}_8 = 0.28 \text{ g (0.35\%}^*)$

Reductant: $\text{Na}_2\text{S}_2\text{O}_5 = 0.28 \text{ g (0.35\%}^*)$

- H_2O : 152.0 g

* Based on total monomer weight (80 g)

Theoretical solids content: 35 wt%

Reaction temperature: 25°C

Monomer feed rate: 0.27 wt%/minute

3) 33:67 molar ratio VDC-BMA emulsion polymerization

- Monomer: 80 g; VDC = 20.0 g; BMA = 60.0 g

Monomer for seeding: 10.0 wt%^{*} = 8.0 g; VDC = 4.0 g; BMA = 4.0 g

Monomer for addition: 90.0 wt%^{*} = 72.0 g; VDC = 16.0 g; BMA = 56.0

g

- Emulsifier: 1.6 wt%^{*}; Aerosol MA (80%) = 1.6 g

- Catalyst:

Activator: $\text{FeSO}_4 \cdot 7\text{H}_2\text{O} = 2.20 \times 10^{-3} \text{ g (0.0027\%}^*)$

Oxidant: $(\text{NH}_4)_2\text{S}_2\text{O}_8 = 0.28 \text{ g (0.35\%}^*)$

Reductant: $\text{Na}_2\text{S}_2\text{O}_5 = 0.28 \text{ g (0.35\%}^*)$

- H_2O : 152.0 g

* Based on total monomer weight (80 g)

Theoretical solids content: 35 wt%

Reaction temperature: 25°C

Monomer feed rate: 0.27 wt%/minute

3.2.3 Experimental Procedure

3.2.3.1 Batch Polymerizations

- 1) The constant-temperature water bath was first adjusted to 25°C.
- 2) A 500-ml four-necked round-bottom flask was placed in the water bath, adjusted, and clamped in a convenient position. The stirrer speed was adjusted to 250 rpm using stroboscopy, and the balance of the apparatus was set up according to Figure 3.1, but without the feeding stream from the syringe pump.
- 3) -15°C ethylene glycol coolant was circulated through the spiral reflux condenser in the sideneck of the flask.
- 4) Prior to the start of polymerization, 134.4 ml deionized water, and 1.6 g emulsifier were charged to the reactor, and the dissolved oxygen was removed by bubbling nitrogen gas through the solution for 30 minutes.
- 5) The monomer mixture was charged to the reactor using the 100 ml syringe with the two-way stopcock and emulsified under nitrogen.
- 6) After 15 minutes, 1.6 ml activator solution of 0.14 wt% $\text{FeSO}_4 \cdot 7\text{H}_2\text{O}$ and 8 ml oxidant solution of 3.5 wt% $(\text{NH}_4)_2\text{S}_2\text{O}_8$, which were freshly made just prior to the start of polymerization, were injected into the reactor using disposable plastic syringes.
- 7) After 5 minutes, 8 ml reductant solution of 3.5 wt% $\text{Na}_2\text{S}_2\text{O}_5$ was added using a disposable plastic syringe, and the polymerization began within one minute, with the appearance of an exothermic reaction; the maximum reaction temperature found was 26.9°C. The polymerization was allowed to proceed until the conversion reached almost 100%.
- 8) The latex obtained was filtered through glass wool, cooled, and stored at room temperature.

3.2.3.2 Semi-continuous Polymerizations

A. Preparation of Seed Latex

- 1) The constant-temperature water bath was first adjusted to 25°C.
- 2) A 500-ml four-neck round-bottom flask was placed in the water bath, adjusted, and clamped in a convenient position. The stirrer speed was adjusted to 250 rpm using stroboscopy, and the balance of the apparatus was set up according to the Figure 3.1.
- 3) -15°C ethylene glycol coolant was circulated through the spiral reflux condenser in a sideneck of the flask.
- 4) Prior to the start of the polymerization, 134.4 ml deionized water, and 1.6 g emulsifier were charged to the reactor, and the dissolved oxygen was removed by bubbling nitrogen gas through the solution for about 30 minutes.
- 5) 10 wt% of the monomer mixture (VDC = 4.0 g; BMA = 4.0 g) based on total monomer weight was added into the reactor using syringe and was emulsified under nitrogen.
- 6) After 15 minutes, 1.6 ml activator solution of 0.14 wt% $\text{FeSO}_4 \cdot 7\text{H}_2\text{O}$ and 8 ml oxidant solution of 3.5 wt% $(\text{NH}_4)_2\text{S}_2\text{O}_8$, which were freshly made, were added to the reactor using disposable plastic syringes.
- 7) After 5 minutes, 8 ml reductant solution of 3.5 wt% $\text{Na}_2\text{S}_2\text{O}_5$ was added using a disposable plastic syringe, and the polymerization began within one minute; the temperature increased to a maximum of 26.0°C, and then decreased to 25°C. The exothermic reaction was completed within 30 minutes.
- 8) After the exothermic reaction was completed, the seed latex was allowed to stay for 20 minutes at 25°C to complete its formation.

B. Addition of Monomer Mixture

1) The rest of the monomer mixture (72.0 g) was purged with pure nitrogen, and placed into the 100-ml glass syringe. The syringe was connected to the Teflon tubing with the two-way Teflon valve.

2) The 100-ml syringe with 72.0 g of monomer mixture was placed on the syringe holder of the syringe pump and fixed into position with the spring clamp.

3) The Teflon tubing was carefully filled with monomer by using the flow selector at a fast flow rate. The flow was stopped, and the flow selector was positioned at the preselected flow rate.

4) The monomer mixture was added continuously to the reactor containing the seed latex at 25°C and 250 rpm. The flow time was counted beginning with the first drop of the monomer into the reactor. The polymerization proceeded with the usual exothermic reaction.

5) When the desired amount of the monomer mixture was added, the monomer addition procedure was stopped, and the polymerization was allowed to proceed for an additional four hours to complete the reaction.

6) The latex was filtered through glass wool, cooled, and stored at room temperature.

3.3 Conversion Measurement

After the polymerization was started, 1-2 ml of the reaction mixture was sampled through the Teflon stopcock into a small polyethylene vial with rubber cap using a disposable plastic syringe at appropriate intervals throughout the polymerization. The sample weight was measured by weighing the polyethylene vial with rubber cap before and after addition of the latex. The latex was placed in a tared aluminum weighing dish along with three drops of shortstop

solution (0.06 g monomethyl ether of hydroquinone in 20 ml isopropanol) and dried in an oven at 70°C overnight. The percent solids and percent conversion of each sample were determined gravimetrically from the dried sample weights based on the total amount of monomer in the recipe.

$$\text{Solids Content}(\%) = (A_2 - A_1)/(V_2 - V_1) \times 100 \quad (3.1)$$

$$\text{Conversion } \% = (\text{Experimental Solids Content} / \text{Theoretical Solids Content}) \times 100 \quad (3.2)$$

where V_1 = Weight of polyethylene vial with rubber cap

V_2 = Weight of polyethylene vial with rubber cap and wet latex sample

A_1 = Weight of aluminum weighing dish

A_2 = Weight of aluminum weighing dish and dried latex sample

3.3.1 Instantaneous Conversion, X_t Measurement

The instantaneous conversion at a given time during the course of polymerization was determined from the ratio of the amount of the polymer formed to the total amount of monomer added up to that time (excluding polymer formed in the seeding reaction).

3.3.2 Conversion X_t at time t, Measurement

The conversion at time t was determined by the calculation of the ratio of the amount of polymer formed to the total amount of monomer added up to the time t (including the amount of monomer in the seeding reaction).

3.3.3 Monomer Concentration, $[M_p]$ in the Latex Particles

The monomer concentration in latex particles at a given time was determined from the ratio of the moles of unreacted monomer at that time (corrected for the water solubility of vinylidene chloride monomer) to the volume of both polymer and monomer phases at that time, assuming that the monomer and polymer volumes are additive.

3.4 Characterization of the Latexes and Latex Films

3.4.1 Particle Size Measurements

The transmission electron micrographs of the latexes were taken using a Philips 300 transmission electron microscope. A drop of latex with a concentration of 1-3% was placed on a carbon-coated Formvar electron microscope grid, and most of the drop was removed by contacting it with filter paper. The sample was then stained with 2% phosphotungstic acid to improve the contrast. The transmission electron micrographs of the latex were taken at room temperature. In order to calibrate the magnification of the electron microscope, a micrograph of a carbon replica of a diffraction grating was taken at the same setting as that used for the latex particles. The diameter of the latex particles was measured by using a Carl Zeiss Mop-3 instrument. A computer program was used to determine the weight-average and number-average particle diameters, as well as particle size distribution. The polydispersity index (PDI) was calculated using the formula:

$$PDI = D_w / D_n \quad (3.3)$$

$$D_w = (\sum n_i D_i^4) / (\sum n_i D_i^3) \quad (3.4)$$

$$D_n = (\sum n_i D_i) / (\sum n_i) \quad (3.5)$$

Where n_i = the number of particles having a diameter of D_i

D_w = the weight-average particle diameter

D_n = the number-average particle diameter

3.4.2 Infrared Spectroscopy

Poly(vinylidene chloride) and its copolymers containing a high proportion of vinylidene chloride are known to be crystalline. The infrared spectrum of poly(vinylidene chloride) in the 100-3600 cm^{-1} region is shown in Figure 3.2. The assignments for the principal bands made by Krimm and Liang (54) are given in Table 3.2.

Narita et al. (55, 56) reported that the 887, 753, 655, 600, 565, and 450 cm^{-1} bands of poly(vinylidene chloride) become very weak in the amorphous state, as shown in Figure 3.3, and the strong doublet at 1046 and 1070 cm^{-1} is a characteristic feature of poly(vinylidene chloride) as well as its copolymers. Especially, the bands at 887 and 753 cm^{-1} are crystallization-sensitive bands. They also reported that the doublet at 1070 and 1048 cm^{-1} in vinylidene chloride-vinyl chloride copolymers loses its identity when the vinyl chloride concentration reaches approximately 50%; at this concentration, a single peak with the maximum at about 1070 cm^{-1} and a shoulder at 1048 cm^{-1} replaces the doublet, signifying amorphous polymer. It is also known (57, 58) that the 1070 cm^{-1} band is stronger than that at 1048 cm^{-1} in the spectrum of unoriented samples, whereas the intensities are reversed in oriented samples.

In the present studies, Fourier-transform infrared spectroscopy (Mattson Instruments Inc, Sirius 100) was employed to determine the crystallinity of the VDC-BMA copolymers prepared by both batch and semi-continuous polymerizations. Films dried from the VDC-BMA copolymer latexes on glass plates or photographic paper described in the literature (59, 60) were used as

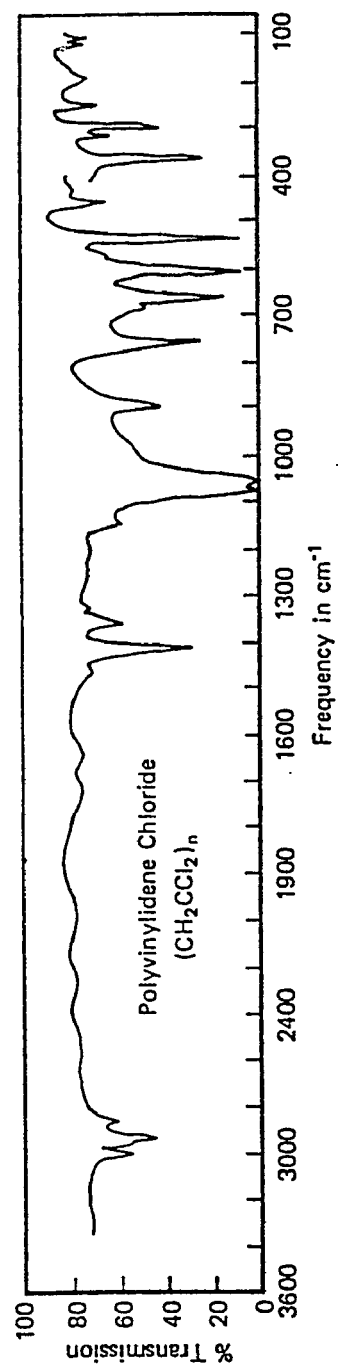


Figure 3-2: Infrared spectrum of poly(vinylidene chloride).

Table 3-2: Assignment of infrared spectrum bands in poly(vinylidene chloride).

Frequency, cm ⁻¹	Wavelength, μ	Polarization	Intensity	Probable group assignment
2990	3.34	\perp	w	CH ₂
2948	3.39	\perp	vw	CH ₂
2930	3.41	\perp	mw	CH ₂
2850	3.51	\perp	w	CH ₂
1460	6.85	\perp	vw	CH ₂
1407	7.11	\perp	m	CH ₂
1360	7.35	\parallel	m	CH ₂
1325	7.55	\perp	w	CH ₂
1142	8.76	\parallel	m	Skeletal
1070	9.35	\perp	vs	Skeletal + CCl ₂
1046	9.56	\perp	vs	Skeletal + CCl ₂
980	10.20	\perp	w	CCl ₂
887	11.27	\perp	m	Skeletal
778	12.85	\perp	vw	CH ₂
754	13.26	\perp	m	CCl ₂
657	15.22	\perp	m	CCl ₂
603	16.58	\perp	s	CCl ₂

* Key: vs, very strong; s, strong; m, medium; mw, medium weak; w, weak; vw, very weak.

specimens in the infrared spectroscopy. Poly(vinylidene chloride) was scanned as a KBr pellet.

3.4.3 Minimum Film Forming Temperature (MFFT)

The minimum film-forming temperature (61) is defined as the minimum temperature at which the polymer latex forms a continuous film upon drying. This minimum film-forming temperature is important for coatings to show sufficient coalescence of the polymer particles to achieve continuity in the film and adhesion to the surface. The minimum film-forming temperature is always found to be lower than the T_g of the polymer. In the present study, the

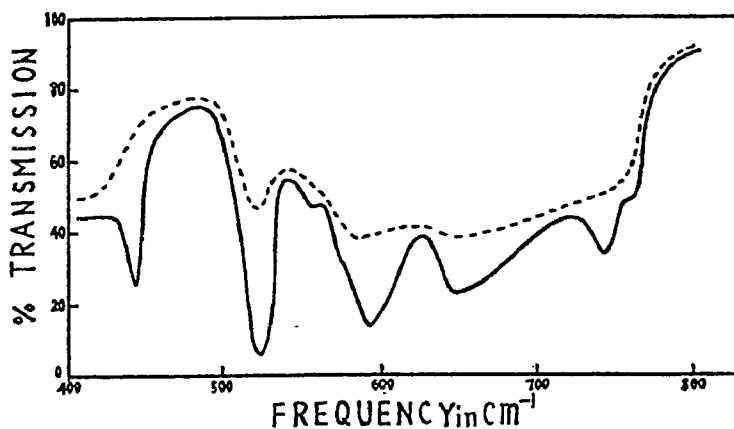


Figure 3-3: Infrared spectrum of molten VDC-VC (vinyl chloride) copolymer containing high amount of VDC; (--)160°C, (—)Room temperature.

minimum film-forming temperature apparatus (Sheen Instrument Co.) was employed to determine the minimum film-forming temperature of the VDC-BMA copolymer latexes.

The test procedure used was as follows:

- 1) After thermal equilibrium was reached on the copper slab, 1-2 ml of 35%-solids latex was placed on the test strip with an eyedropper.
- 2) The latex was spread uniformly along the test strip with a Plexiglas spreader.
- 3) The glass cover was placed over the test slab.
- 4) The latex was observed periodically until dry.

The point at which the film became discontinuous was noted and recorded. The reported minimum film-forming temperature values in present study were average values of at least three measurements.

3.4.4 T_g and T_m Measurements

The T_g (glass transition temperature) and T_m (crystalline melting temperature) of the VDC-BMA latex copolymers were determined using the Du Pont-1090, and Perkin-Elmer Model DSC-1B differential scanning calorimeters. Indium which has a melting point of 429°K was used as a reference. The latexes were dried at room temperature to form films of about 1 mm thickness, which were heat-treated for 30 minutes at 70°C before use as the specimens for T_g and T_m measurements. About 5 mg of sample was placed in an aluminum sample pan and sealed with an aluminum cover. In some T_g measurements, liquid nitrogen was used to lower the sample temperature to 233°K; then the temperature was increased at a rate of 20°C/minute. The T_g was taken as the temperature of the first inflection point, which was recorded automatically. The T_m was taken as the temperature of the endotherm peak.

3.4.5 Determination of Percent Crystallinity (62)

The percent crystallinities of the VDC-BMA copolymers, as well as poly(vinylidene chloride), were determined from the heat of fusion using DSC at a heating rate of 20°C/minute. The heat of fusion of the polymer sample was determined using the latent heat of fusion of indium as a reference. The areas of the endotherm peaks were determined by using a Carl Zeiss Mop-3 instrument. The heats of fusion of the copolymers were calculated using the following equations (63).

$$\Delta H_{\text{polymer}} = (\Delta H_{\text{In}} \times \text{Area}_{\text{polymer}} \times \text{Standard Sample Weight}_{\text{In}}) / (\text{Area}_{\text{In}} \times \text{Polymer Sample Weight}) \quad (3.6)$$

The percent crystallinities of the polymers were determined by

$$\% \text{ CRYSTALLINITY} = \Delta H_{\text{polymer sample}} / \Delta H^* \quad (3.7)$$

where ΔH^* is the heat of fusion of 100% crystalline poly(vinylidene chloride), 1500 cal/mol (9).

3.4.6 X-ray Powder Diffraction

X-ray studies of poly(vinylidene chloride) showed that the polymer becomes amorphous when it is molten and quenched but recrystallizes when kept at room temperature (64). Okuda et al. (65) have indexed some of the important reflections in both poly(vinylidene chloride) and its copolymers with vinyl chloride (VC), and found that d-spacings calculated for the copolymers were the same as those of poly(vinylidene chloride) as shown in Table 3.3, indicating that the structure of poly(vinylidene chloride) is retained in the copolymers.

Table 3-3: d-Spacings of VDC-VC Copolymers.

Composition (molar fraction of VDC)	Observed spacings, Å						
	Lattices of the plane						
	100 + $\bar{1}02$	002	$\bar{1}04$	200 + $\bar{2}04$	$\bar{1}05$ + $\bar{2}05$	005 + $\bar{3}05$	020
1.000 (PVDC)	5.61	5.35	3.11	2.804	2.440	2.081	2.343
0.905	5.61	5.28	3.10	2.804	2.440	2.089	2.343
0.820	5.63	5.28	3.11	2.809	2.443	2.086	2.343
0.745	5.61	5.28	3.11	2.809	2.443	2.086	2.343
0.685	5.63	5.28	3.11	2.809	2.450	2.089	2.350
0.603	5.63		3.13	2.809	2.450	2.089	2.343
0.560	5.57			2.809			2.350

In the present study, X-ray powder diffraction patterns of PVDC and the VDC-BMA copolymers prepared by both batch and semi-continuous polymerizations, and heat-treated at 70°C for 30 minutes were obtained with a Philips Automated X-ray powder diffractometer using Ni-filtered $\text{CuK}\alpha$ radiation; Debye-Scherrer ring patterns of these polymers were also taken.

3.4.7 Solubility (66)

Poly(vinylidene chloride) is insoluble in most common solvents at ambient temperature because of its high crystallinity and high melting temperature. It dissolves readily, however, in a wide variety of solvents at temperatures above 130°C. Copolymers with a high enough vinylidene chloride content to be crystalline behave in a manner similar to that of poly(vinylidene chloride). They are more soluble, however, because of their lower melting temperatures. The solubility of copolymers which are amorphous is much higher. Table 3.4 lists some of the more common solvents for Saran copolymers. Saran is a generic name for high VDC-content copolymers with vinyl chloride (VC), acrylonitrile (AN), or various alkyl acrylates. Solvents that dissolve poly(vinylidene chloride) generally dissolve the copolymers, but at lower temperatures.

Table 3-4: Common Solvents of Saran Copolymers (67).

Solvent	Copolymer type	Range °C
Tetrahydrofuran (THF)	All	<60
Methyl ethyl ketone (MEK)	Low crystallinity polymers	<80
1,4-dioxane	All	50-100
Cyclohexanone	All	50-100
Cyclopentanone	All	50-100
Ethyl acetate	Low crystallinity polymers	<80
Chlorobenzene	All	100-130
Dichlorobenzene	All	100-140
Dimethyl formamide (DMF)	High acrylonitrile (AN)	<100

In the present study, 0.2 g VDC-BMA latex film samples before and after heat treatment at 70°C for 30 minutes were placed in 3 ml of various common solvents at room temperature and the solubility was observed.

3.4.8 Dynamic Mechanical Spectroscopy (68)

Latex samples were dried at 50°C in small plastic petri dishes to give films of 4 mm thickness. The plastic petri dishes used for film formation of the latexes were pretreated with Parafilm (Price-Driscoll Co.) mold release agent. The films were aged at room temperature for 120 days to ensure that the further gradual coalescence and crystallinity were complete. The film was cut into 40×6×4 mm specimens for dynamic mechanical spectroscopy. The storage modulus (E'), loss modulus (E''), and loss tangent (δ) were measured using a Rheovibron Viscoelastomer Model DDV-II (Toyo Measuring Instrument Co.). Liquid nitrogen was used to decrease the testing temperature. The temperature range employed ranged from -25° to 100°C, the heating rate was 1°C/minute, and the frequency was 110 Hz. The T_g values for all films were determined from the peak of the loss modulus spectrum.

3.4.9 Tensile Properties

Tensile measurements of the VDC-BMA latex films were carried out at room temperature using the Instron (Instron Engineering Corp.). The latex samples were dried at 50°C in small plastic petri dishes to give films of 3 mm thickness. The plastic petri dishes used for the film formation of latexes were pretreated with Parafilm mold release agent. The films were aged at room temperature for 120 days to ensure that the further gradual coalescence and crystallization were complete. The films were cut to the size as described in ASTM D-1708 (for tensile measurements) using the microtensile specimen cutter. A crosshead speed of 0.5 inch/minute was found most suitable to cover the entire range of compositions of the copolymers. The Young's modulus (E) was determined from the initial slope of the stress-strain curves, and the energy to

break (σ) was determined from the area under the stress-strain curves. The ultimate strength (σ_u) and percent elongation were also determined

3.4.10 Water Vapor Transmission Rate Measurements (WVTR)

Vinylidene chloride copolymers as well as poly(vinylidene chloride) are less permeable to a wide variety of gases and liquids than other polymers, which is one of their most valuable properties. This is a consequence of the combination of high density and high crystallinity in the polymers. An increase in either tends to reduce the permeability (69). Table 3.5 shows the WVTR values of polymer films, including Saran-type polymers (70).

In the present study, the films were prepared using the photographic paper method (59), which produces thin latex films with smooth surfaces as thin as 1 mil. 1-2 ml of 35%-solids latex was placed on the photographic paper using an eyedropper, spread uniformly on the paper with a Plexiglas spreader, and dried at 70°C in a drying oven. After the film was dried, the photographic paper was soaked in water to dissolve the gelatin, and the film was peeled from the paper. The film was washed with a large volume of water to remove the gelatin and dried at room temperature. The film thicknesses were measured to within 1 mil using a Starret Micrometer with subdivisions of 0.01 mm. Glass vials (10×60 mm; 2 dram; Kimble Co.) were used as cells for the water vapor transmission rate study (71). A hole of diameter equal to the inside diameter of the vial lip (9.4 mm) was drilled in the center of the cap and rubber gasket. The rubber gasket and the threads on the vial lip were lightly coated with silicone vacuum grease (Dow Corning Co.), and the film was carefully placed between them. The cap was gently screwed on the vial until it touched the film. A slight pressure was applied to obtain a seal. For the WVTR determinations, the cell was

Table 3-5: Water transmission rates of Polymer films.

(gm-mil/cm ² -min)	
Sample	Rate *
Saran Type M ^a	1.2×10^{-7}
Saran Type M recast ^a	8.4×10^{-8}
Saran B-115 ^a	1.3×10^{-7}
Saran B-118 ^a	2.6×10^{-7}
Saran B-130 ^a	3.1×10^{-7}
Saran F-120 ^a	1.4×10^{-7}
92:8 VeCl ₂ -VCl ^b	1.2×10^{-7}
80:20 VeCl ₂ -VCl	1.9×10^{-7}
66:34 VeCl ₂ -VCl	5.4×10^{-7}
60:40 VeCl ₂ -VCl	6.0×10^{-7}
50:50 VeCl ₂ -VCl	6.1×10^{-7}
92:8 VeCl ₂ -VCN ^b	6.8×10^{-7}
80:20 VeCl ₂ -VCN	1.7×10^{-7}
75-80:10:10-15 VeCl ₂ -VCN-VCl	2.3×10^{-7}
70:30 VeCl ₂ -IB ^b	7.2×10^{-7}
81:19 VeCl ₂ -VCN	1.5×10^{-8}
Saran ^a	$4.0-5.2 \times 10^{-10}$
PVeCl ₂	$0.7-4.8 \times 10^{-9}$
PVeCl ₂	3.8×10^{-9}
amorphous PVeCl ₂	9.5×10^{-8}
PMMA ^b	1.8×10^{-5}
PMMA	4.8×10^{-6}
PB ^b	2.1×10^{-5}
cis-PB	5.6×10^{-5}
24:76 S-B ^b (standard SBR) ^b	2.8×10^{-5}
39:61 S-B (Synpol 8401 high-styrene SBR)	1.4×10^{-5}
90:10 S-B	1.8×10^{-5}
Styroflex A & B ^c PS ^b	1.9×10^{-6}
PS	$1.6-1.7 \times 10^{-6}$

^aThe Dow Chemical Company.

^bVeCl₂: vinylidene chloride; VCl: vinyl chloride; VCN: acrylonitrile; IB: isobutylene; PMMA: polymethyl methacrylate; PB: polybutadiene; S: styrene; B: butadiene; SBR: styrene-butadiene rubber; PS: polystyrene.

^cD. Seekabelwerke.

* References given in (70)

filled with 4 ml of water, and the film was placed in position as described above. The experiments were carried out at 72°F and 50% relative humidity by a Honeywell 60 controller under static air conditions. The weight loss was measured as a function of time. The experiments were continued until the value of the WVTR reached a constant value.

3.4.11 Molecular Weight Determination

The molecular weights of the polymers were determined by gel permeation chromatography (GPC) using a Waters Associates 201A instrument coupled to a differential refractometer detector. The measurements were performed at ambient temperature using nonaqueous Microstyrogel Columns (pore sizes 10^3 , 10^4 , 10^5 , and 10^6 Å² units) and tetrahydrofuran (THF) as the solvent. Monodisperse polystyrene samples with the molecular weights of 4,000, 17,500, 35,000, 128,000, 390,000, 770,000, 3,000,000 were used as references. The standard polystyrene had a concentration of 0.2 % in THF; the flow rate was 1.2 ml/minute, and the sample size was 0.1 ml.

To recover the polymer, the latexes were frozen, and the coagulated polymer was washed with deionized water, filtered, dried, dissolved in THF, precipitated in 50:50 vol% water-methanol mixture, filtered, washed, and dried under vacuum at room temperature. The purified polymer sample was then dissolved in THF at a concentration of 0.1 wt%. Before injection into the sampling loop, each sample was filtered to remove any particulates. The sample injection volume was 0.2 ml. A computer program was used to calculate the number-average and weight-average molecular weights, as well as the molecular weight distributions.

3.4.12 Latex Cleaning and Surface Characterization (72-74)

The latexes were cleaned with distilled-deionized-water (DDI) using serum replacement and characterized by conductometric titration (73, 74). The latex samples were diluted to 2.5-3.0% solids with DDI-water and placed in the serum replacement cell equipped with 0.1 or 0.2 μ m-diameter Nuclepore membrane. The capacity of the cell was 400 ml; filtration membrane diameter was 76 mm. DDI-water was fed into the cell from a water reservoir positioned above the cell, and the diluted serum or filtrate was collected from the bottom while the latex was agitated continuously by the stirring bar. This process was continued until the conductance of the filtrate was about the same as that of the feed water, to remove adsorbed emulsifier from the latex particle surface as well as solute emulsifier, residual initiator, and their decomposition products from the aqueous phase. The cleaned latex was treated with about 1 gal of 10^{-5} N hydrochloric acid to replace the Na^+ and NH_4^+ ions by H^+ ions, and was again washed with DDI-water until the conductance of the filtrate was about the same as that of the feed water. Generally, 1-2 weeks were required for the complete serum replacement process. After cleaning the latex, the monodisperse latexes displayed their characteristic interference colors.

In order to determine the number of surface strong acid and weak acid groups, the cleaned latexes were titrated conductometrically. An amount of latex containing about 1 g solids was weighed into a 250 ml beaker, diluted to 200 ml with DDI-water, and titrated under nitrogen using 0.02 N standard sodium hydroxide. The sodium hydroxide solution was added continuously using an automatic constant-rate burette (Sargent Welch Instrument Co.). The conductance was recorded continuously using the conductivity meter, and the

endpoints for the strong acid and weak acid groups were determined from the intersections of the extrapolated linear portions of the ascending and descending legs of the titration curves. The samples were back-titrated with 0.02 N standard hydrochloric acid to check the concentration of weak acid groups, as shown in Figure 3.4.

3.4.13 Determination of Copolymerization Reactivity Ratios in VDC-BMA Emulsion Polymerization (75, 76)

In order to determine the copolymerization reactivity ratios in VDC-BMA emulsion polymerization, Six pairs of monomer mixtures over the entire range of compositions were prepared as described in Table 4.1 and polymerized using the same recipe and the same polymerization conditions as those described in sections 3.2.2.1 and 3.2.3.1. The polymerizations were shortstopped at about 5 % conversion by adding a shortstopper solution, and the samples were poured in cold methanol to precipitate the polymer, which was washed with a large volume of the 50:50 vol% methanol-water mixture, and dried under vacuum at room temperature. The dried copolymers were analysed for the C, H, and Cl content using the combustion method (from Robertson Laboratory) to determine the monomer compositions in copolymers.

The copolymerization reactivity ratios were determined using the Lewis-Mayo equation (77) and the compositions of the copolymers.

$$r_2 = r_1 H^2 / h + H(1 - h) / h \quad (3.8)$$

$$h = d[M_1] / d[M_2] \quad (3.9)$$

$$H = M_1 / M_2 \quad (3.10)$$

where r_1 and r_2 are the reactivity ratios, h is the mole ratio of VDC to BMA in the copolymer, and H is the same ratio in the monomer.

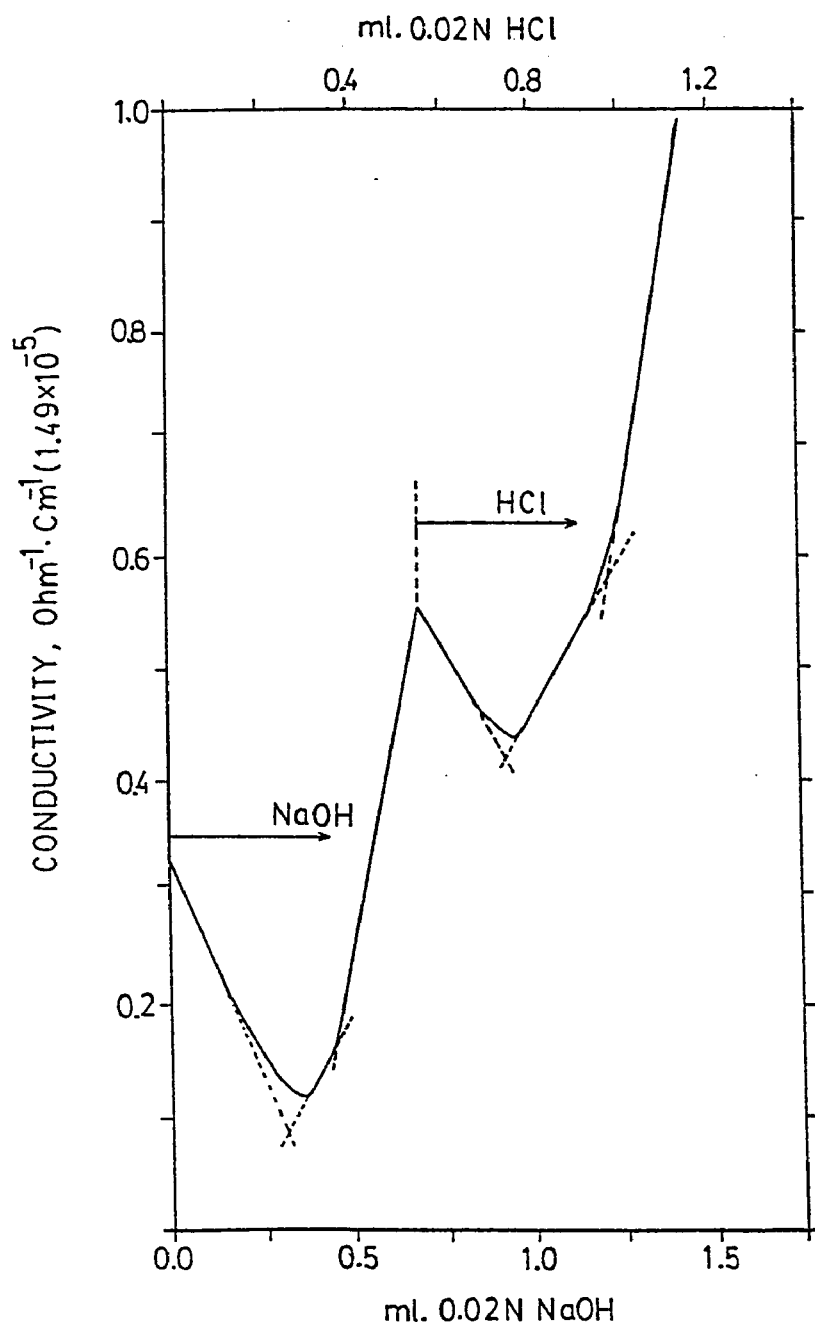


Figure 3-4: Conductometric titration of cleaned 83:17 VDC-BMA latex prepared by batch polymerization.

3.4.14 Nuclear Magnetic Resonance Spectroscopy

3.4.14.1 Carbon-13 NMR Spectroscopy

The 50.32 MHz ^{13}C NMR spectrum of the 83:17 VDC-BMA copolymer prepared by semi-continuous polymerization was obtained at 50°C using a Bruker WP200 spectrometer. A 20 wt% sample in deuterated nitrobenzene in a 10-mm diameter tube was used to reduce the total scan time and improve the signal-to-noise ratio. The sweep width of the spectrometer was 16000 Hz, and a pulse width of 6 microseconds (corresponding to a 45° pulse angle) was chosen. 16384 data points were taken. A pulse delay of 10 seconds and gated decoupling were used to suppress the Nuclear Overhauser Enhancements (NOE) for quantitative measurements.

3.4.14.2 Solid-State NMR Spectroscopy

Solid-state NMR experiments were performed using a General Electric NMR Instrument GN-300 spectrometer operating at 75.4 MHz for Carbon-13 at room temperature. The standard cross polarization Magic Angle Sample Spinning (CP/MASS) with spinning speeds of greater than five hundred Hz were typical. The maximum ^{13}C and ^1H RF field strengths were approximately 35 and 60 KHz, respectively. The CP contact time was 1 millisecond with a recycle delay of 6 seconds. For one-pulse experiments, the recycle delay was 30 seconds. Overnight accumulations of approximately 10,000 (CP/MASS) and 2,000 (one-pulse) transients were obtained. The sample volume was approximately 0.35 ml in a Doty Scientific, Inc., spinning assembly in a homemade probe. Deuterated benzene-swollen samples containing 50 wt% solvent were used. Acquisition times were approximately 40 milliseconds (CP/MASS) and 80 milliseconds (one-pulse).

Chapter 4

RESULTS AND DISCUSSION

4.1 Reactivity Ratios of VDC-BMA in Emulsion

Copolymerization

The reactivity ratios of VDC and BMA in emulsion copolymerization were determined by elemental analysis method, using the method of Lewis and Mayo described in section 3.4.14. The results are shown in Table 4.1.

Table 4-1: Emulsion copolymerization of VDC (M_1) and BMA (M_2).

SAMPLE No.	MONOMER(mol%)		C, H, Cl wt% in POLYMER*			POLYMER(mol%)	
	M_1	M_2		C	H	Cl	$d(M_1)$ $d(M_2)$
1	96.53	3.47	E	37.96	4.22	50.87	77.05 22.95
			T	37.75	4.43	50.87	
2	80.39	19.61	E			33.04	54.64 45.36
			T			33.04	
3	64.15	35.85	E	55.14	7.89	21.02	37.09 62.91
			T	55.29	7.62	21.02	
4	54.50	45.50	E	57.61	8.38	16.92	30.17 69.83
			T	57.84	8.08	16.92	
5	38.55	61.45	E			10.11	19.00 81.00
			T			10.11	
6	20.53	79.47	E			4.73	9.18 90.82
			T			4.73	

* determined by elemental analysis
 E = experimental value
 T = calculated value

The calculated values of the proportions of C and H in the copolymers, based on the %Cl determined by elemental analysis, agreed well with the experimentally determined values. The reactivity ratios determined in the present study were $r_1 = 0.22$ and $r_2 = 2.41$, as shown in Figure 4.1, in which r_1 was derived from the slope of the curve, and r_2 from the intercept on Y-axis.

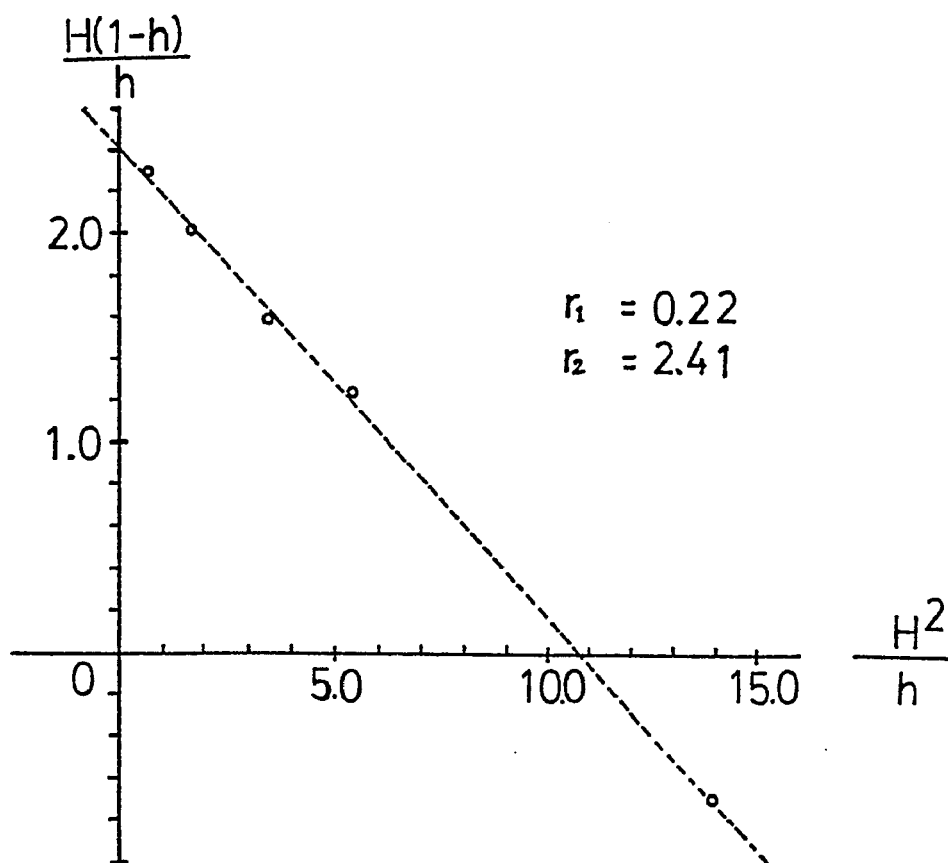


Figure 4-1: Reactivity ratios determined by Lewis and Mayo equation.

Therefore, in batch polymerization, the copolymer composition will drift with conversion, resulting in BMA-rich copolymers at the beginning and VDC-rich copolymers at the end of the copolymerization.

Table 4-2: Reactivity ratios in VDC-BMA copolymerizations.

r_1	r_2	CONDITIONS
0.22	2.41	25°C, Emulsion
0.35	2.20	68°C, Bulk (75)
0.35	2.80	From Q and e values

The reactivity ratios determined in this study agreed well with the values reported for bulk polymerization at 68°C (75), as shown in Table 4.2, indicating that the emulsion copolymerization of VDC-BMA takes place mostly in monomer-polymer particles rather than in the aqueous phase. The monomer reactivity ratios calculated from the Q and e parameters (8) were also similar to the values determined experimentally.

4.2 Syntheses of 83:17 VDC-BMA Emulsion Copolymers by Batch and Semi-Continuous Polymerization

4.2.1 Kinetics

Seven 83:17 mol% VDC-BMA copolymer latexes A to G were prepared by both batch and seeded semi-continuous polymerization using the recipes and the experimental procedures described in section 3.2.2 and 3.2.3. Five latexes A to E were prepared by seeded semi-continuous polymerization, in which the monomer feed rates (R_a) were varied from 0.27 wt%/minute to 1.10 wt%/minute. One latex F was prepared by seeded batch polymerization and another latex G by a conventional batch polymerization. These emulsion copolymerizations resulted in stable latexes of almost 100% conversion with negligible amounts of coagulum.

Figure 4.2 shows the overall conversion versus time curves of these seven emulsion copolymerizations as determined by the gravimetric method. In general, if the feed rate (R_a) is less than the maximum rate of batch polymerization ($R_{p,max}$), the polymerization becomes a "starved" reaction. If the feed rate is higher than the maximum rate of batch polymerization, the reaction becomes flooded and excess monomer is present in the reactor. In the seeded semi-continuous polymerizations A to E, the rate of polymerization (R_p) increased with increasing monomer feed rate, i.e., the rate of polymerization was controlled by the monomer feed rate. Specifically, the monomer feed rates in the polymerizations A to D (1.40 - 4.12×10^{-4} mol·l⁻¹·sec⁻¹) were less than the observed maximum rate of batch polymerization (5.79×10^{-4} mol·l⁻¹·sec⁻¹), indicating that the monomer concentrations in latex particles in the polymerizations A to D are much lower than those of the batch and seeded batch polymerization G and F,

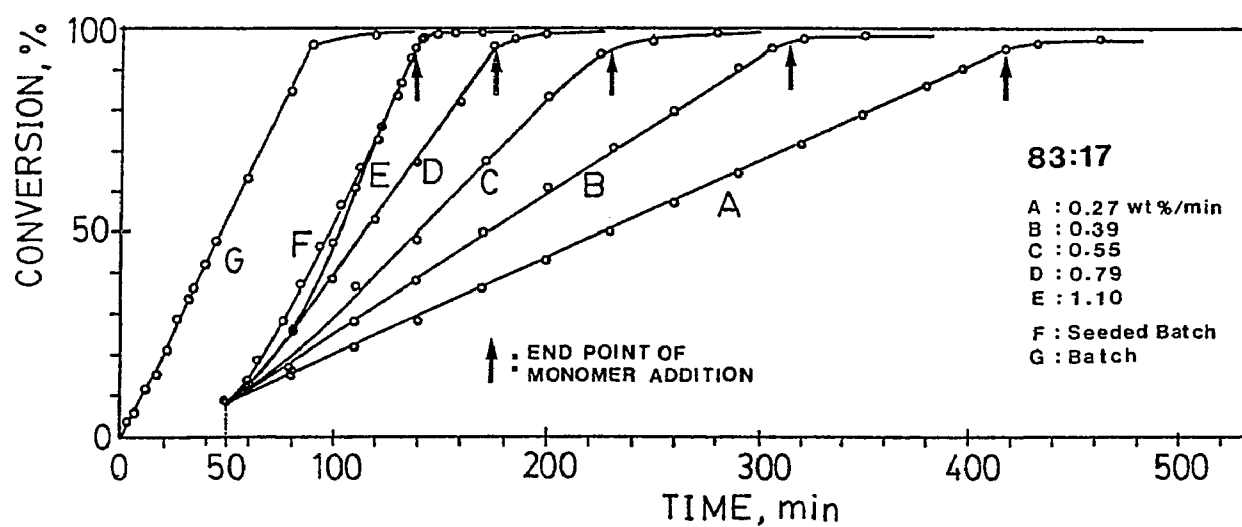


Figure 4-2: Overall conversion versus time curves of 83:17 VDC-BMA emulsion copolymerizations.

respectively. In other words, the polymerizations A to D occurred under monomer-starved conditions. However, for the polymerization E, which used the highest monomer feed rate ($5.77 \times 10^{-4} \text{ mol} \cdot \text{l}^{-1} \cdot \text{sec}^{-1}$), the corresponding conversion versus time curve was nearly the same as those obtained in the batch copolymerization G and the seeded batch polymerization F, indicating that the polymerization E occurred under near-flooded conditions.

Figure 4.3 shows the temperature inside the reactor as a function of time during these seven copolymerizations. In the seeded polymerizations A to F, the temperatures rose from the designated polymerization temperature, 25°C , during the formation of the seed, and returned to the designated temperature at the end of the polymerization. With the addition of the monomers, the temperature rose again to a maximum, and leveled off. During the seed formation of polymerizations A to F, the maximum reaction temperature was 26.0°C . The maximum reaction temperatures found during the monomer feed increased with increasing monomer feed rate (R_a), i.e., the maximum reaction temperature was controlled by the feed rate. In polymerizations A and B, the reaction temperature was constant at 25.5°C throughout the monomer addition period. However, in polymerizations C to E, the maximum reaction temperatures observed at the end of monomer feed period were 26.1 , 26.2 , and 26.9°C , respectively. For polymerization E, which used the highest monomer feed rate, the corresponding maximum reaction temperature was the same as those obtained for seeded batch (F) and batch polymerizations (G).

Figures 4.4 and 4.5 show the instantaneous conversion (X_I) versus time curves, and the conversion at time t (X_t) versus time curves obtained in the seeded semi-continuous copolymerizations A to E. In general, the instantaneous

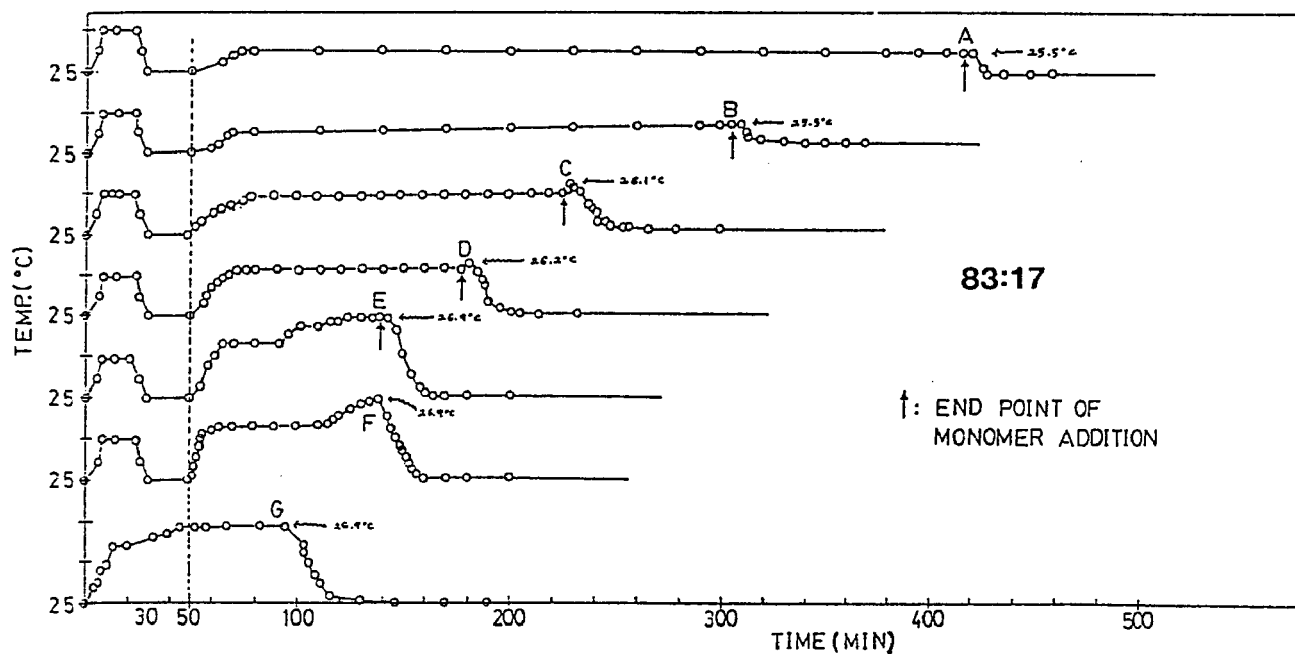


Figure 4-3: Reaction temperature versus time curves of 83:17 VDC-BMA emulsion copolymerizations.

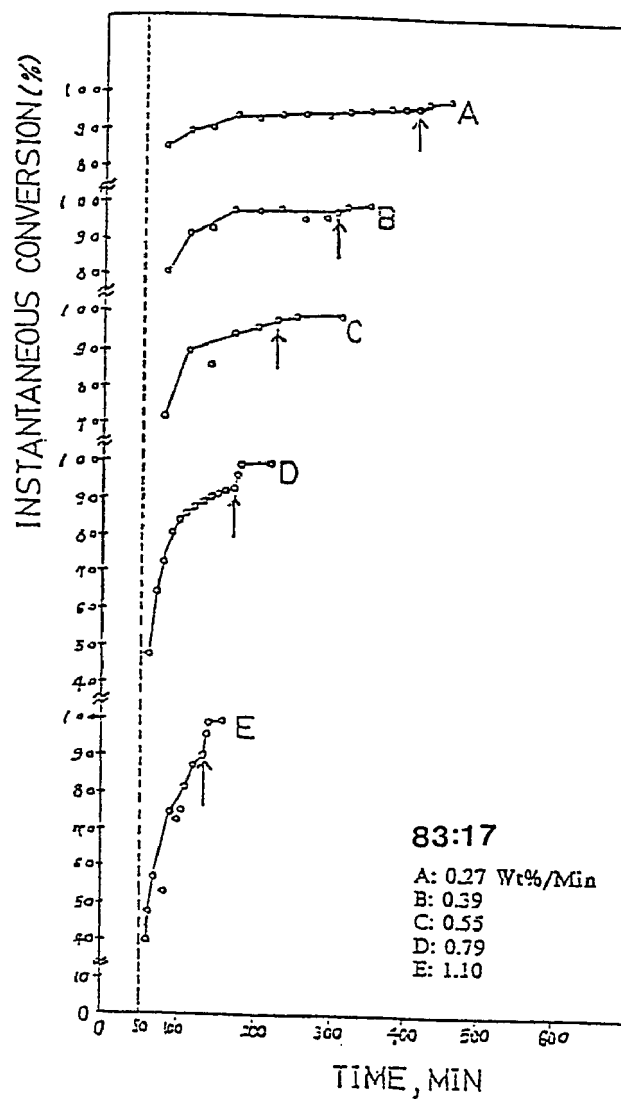


Figure 4-4: Instantaneous conversion versus time curves of 83:17 VDC-BMA emulsion copolymerizations.

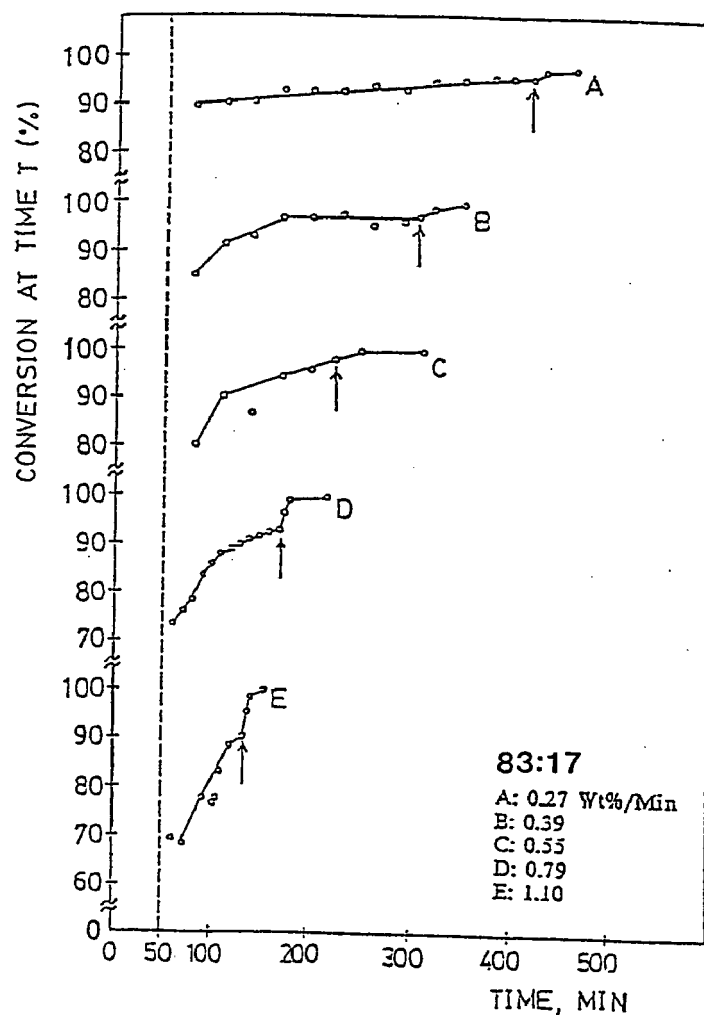


Figure 4-5: Conversion at time t versus time curves of 83:17 VDC-BMA emulsion copolymerizations.

conversion and the conversion at time t at the beginning of the monomer addition increased with decreasing monomer feed rate (R_a). Especially, in polymerization A, which used the slowest monomer feed rate, the instantaneous conversion at the beginning of the polymerization was the highest of the five polymerizations, and the conversion at time t versus time curve tended to be the most horizontal, indicating that the polymerization reached a steady state.

Figure 4.6 shows the concentration of monomer in the latex particles, $[M_p]$ versus % conversion curves in these five seeded semi-continuous polymerizations. It is shown that the concentration of monomer in the latex particles in the polymerizations A to E varies with the monomer feed rate. After the seeding process, and at the beginning of the monomer addition, the monomer concentration in the latex particles increased with increasing monomer feed rate and approached a maximum, then decreased with time as shown in Figure 4.6. For polymerization A, which used the slowest monomer feed rate, the corresponding $[M_p]$ versus % conversion curve was the most horizontal.

These results indicate that the concentration of monomer which built up from the beginning of the monomer addition period increased with increasing monomer feed rate. As the polymerizations became increasingly flooded with monomer with increasing feed rate, the instantaneous conversions at the beginning of the polymerization decreased. The magnitude of the gel effect increased with increasing amounts of monomer initially accumulated, the rates of polymerization became increasingly faster and as a result the temperature of the reactor increased with increasing feed rate.

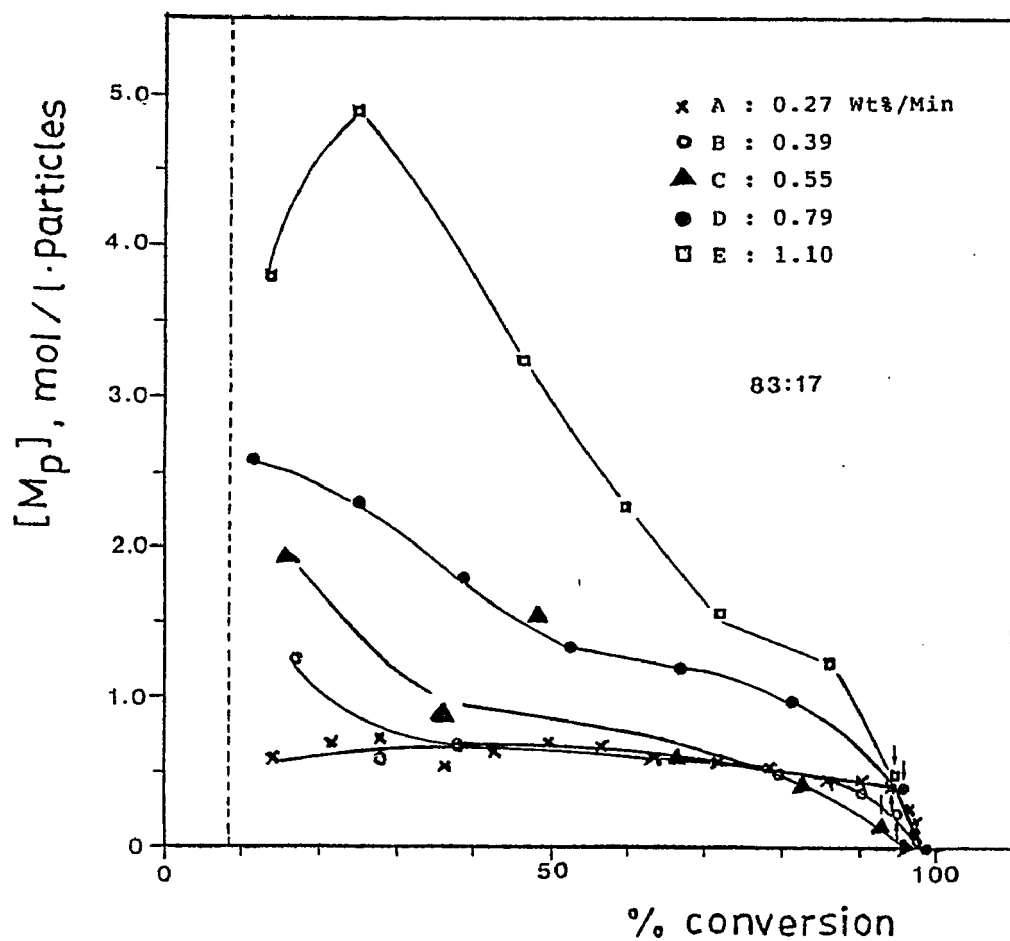


Figure 4-6: Monomer concentration in latex particles versus % conversion curves of 83:17 VDC-BMA emulsion copolymerizations.

4.2.2 Characterization of 83:17 VDC-BMA Latex Copolymers

4.2.2.1 Particle Size and Particle Size Distribution

Table 4-3: Particle sizes of 83:17 VDC-BMA copolymer latexes.

LATEXES	PARTICLE SIZES		D_w/D_n
	D_n (nm)	D_w (nm)	
Seed	56	57	1.022
A	121	124	1.024
B	120	125	1.035
C	125	130	1.033
D	124	126	1.022
E	120	123	1.023
F	124	126	1.018
G	113	116	1.020

Table 4.3 shows the average particle diameters of the latexes determined by transmission electron microscopy. The copolymer latexes A to F prepared by seeded polymerization showed almost the same number-average particle diameters of about 120-125 nm, all with narrow size distributions. Figure 4.7 shows transmission electron micrographs of these latexes. These results indicate that no secondary particle nucleation took place after the seeding process. The seeding with 10 wt% of the monomer ensured that most of the emulsifier was adsorbed on the particle surface, so that the secondary generation of new particles would be avoided. The copolymerization G, carried out by conventional batch polymerization, resulted in a latex with a number-average particle diameter of 113 nm and a narrow size distribution. This average particle size was slightly smaller than that of the latexes prepared by seeded polymerization. Vinylidene chloride is much more water soluble than butyl methacrylate, as shown in Table

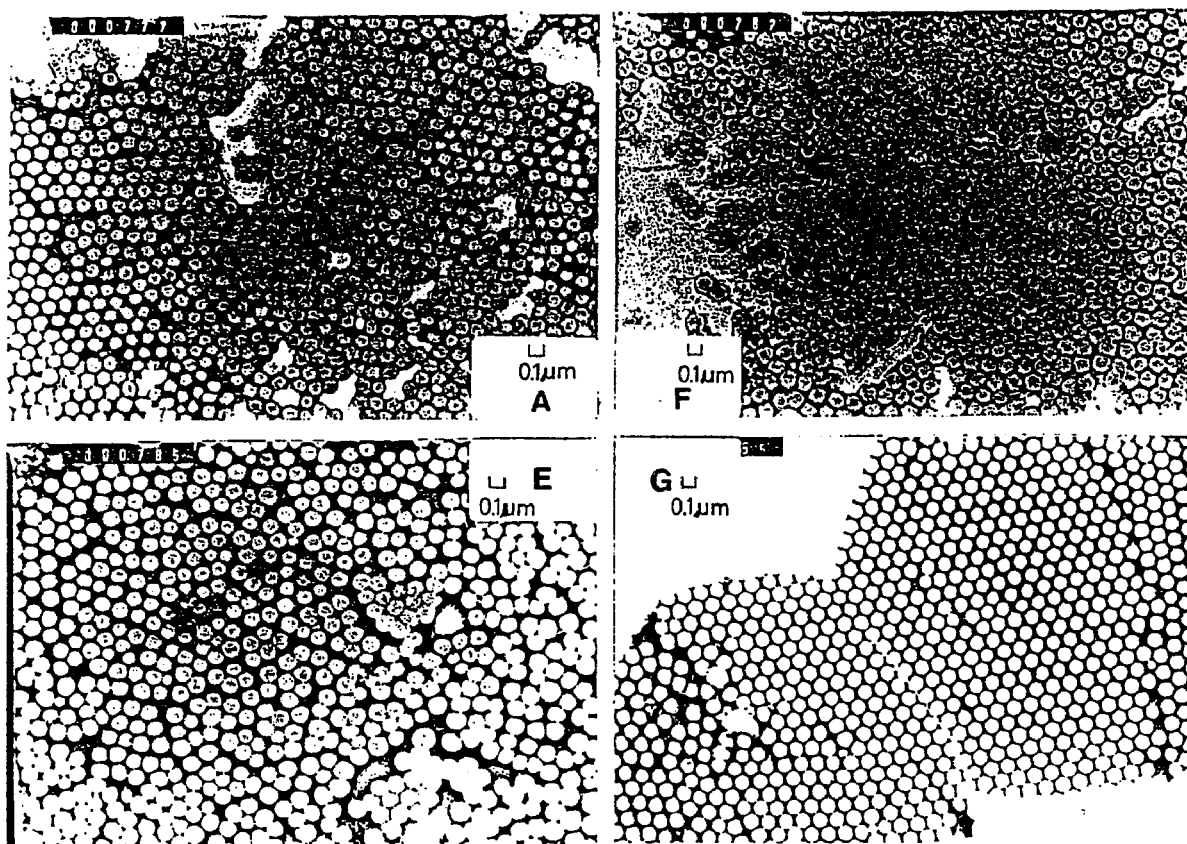


Figure 4-7: Transmission electron micrographs of 83:17 VDC-BMA copolymer latexes.

1.1. If the copolymerization favors initiation in the aqueous phase (homogeneous nucleation), the radicals generated in the aqueous phase add vinylidene chloride monomer and polymerize until the oligomeric radicals exceed their solubility and precipitate. The precipitated oligomeric radicals adsorb emulsifier and absorb monomer to become primary particles. These primary particles formed in the early stage of polymerization may persist as nuclei for the capture of other primary particles. Therefore, in the copolymerization of VDC-BMA mixture, the number of nuclei generated would be proportional to the content of vinylidene chloride monomer in the monomer mixture. In the same way, the latex G prepared by batch polymerization has a larger number of nuclei than those of latexes prepared by seeded polymerization.

4.2.2.2 Infrared Spectra of 83:17 VDC-BMA Latex Films

For poly(vinylidene chloride) and its copolymers, the infrared bands at 1048, 884, 753, 655, 600, 565, and 450 cm^{-1} are related to the crystallinity of the polymers (54-57).

Figures 4.8 and 4.9 show the infrared spectra of 83:17 VDC-BMA copolymer latex films before and after heat-treatment for 30 minutes at 70°C, respectively. The seven VDC-BMA copolymer latexes were all film-forming at room temperature. The infrared spectra of the latex films before the heat-treatment did not show any of the characteristic crystallinity peaks that appear for poly(vinylidene chloride), independent of the method of the monomer addition. This seems to be an indirect indication that the latex particles do not contain crystalline domains as they are synthesized. However, the infrared spectra of the 83:17 VDC-BMA copolymer latex films heated for 30 minutes at 70°C showed that, while the VDC-BMA copolymers A to E prepared by semi-continuous polymerization, still did not show any crystallinity peak, the VDC-BMA copolymers F and G prepared by seeded batch and batch polymerization did show crystallinity peaks.

These latex films were also aged for 6 months at room temperature. Figures 4.10, 4.11, and 4.12 show the infrared spectra of latex films A, F, and G, respectively, for different aging times. Interestingly, these spectra were found to be similar to those obtained from the samples heated for 30 minutes at 70°C and shown in Figure 4.9. Latex film A, prepared by the seeded semi-continuous polymerization with the slowest monomer feed rate, did not show any sign of crystallinity after aging for up to 6 months, indicating that the film was still amorphous in character. However, latex films F and G, prepared, respectively

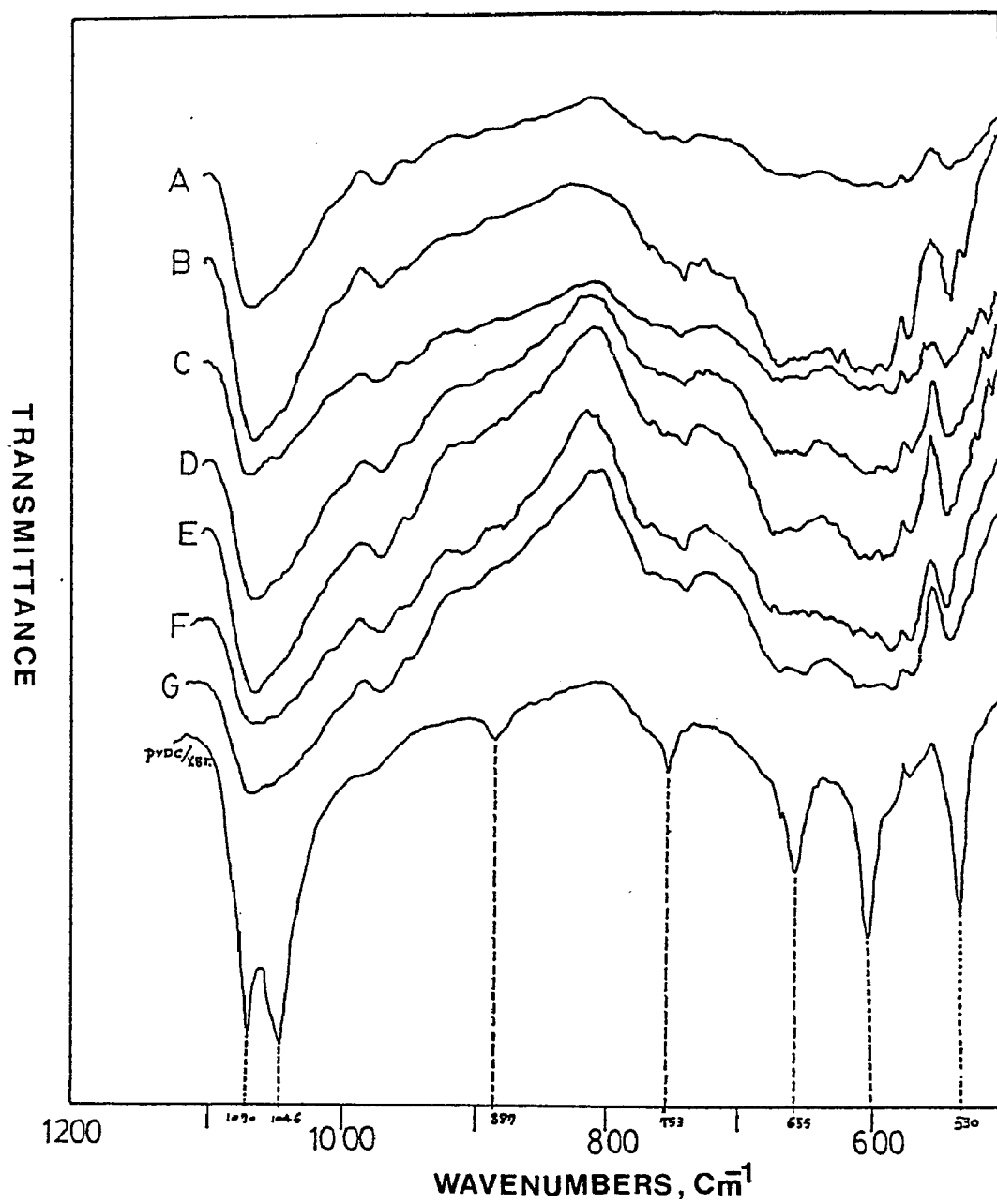


Figure 4-8: Infrared spectra of 83:17 VDC-BMA copolymer latex films A to G without heat-treatment (see Table 3.1 for identification).

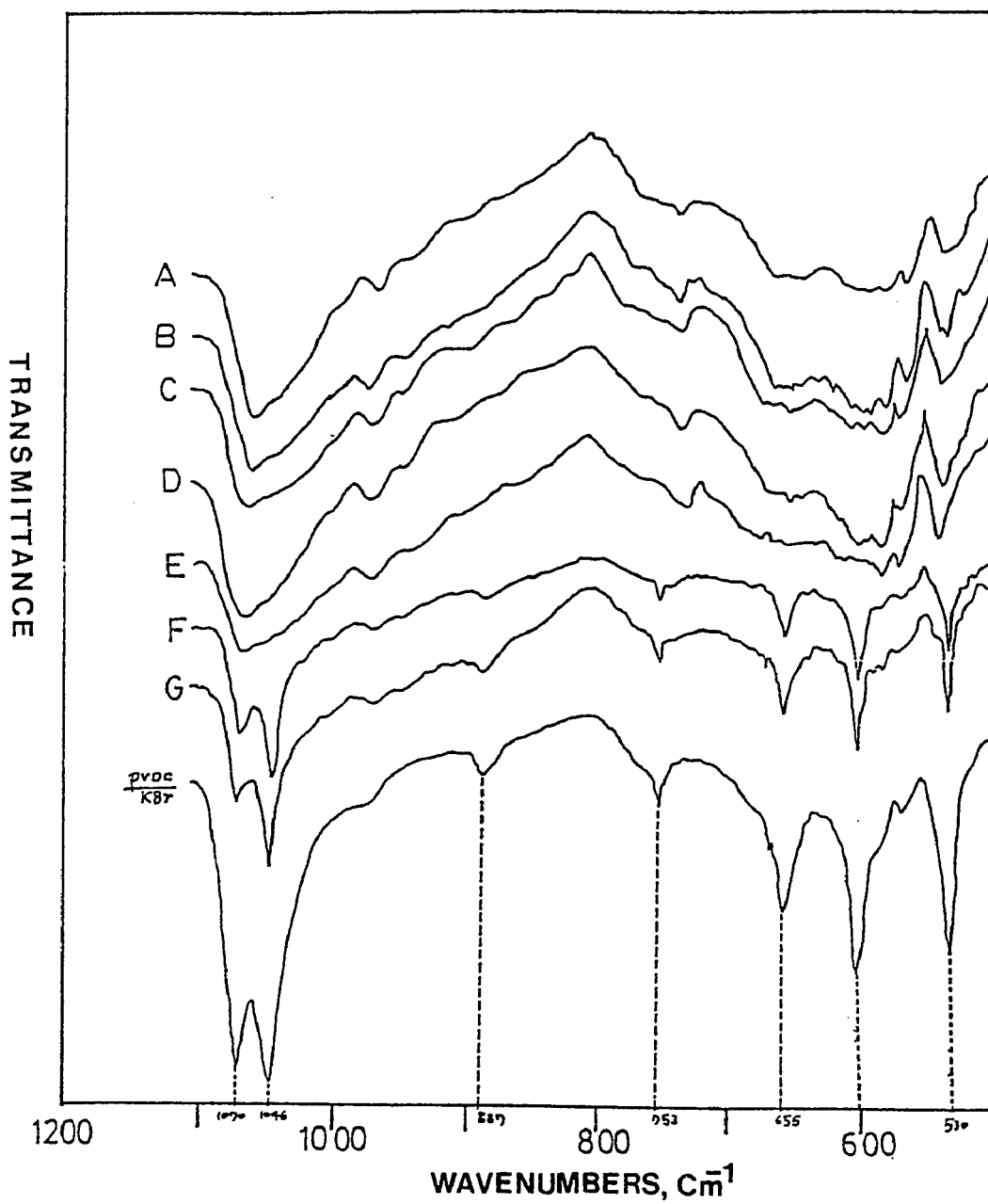


Figure 4-9: Infrared spectra of 83:17 VDC-BMA copolymer latex films A to G with heat-treatment for 30 minutes at 70°C (see Table 3.1 for identification).

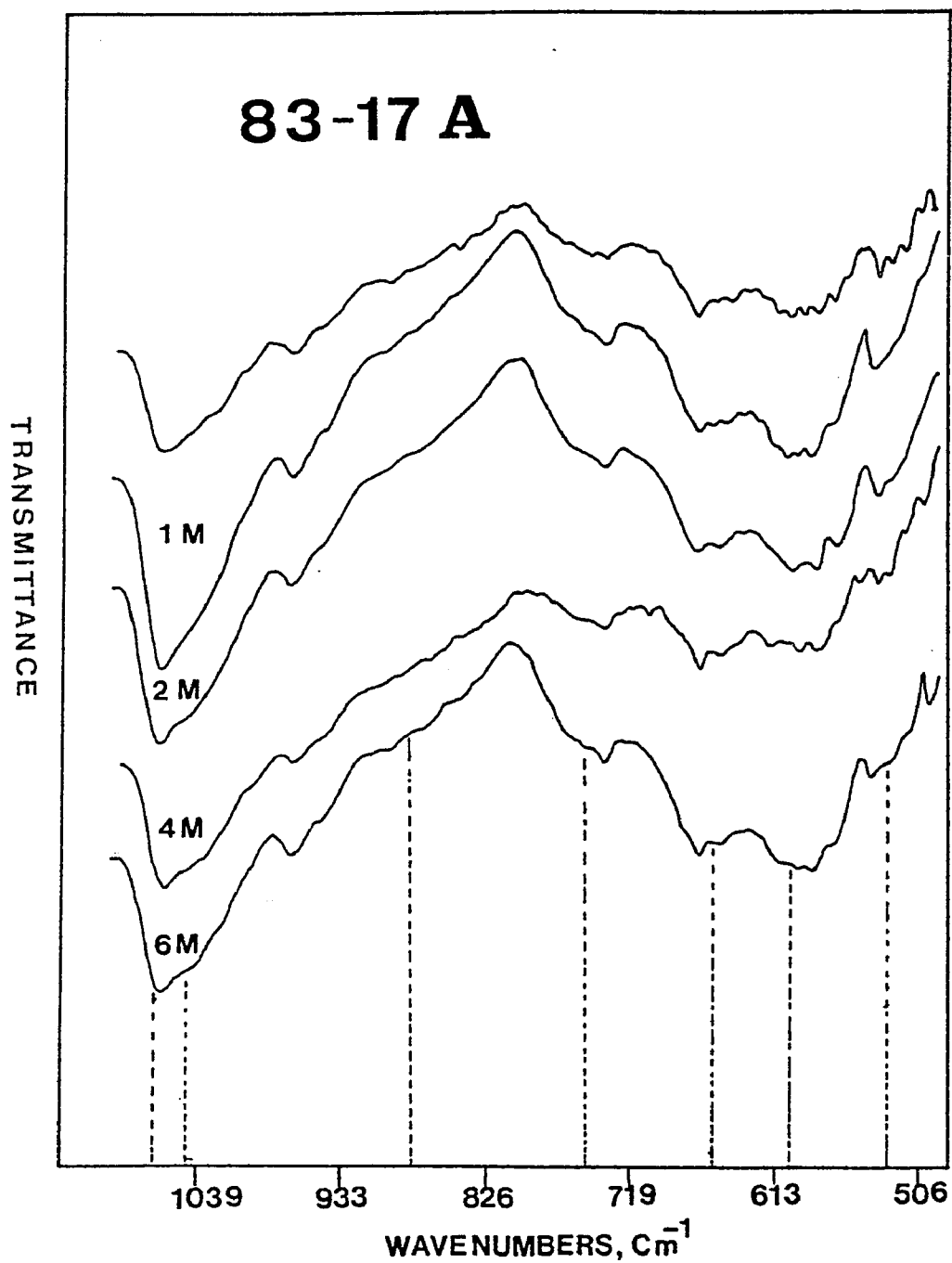


Figure 4-10: Infrared spectra of 83:17 VDC-BMA copolymer latex film A aged for 6 months at room temperature.

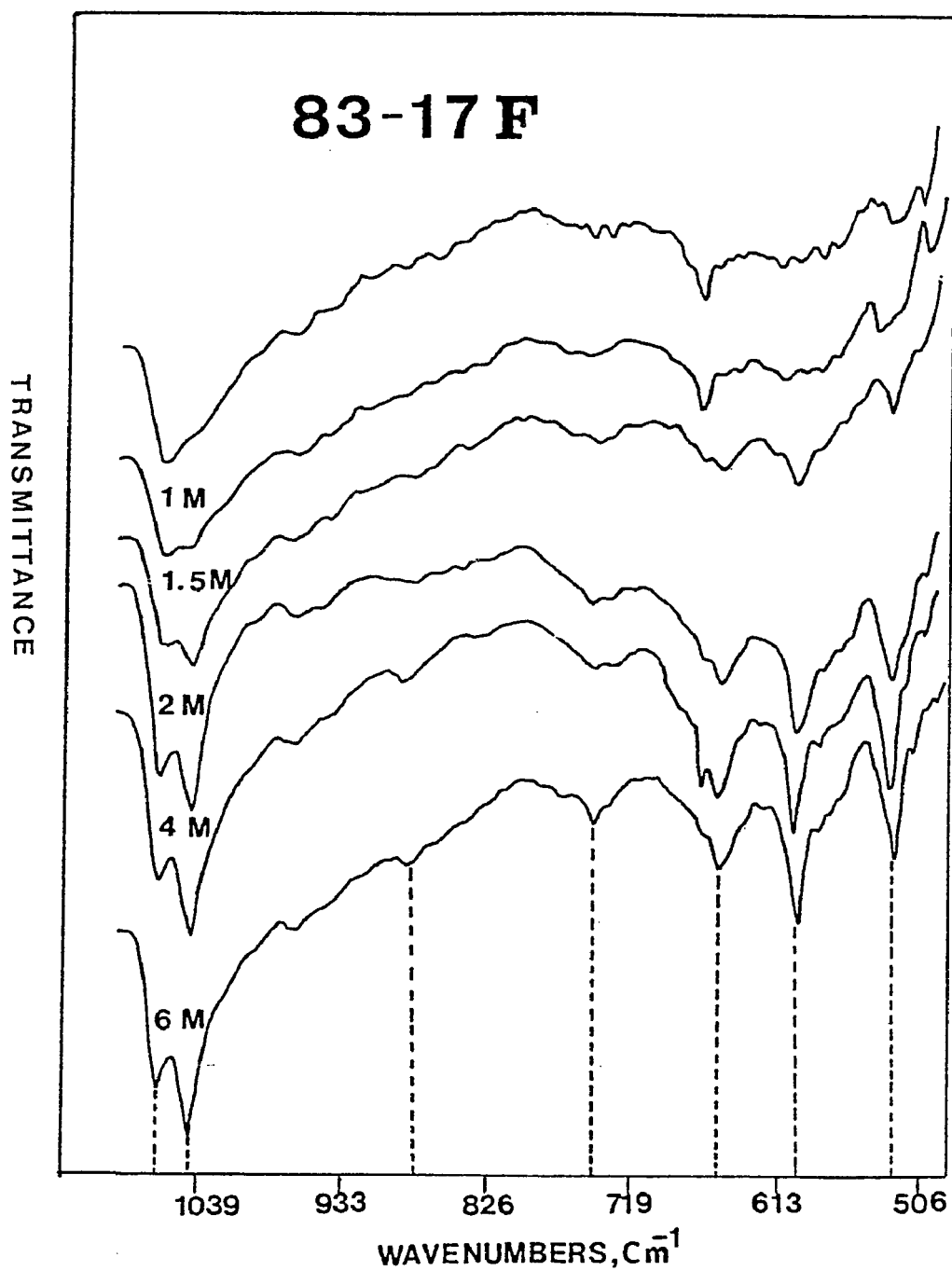


Figure 4-11: Infrared spectra of 83:17 VDC-BMA copolymer latex film F aged for 6 months at room temperature.

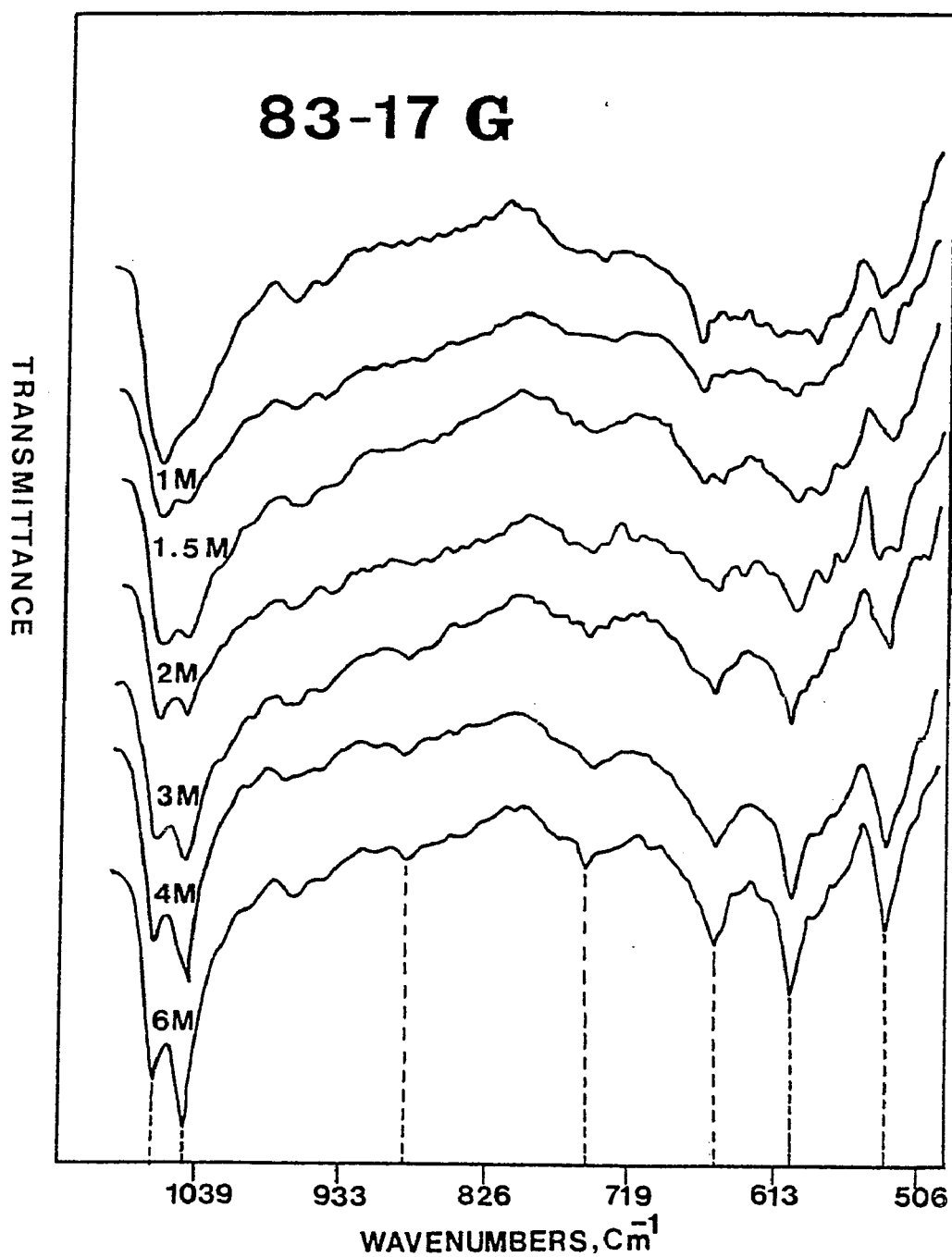


Figure 4-12: Infrared spectra of 83:17 VDC-BMA copolymer latex film G aged for 6 months at room temperature.

by seeded batch and conventional batch polymerization and aged for up to six months at room temperature, showed the characteristic crystallinity peaks. It is known (55, 56, 58) that the doublet at 1070 and 1048 cm^{-1} for the crystalline copolymers of vinylidene chloride is replaced by a single peak with the maximum at 1070 cm^{-1} and a shoulder at 1048 cm^{-1} for the amorphous copolymers. The band at 1070 cm^{-1} is stronger than that at 1048 cm^{-1} for the unoriented crystalline samples, whereas the intensities are reversed as the unoriented samples are oriented. In the infrared spectra of latex films F and G, heat-treated or aged for up to 6 months, the bands at 1070 cm^{-1} became weaker, while the band at 1048 cm^{-1} became stronger, indicating that these latex films were oriented under the heating and aging conditions, and became crystalline in character, i.e., crystallization took place.

In summary, the 83:17 VDC-BMA copolymer latex films freshly made at room temperature are amorphous in character, irrespective of the method of monomer addition used for the polymerization. Upon heat-treatment or aging, the latex films F and G prepared by seeded batch and batch polymerization, respectively, were crystalline in character, while the latex films A to E prepared by the seeded semi-continuous polymerization did not show any sign of crystallinity to heat-treatment or to aging, reflecting their amorphous character. As only VDC units can crystallize, these results indicate that, in the batch process, the copolymer composition drifted with conversion, resulting in copolymers having a fraction of chains containing long vinylidene chloride sequences. On the other hand, in the semi-continuous process, the controlled monomer feed technique formed copolymers having shorter vinylidene chloride sequences and with a more uniform copolymer composition. In other words, the

length of the vinylidene chloride sequences in the copolymer was controlled by the mode of monomer addition.

4.2.2.3 X-ray Powder Diffraction of 83:17 VDC-BMA Latex

Copolymers

Figure 4.13 shows X-ray diffraction patterns of the 83:17 VDC-BMA copolymer latex films heated for 30 minutes at 70°C. Latex films F and G, prepared by seeded batch and batch polymerization, respectively, showed the same diffraction peaks as the poly(vinylidene chloride), indicating that these copolymers are crystalline in character. These latex films also showed the regular Debye-Scherrer ring patterns found in poly(vinylidene chloride), as shown in Figure 4.14. In contrast, latex films A to E, prepared, by seeded semi-continuous polymerization, did not show any characteristic crystalline peaks or regular ring patterns, indicating that these polymers are amorphous in character.

The results from the X-ray diffraction study confirm the crystallinity results obtained by infrared spectroscopy, described in the previous section.

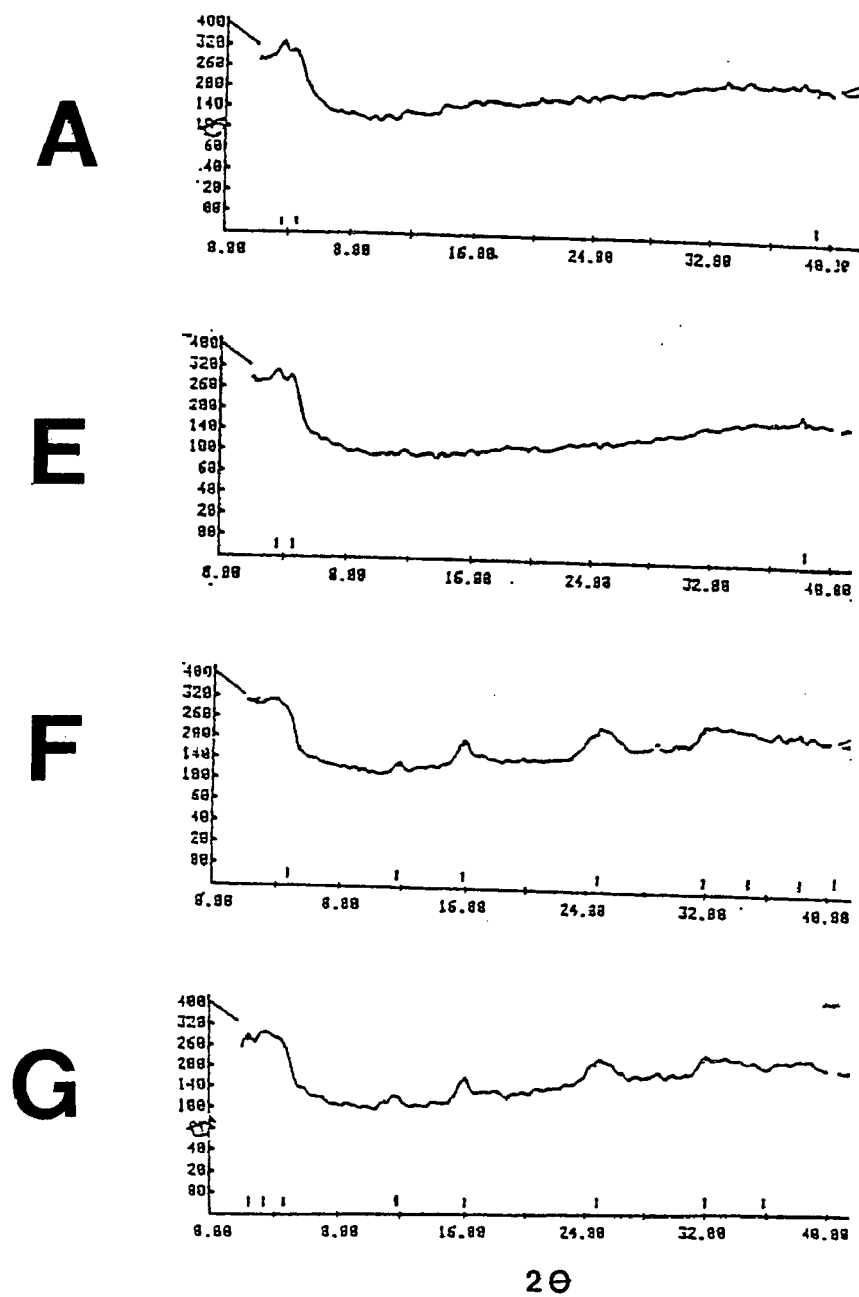


Figure 4-13: X-ray diffraction patterns of the 83:17 VDC-BMA copolymer latex films heated for 30 minutes at 70°C.

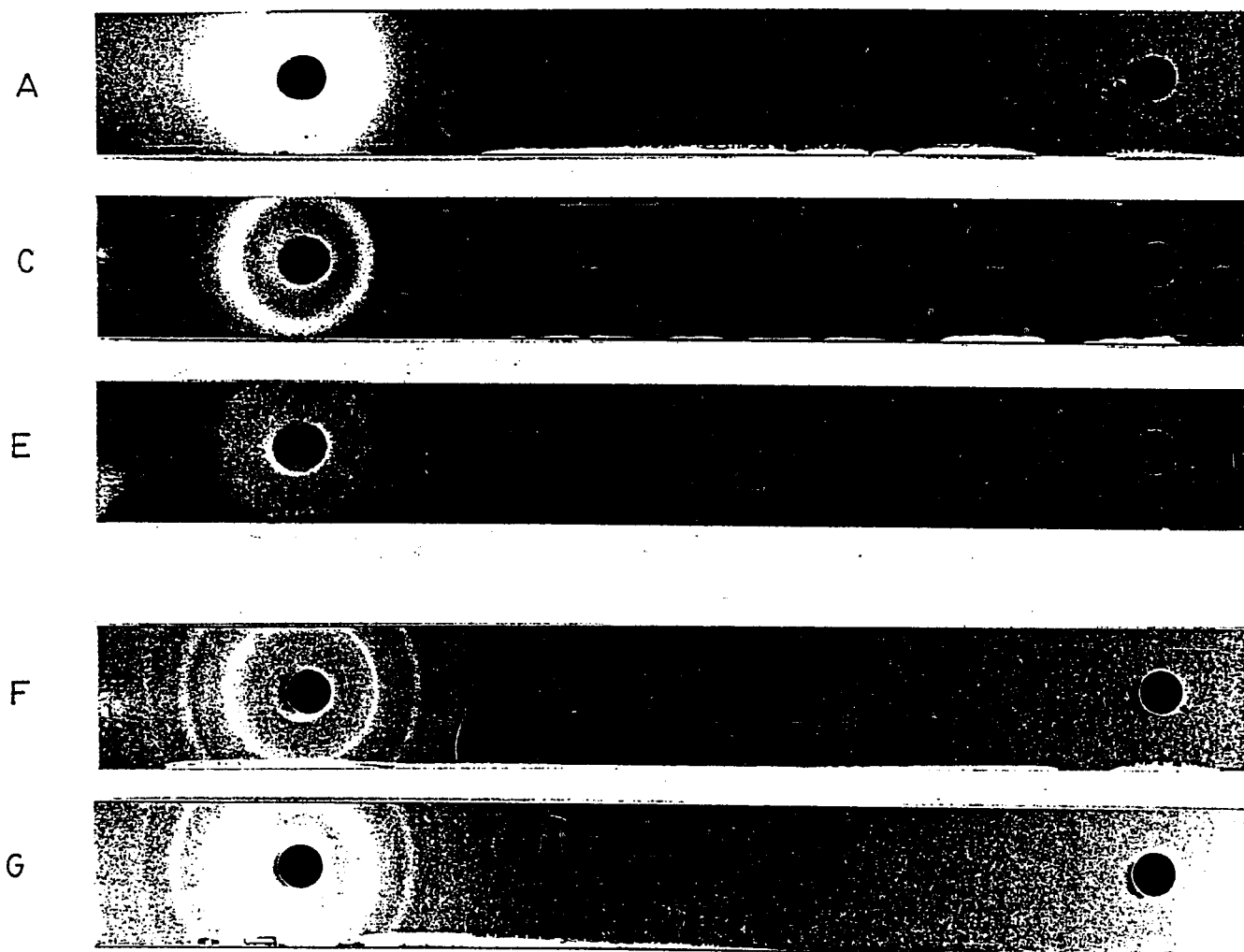


Figure 4-14: Debye-Scherrer ring patterns of the 83:17 VDC-BMA copolymer latex films heated for 30 minutes at 70°C.

4.2.2.4 T_g , T_m , and Minimum Film Forming Temperature (MFFT).

Table 4-4: T_g , T_m , and MFFT for heat-treated 83:17 VDC-BMA copolymer latex films.

(°C)	SEMI-CONTINUOUS					BATCH	
	A	B	C	D	E	F	G
T_g	16.3	16.3	15.8	15.7	16.9	23.2	24.2
T_m	=	=	=	=	=	184.0	187.0
MFT	+	+	+	+	+	+	+

= : no T_m observed

+ : lower than 5°C

Table 4.4 shows the glass transition temperature (T_g) and the crystalline melting temperature (T_m) determined by differential scanning calorimetry (heating rate 20°C/minute) for the seven latex films heated for 30 minutes at 70°C, and the minimum film forming temperature values of these latexes. These seven latexes were all film-forming at room temperature, and all of the MFFT values were below 5°C. Latex films A to E, prepared, by seeded semi-continuous polymerization, showed almost the same 16-17°C T_g value, shown in Figures 4.15 to 4.19. In contrast, latex films F and G, prepared respectively, by the seeded batch and batch polymerization showed T_g values 7-8°C higher than those for the copolymers prepared by semi-continuous polymerization, as shown in Figures 4.20 and 4.21. As mentioned before, the difference in T_g between the latex films prepared by batch and semi-continuous polymerization reflects that, in conventional batch and seeded batch copolymerizations, the copolymer composition drifted with increasing conversion, resulting in copolymers having a fraction of chains containing vinylidene chloride sequences long enough

Sample: A
Size: NOT WEIGHED/15 MG.
Rate: 20C/MIN 25CC/MIN N2
Program: Interactive DSC V3.0

DSC

Date: 23-Oct-85 Time: 10:53:26
File: DS-TGA.77 DAUGH.157
Operator: SPR
Plotted: 24-Oct-85 9:54:41

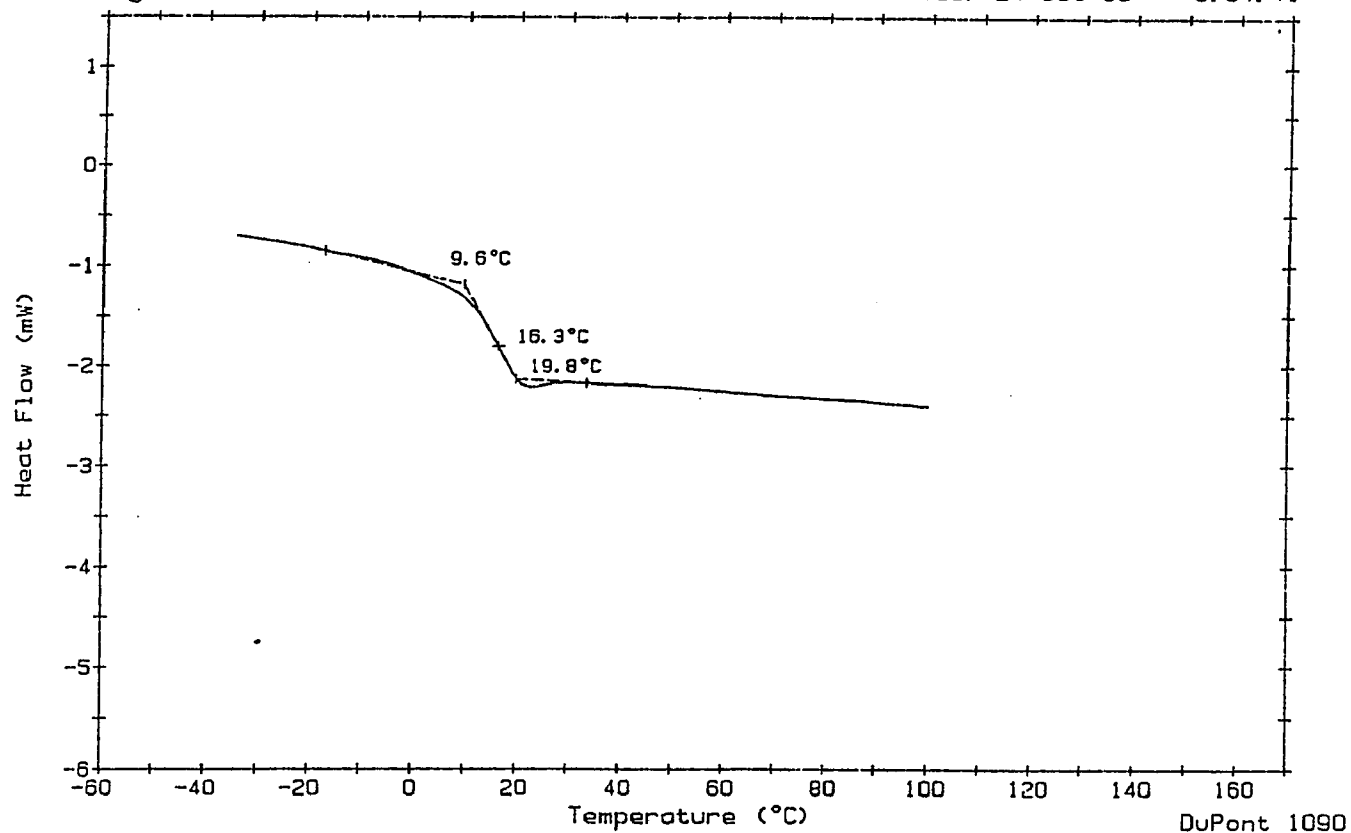


Figure 4-15: Differential scanning calorimetry curve of the 83:17 VDC-BMA copolymer A latex film.

Sample: B
Size: NOT WEIGHED/15 MG.
Rate: 20C/MIN 25CC/MIN N2
Program: Interactive DSC V3.0

DSC

Date: 23-Oct-85 Time: 10:53:26
File: DS-TGB.77 DAUGH.157
Operator: SPR
Plotted: 24-Oct-85 9:57:46

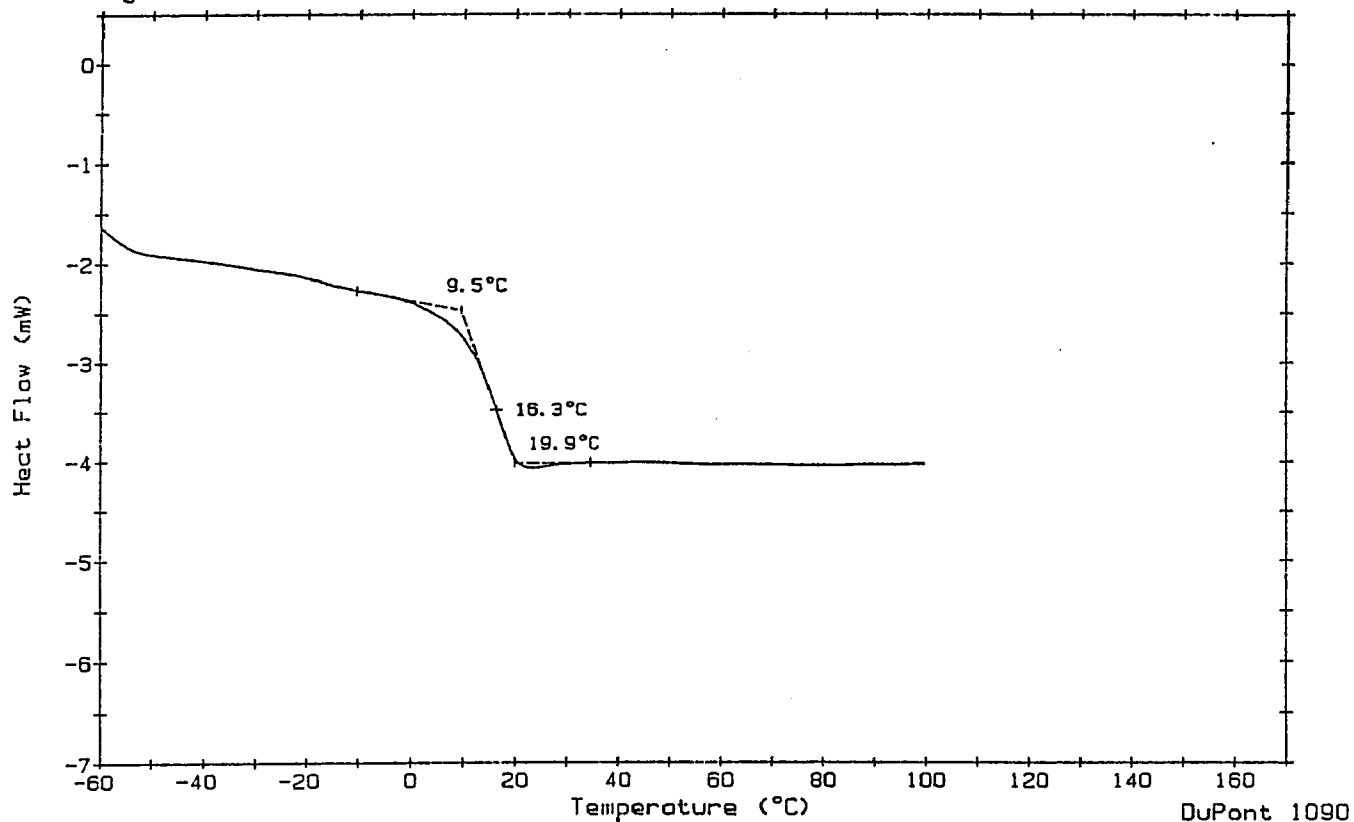


Figure 4-16: Differential scanning calorimetry curve of the 83:17 VDC-BMA copolymer B latex film.

Sample: C
Size: NOT WEIGHED/15 MG.
Rate: 20C/MIN 25CC/MIN N2
Program: Interactive DSC V3.0

DSC

Date: 23-Oct-85 Time: 14:39:37
File: DS-TGB.81 DAUGH.157
Operator: SPR
Plotted: 28-Oct-85 12:08:11

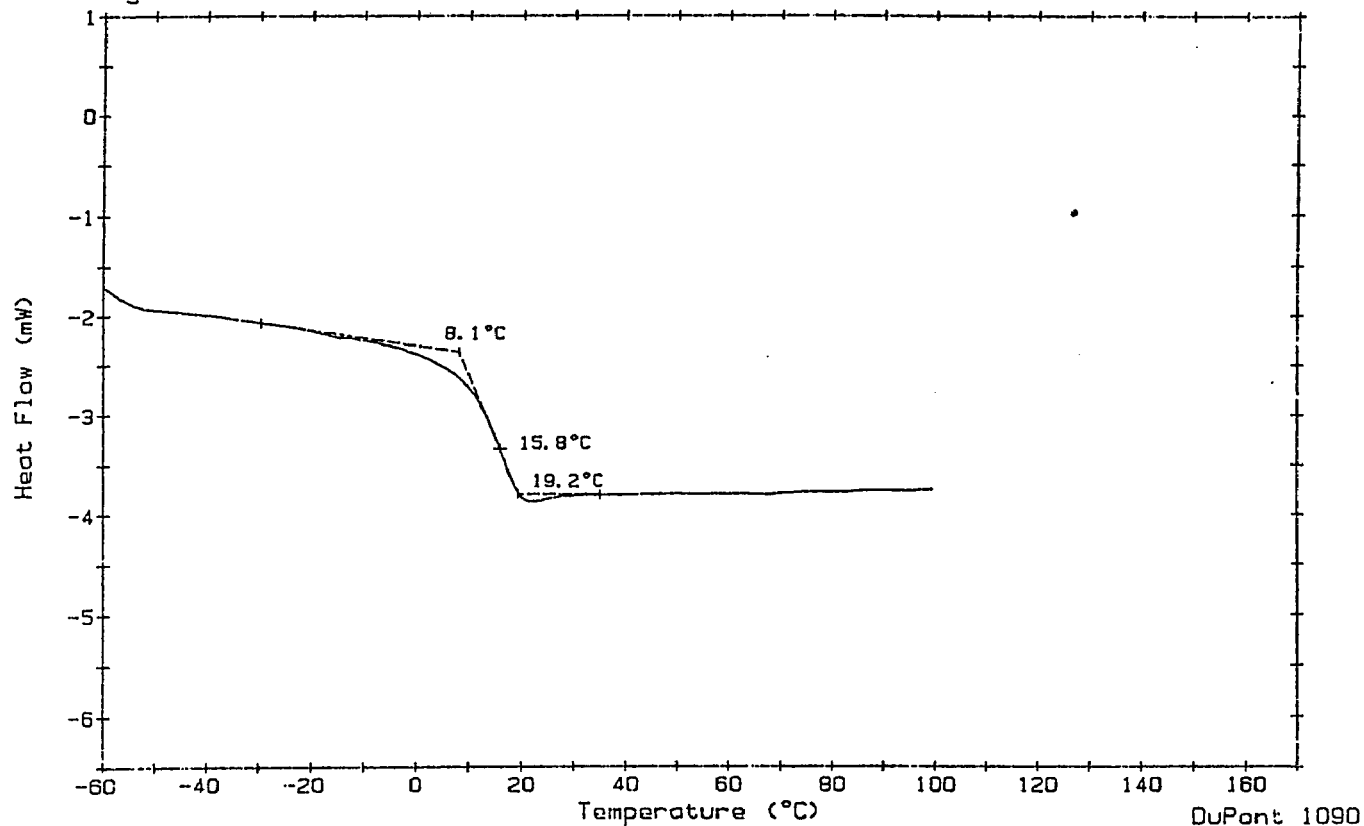


Figure 4-17: Differential scanning calorimetry curve of the 83:17 VDC-BMA copolymer C latex film.

Sample: D
Size: NOT WEIGHED/15 MG.
Rate: 20C/MIN 25CC/MIN N2
Program: Interactive DSC V3.0

DSC

Date: 23-Oct-85 Time: 11:50:01
File: DS-TGB.78 DAUGH.157
Operator: SPR
Plotted: 24-Oct-85 10:06:48

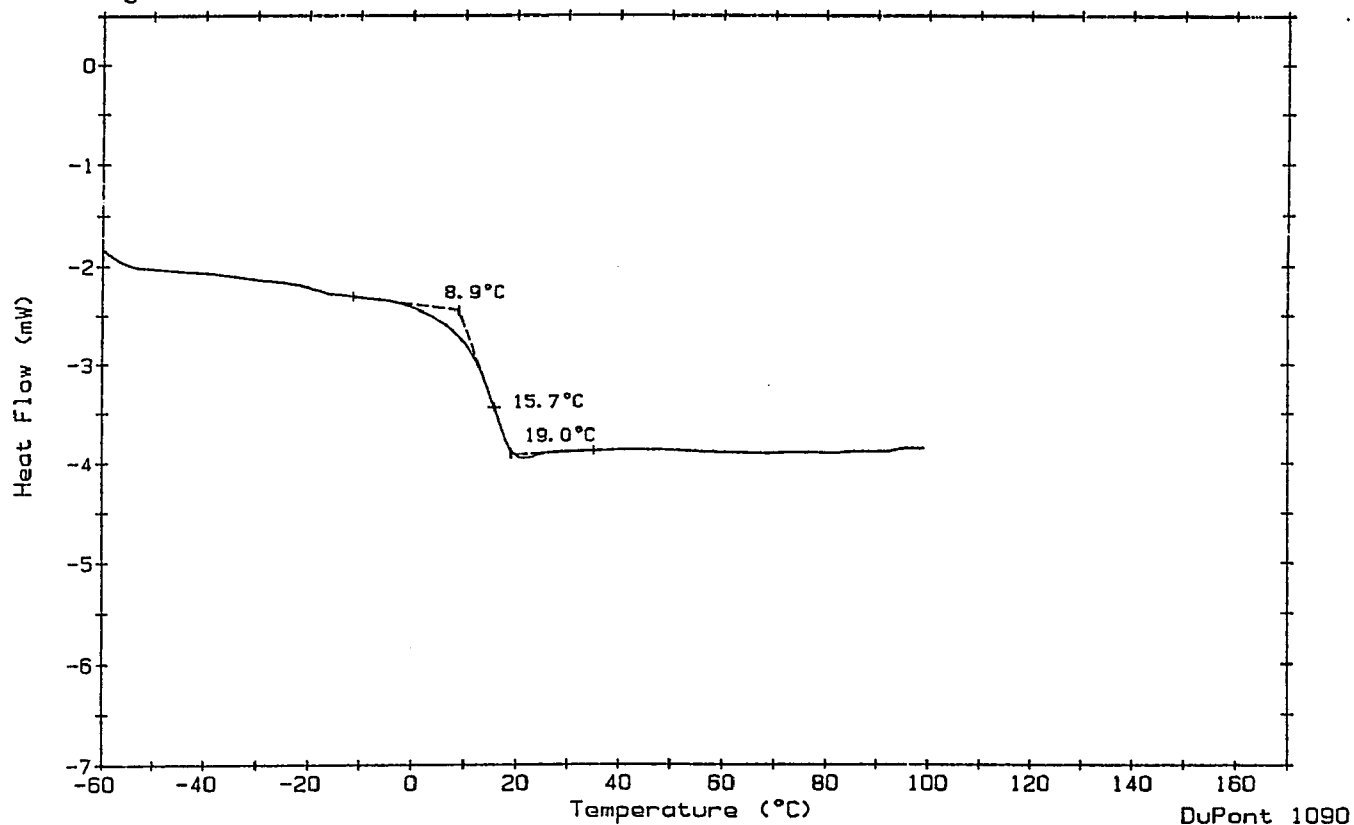


Figure 4-18: Differential scanning calorimetry curve of the 83:17 VDC-BMA copolymer D latex film.

Sample: E
Size: NOT WEIGHED/15 MG.
Rate: 20C/MIN 25CC/MIN N2
Program: Interactive DSC V3.0

DSC

Date: 23-Oct-85 Time: 12:46:35
File: DS-TGA.79 DAUGH.157
Operator: SPR
Plotted: 24-Oct-85 10:10:00

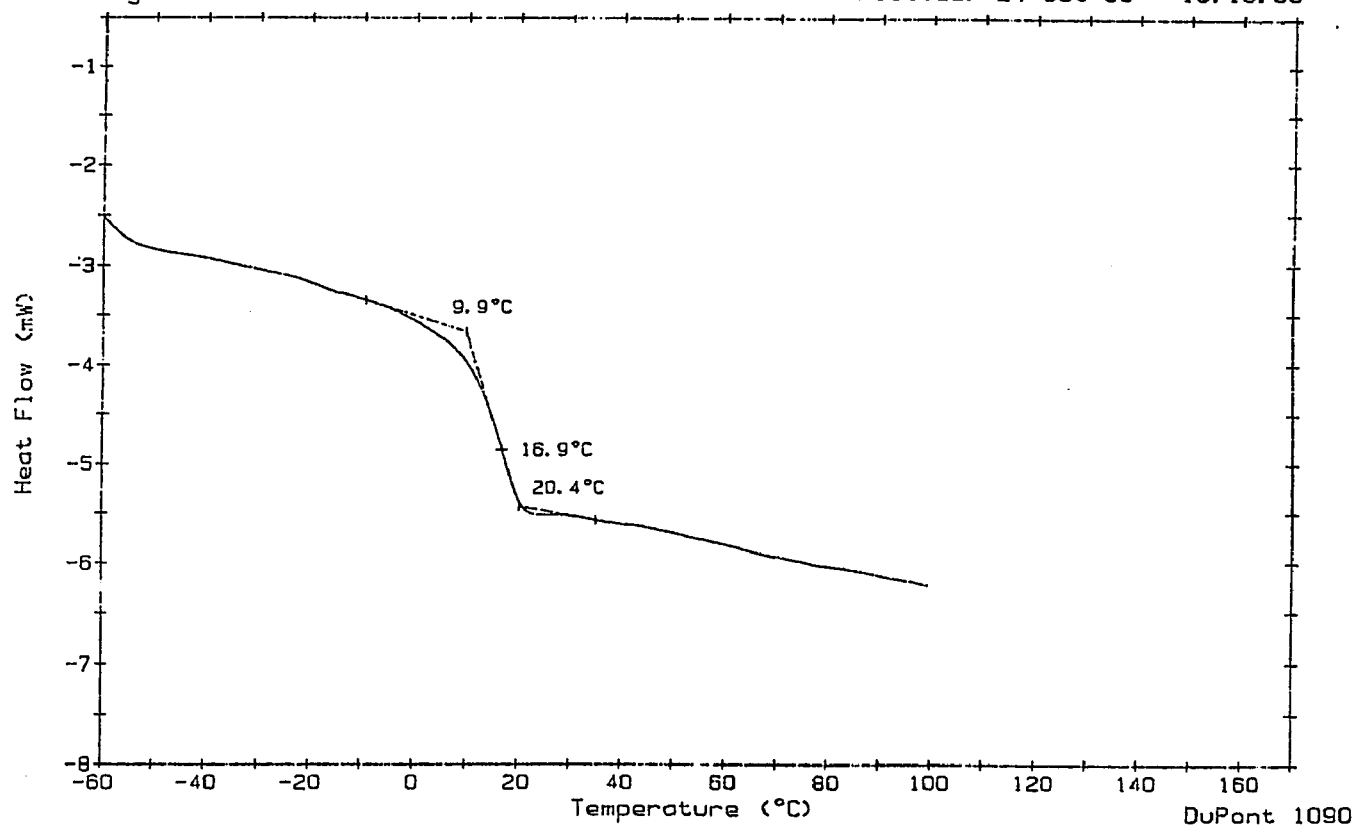


Figure 4-19: Differential scanning calorimetry curve of the 83:17 VDC-BMA copolymer E latex film.

Sample: F
Size: NOT WEIGHED/15 MG.
Rate: 20C/MIN 25CC/MIN N2
Program: Interactive DSC V3.0

DSC

Date: 23-Oct-85 Time: 12:46:35
File: DS-TGB.79 DAUGH.157
Operator: SPR
Plotted: 24-Oct-85 10:25:17

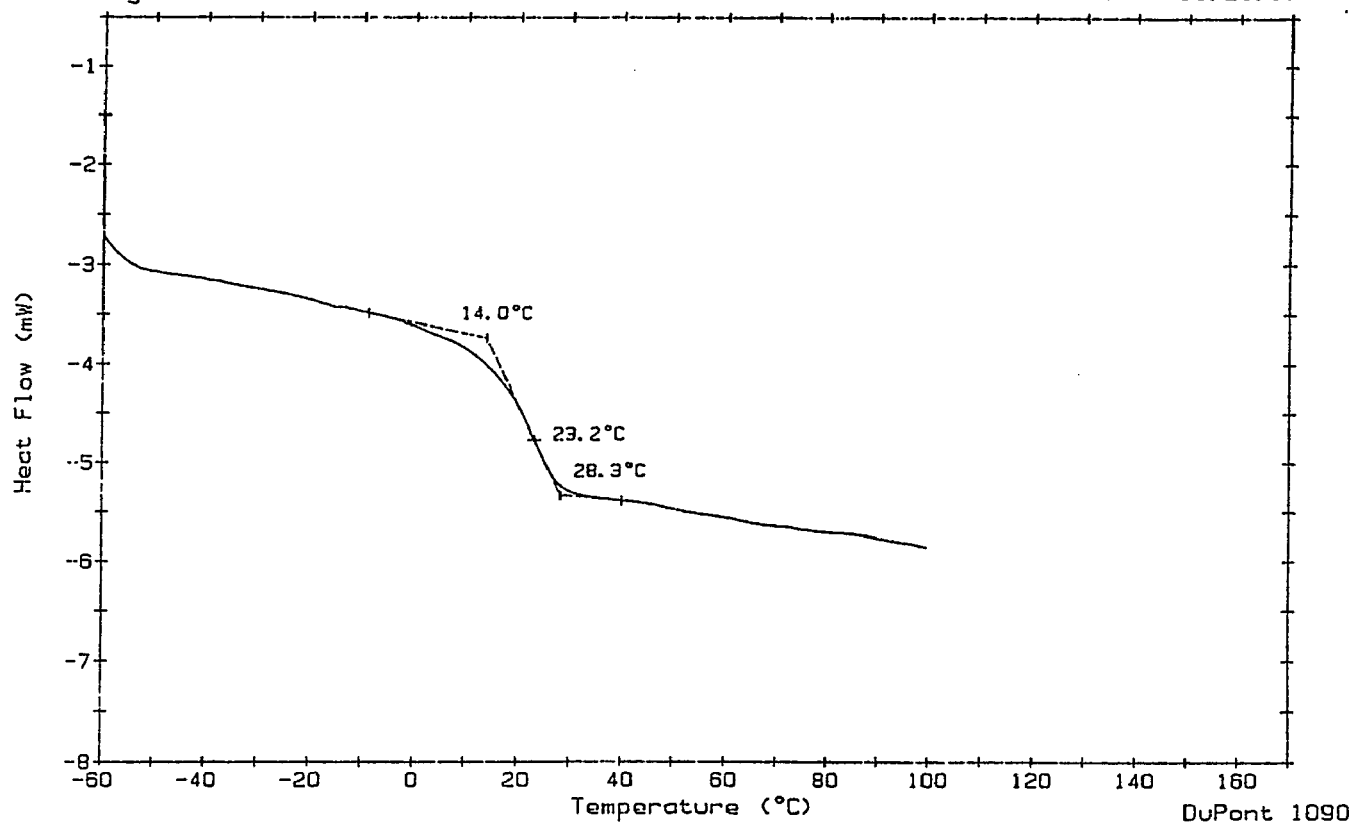


Figure 4-20: Differential scanning calorimetry curve of the 83:17 VDC-BMA copolymer F latex film.

Sample: G
Size: NOT WEIGHED/15 MG.
Rate: 20C/MIN 25CC/MIN N2
Program: Interactive DSC V3.0

DSC

Date: 23-Oct-85 Time: 13:43:07
File: DS-TGA.80 DAUGH.157
Operator: SPR
Plotted: 24-Oct-85 10:41:29

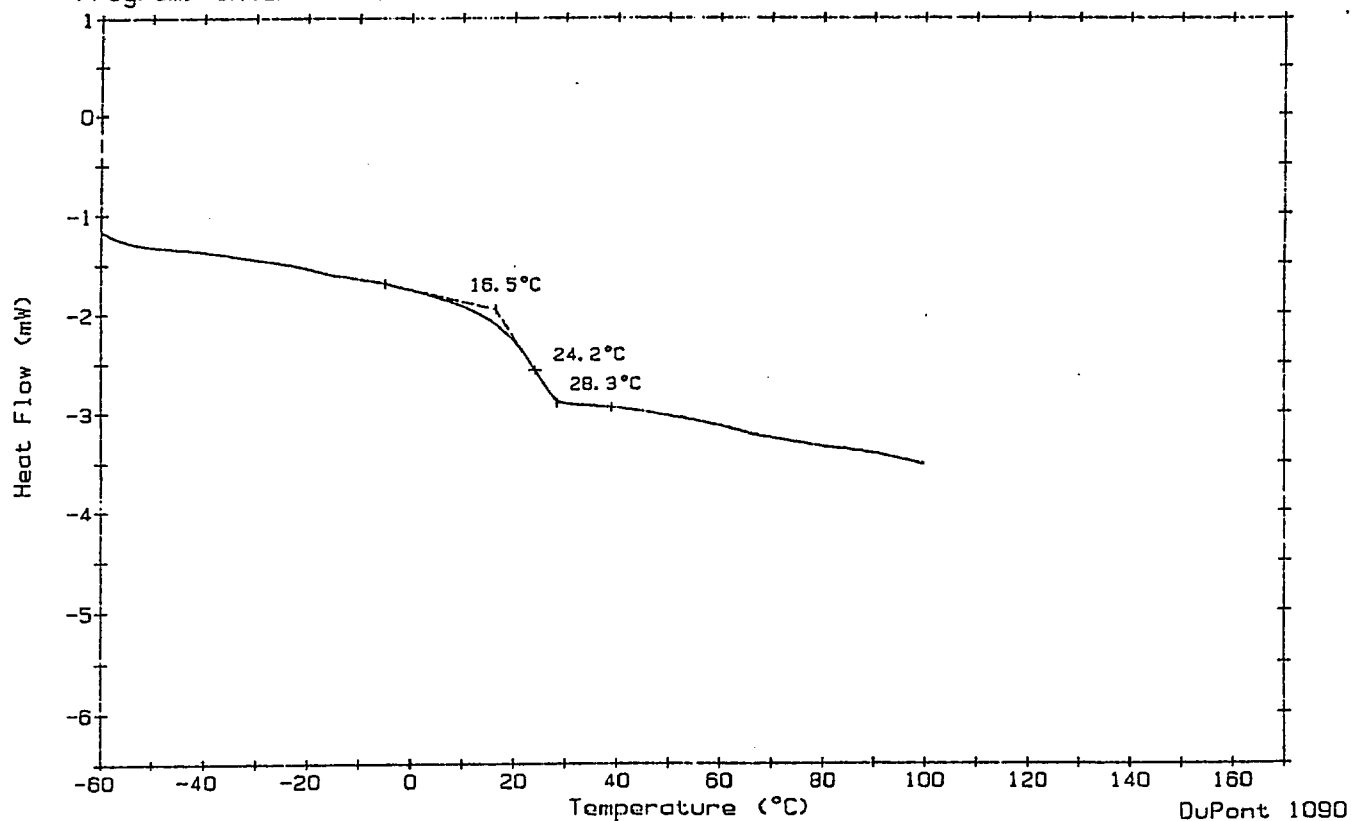


Figure 4-21: Differential scanning calorimetry curve of the 83:17 VDC-BMA copolymer G latex film.

to crystallize. In the semi-continuous polymerizations, on the other hand, the corresponding copolymer compositions were more homogeneous, the vinylidene chloride sequences were shorter, and the resulting copolymers were amorphous in character. The temperature difference between the two inflection points in the DSC curves was greater for the batch copolymer latex films than for the semi-continuous copolymer latex films, as shown in Figures 4.15 to 4.21, confirming again that the batch copolymers have more heterogeneous copolymer compositions. The reason that the latex films F and G, prepared by seeded batch and batch polymerization, have T_g values 7-8°C higher than those of the latex films A to E, prepared by seeded semi-continuous polymerization, might be due to the presence of crystallites in batch copolymers which reduce the mobility of amorphous chains trapped between crystallites, thereby increasing the T_g .

It can be seen in Table 4.4 that only the latex films F and G, prepared by seeded batch and batch polymerization, showed crystalline melting temperatures of 184°C and 187°C, respectively. On the other hand, the latex films A to E, prepared by semi-continuous polymerization, did not show crystalline melting temperatures, indicating that these latex films were amorphous in character. Also, the difference in melting temperatures between the latex films F and G might be due to the difference in size of the crystallites present in copolymers.

It should be also noted that, for the latexes F and G, prepared by seeded batch and batch polymerization, respectively, which are film-forming at room temperature with amorphous character, the corresponding latex films heated for 30 minutes at 70°C or aged for up to several months at room temperature,

however, were crystalline in character, having many valuable properties such as low permeability against most gases and vapors, solvent-resistance, and good mechanical properties.

4.2.2.5 Dynamic Mechanical Properties

The latex films dried at 50°C and aged for about a four month period, were used for dynamic mechanical analysis using the Rheovibron Viscoelastomer at 110 Hz and a heating rate of 1°C/minute. The results are shown in Figures 4.22 to 4.28. The latex films A to E, prepared by seeded semi-continuous polymerization, showed almost the same 30-31°C T_g . In contrast, the latex films F and G, prepared by seed batch and batch polymerization, respectively, showed a T_g about 10°C higher than those of the latexes prepared by semi-continuous polymerization. The results are similar to the T_g values determined by DSC, as described in section 4.2.2.4.

The latex films prepared by both batch and semi-continuous polymerization showed only one peak in the loss modulus (E'') spectra. That might be due to the small difference in T_g between the homopolymers of VDC and BMA. The width of the peaks in the loss modulus spectra (E'') of the latex films A to E, prepared by semi-continuous polymerization, however, were narrower than those of the latex films F and G, prepared by seeded batch and batch polymerization, respectively, indicating again that the copolymers prepared by the semi-continuous process have more homogeneous copolymer compositions than their counterparts by the batch process. The storage modulus (E') in the latex films A to E, prepared by seeded semi-continuous polymerization, approached a value of about 10^6 pa at 100°C with scattered data points, whereas the storage modulus in the latex films F and G, prepared by seeded batch and batch polymerization, respectively, approached a value of $10^{7.2-7.3}$ pa at 100°C with non-scattered data points, indicating that the latex copolymers F and G have higher moduli at the rubbery plateau region. The latex copolymers F and G

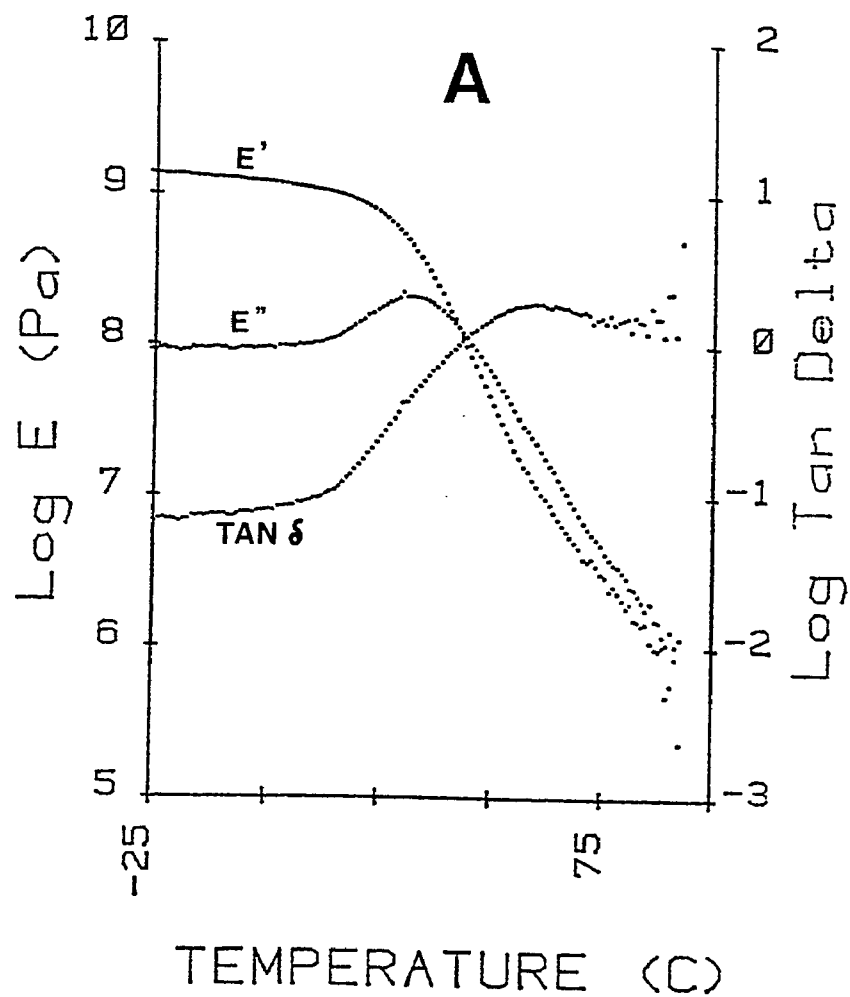


Figure 4-22: Dynamic mechanical spectrum of 83:17 VDC-BMA copolymer A.

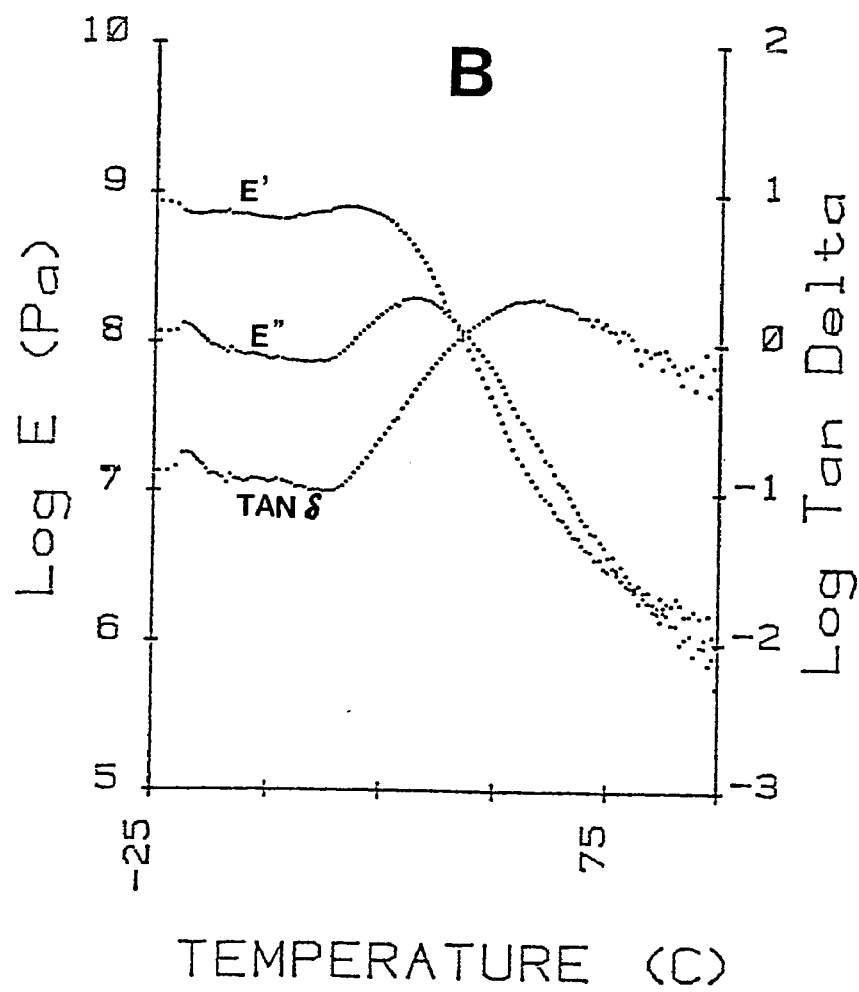


Figure 4-23: Dynamic mechanical spectrum of 83:17 VDC-BMA copolymer B.

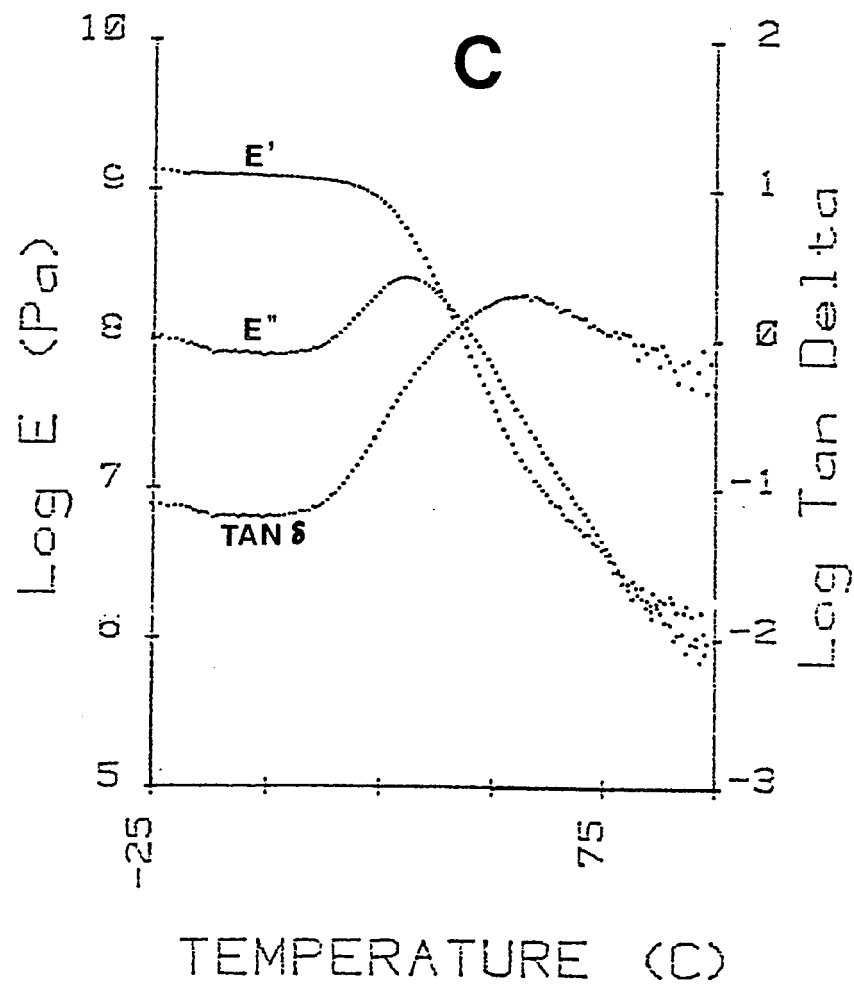


Figure 4-24: Dynamic mechanical spectrum of 83:17 VDC-BMA copolymer C.

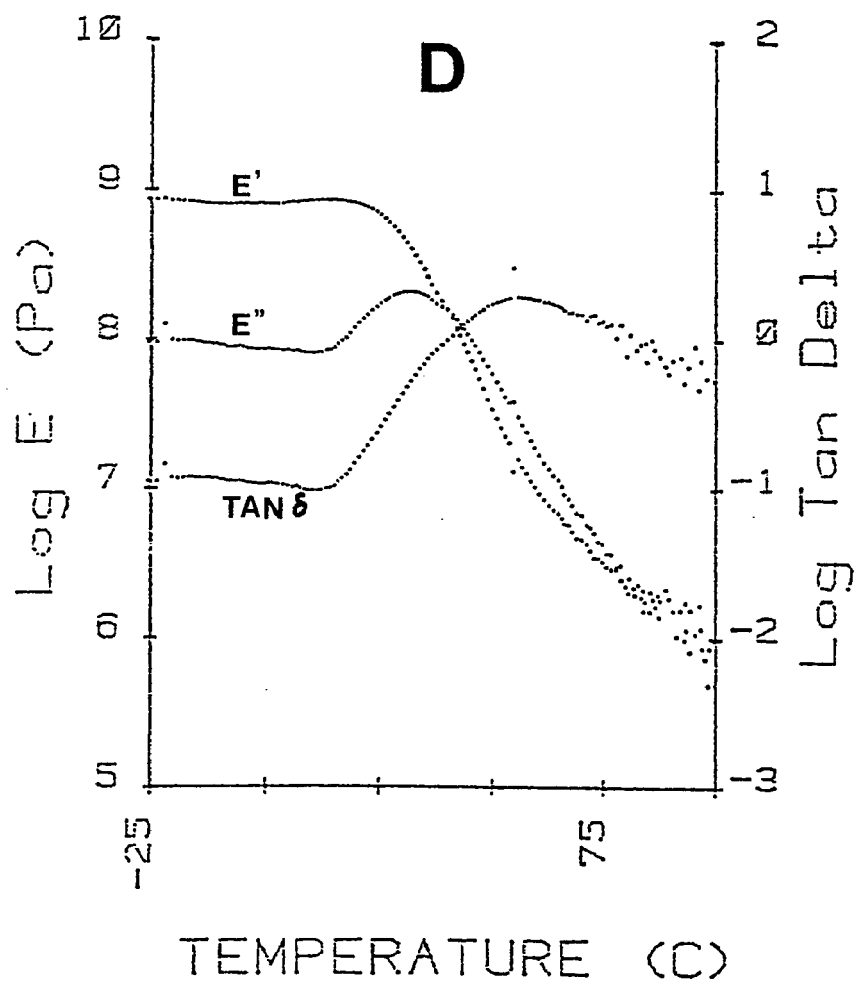


Figure 4-25: Dynamic mechanical spectrum of 83:17 VDC-BMA copolymer D.

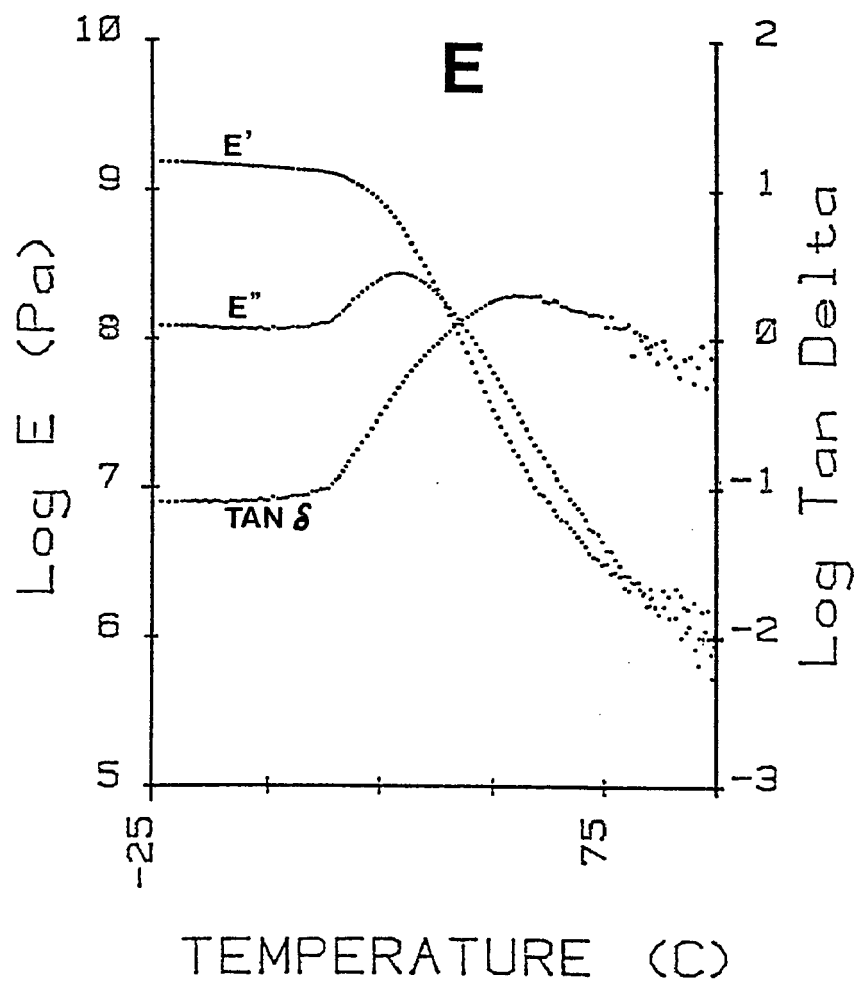


Figure 4-26: Dynamic mechanical spectrum of 83:17 VDC-BMA copolymer E.

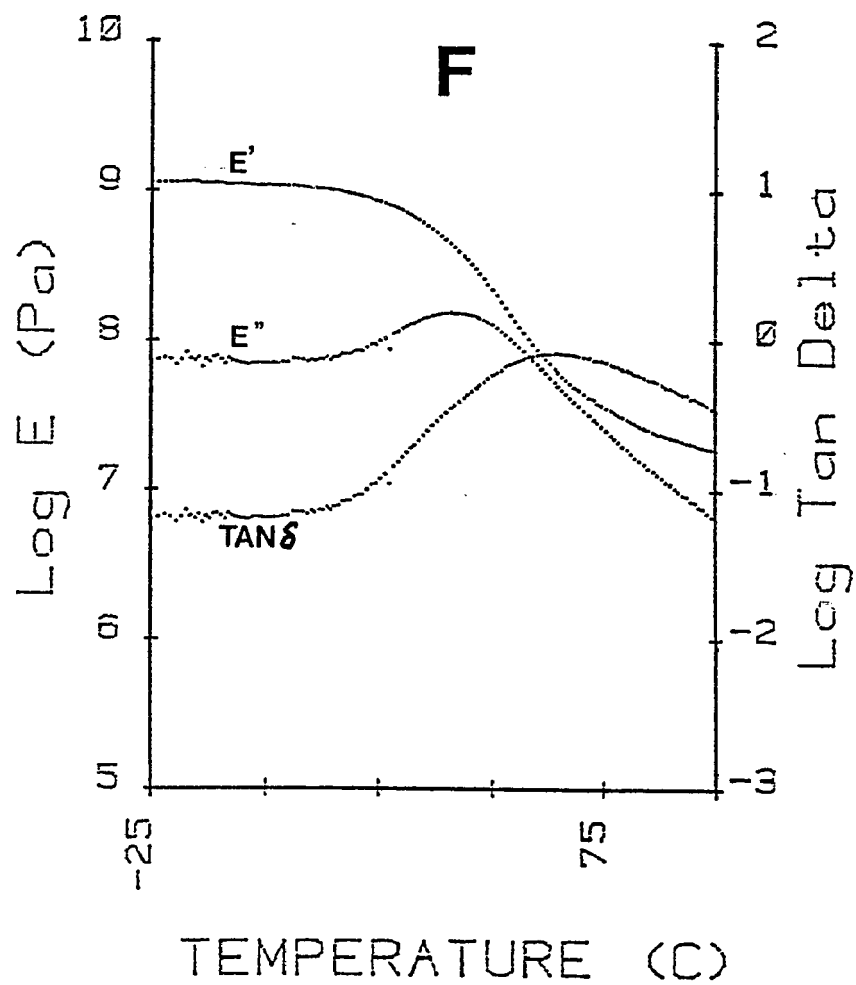


Figure 4-27: Dynamic mechanical spectrum of 83:17 VDC-BMA copolymer F.

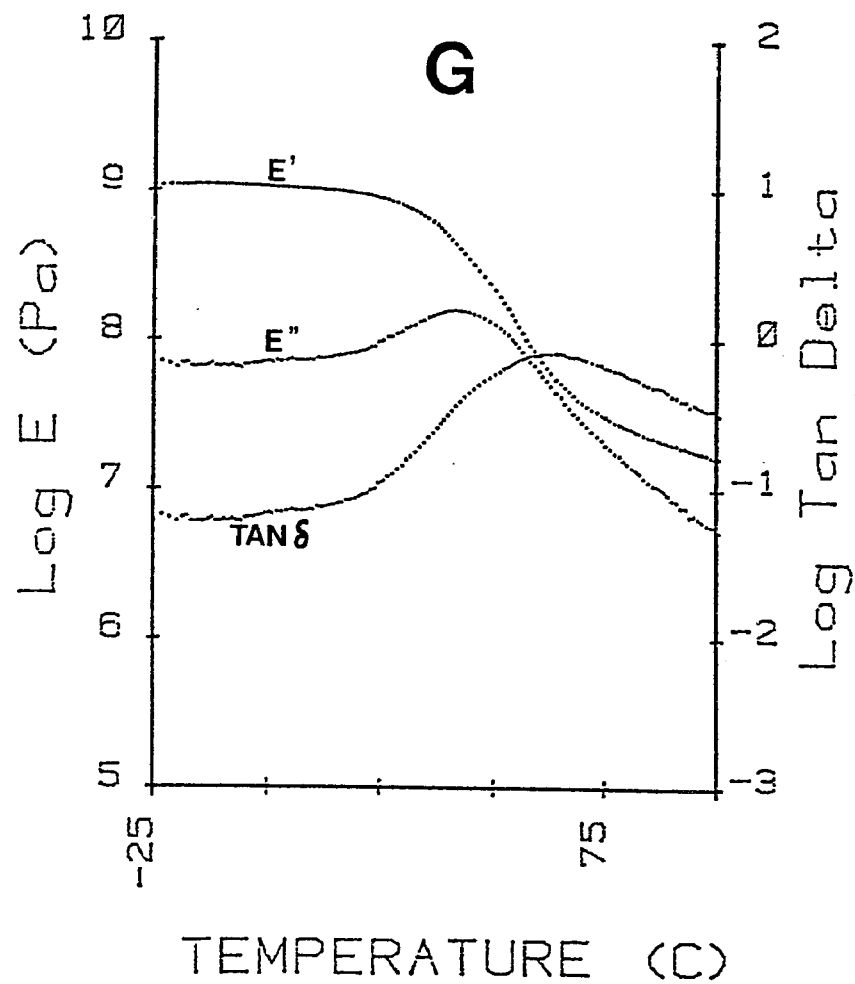


Figure 4-28: Dynamic mechanical spectrum of 83:17 VDC-BMA copolymer G.

were known to be crystalline, as confirmed by the presence of crystalline melting temperatures, higher T_g values, and the presence of crystalline characteristic peaks in the infrared spectra and X-ray diffraction patterns. The crystallites in crystalline materials may act as a reinforcing filler or crosslinker between the amorphous regions, and increase the modulus and the stiffness in the composites (78). This may be the reason why the copolymers F and G have higher moduli, and stiffness in the rubbery plateau region than their counterparts prepared by semi-continuous polymerization. Therefore, it is reasonable to deduce that the mode of polymerization, which controls the length of the vinylidene chloride sequences in the copolymer chain, affects the physical and mechanical properties.

4.2.2.6 Tensile Properties of 83:17 VDC-BMA Copolymer Latex Films

Significant differences were found in tensile properties of these seven latex films.

Table 4-5: Tensile properties of 83:17 VDC-BMA copolymer latex films.

PROCESS	SEMI-CONTINUOUS					BATCH	
	A	B	C	D	E	F	G
Young's modulus, $E^{a,b}$ (MPa)	3.4	6.2	7.3	12.7	12.7	230.1	296.3
ultimate strength, σ_b (MPa)	1.3	2.7	2.7	2.9	2.9	7.6	8.4
elongation to break, (%)	588	483	480	480	468	74	87
energy to break, τ^b (MJ/m ³)	15.6	11.4	9.9	8.3	7.7	5.4	6.1

a : determined from the initial slope of the stress-strain curve

b : based on the initial cross-sectional area

Table 4.5 shows the tensile measurements for these latex films, all dried at 50°C and aged for about a four-month period. In general, latex films A to E, prepared by semi-continuous polymerization, had much lower Young's moduli E , lower ultimate strengths σ_u , higher percent elongations ϵ , and higher energies to break (toughness) τ than those of latex films F and G, which were prepared by seeded batch and conventional batch polymerization. Also, the tensile properties of latex films A to E, prepared by semi-continuous polymerization, varied with the monomer addition rate used in the polymerizations. The Young's modulus and ultimate strength increased, and the percent elongation and toughness decreased with increasing monomer addition rate (R_a). This result indicates that, even in semi-continuous polymerization, the degree of composition drift varies with increasing monomer feed rate. In other words, the unit length

of vinylidene chloride molecule in copolymers is controlled by the monomer feed rate. The result of tensile measurements of these copolymers correlates with the results of solubility in various solvents as stated in next section. The reason that the latex films F and G have higher moduli, higher ultimate strength, lower percent elongation, and lower toughness may be explained by the presence of the crystallites acting as reinforcing fillers or crosslinkers in the copolymers.

4.2.2.7 Solubility Behavior of 83:17 VDC-BMA Copolymer Latex

Films

Poly(vinylidene chloride) and its copolymers of high vinylidene chloride content are insoluble in all solvents at room temperature because of their crystallinity.

Table 4.6 shows the results of the solubility tests of 83:17 VDC-BMA copolymer latex films, prepared by batch and semi-continuous polymerization, before and after heat-treatment for 30 minutes at 70°C, carried out at room temperature with various common solvents. Figure 4.29 also shows a picture of the latex films A to G, heated for 30 minutes at 70°C, after dissolution in tetrahydrofuran (THF) at room temperature. A remarkable difference was found in solubility behavior of these latex films, according to the mode of monomer addition and whether they were heat-treated. Of the latex films heated for 30 minutes at 70°C, the latex copolymers F and G, prepared by seeded batch and batch polymerization, were found to be totally insoluble in these solvents at room temperature. In contrast, for the latex films A to E, prepared by semi-continuous polymerization, the solubility varied from totally soluble to partially insoluble with increasing monomer addition rate (R_a). The freshly made latex films A to G without heat-treatment were found to be more soluble than those

WITHOUT HEAT TREATMENT

SAMPLE*	DIOXANE	MEK	DMF	MC	NB	TOL	THF	NMP
A	S	S	S	S	S	S	S	S
B								
C								
D								
E								
F	P.S	I.S	P.S	I.S	I.S	I.S	P.S	P.S
G	P.S	I.S	P.S	I.S	I.S	I.S	P.S	P.S

WITH HEAT TREATMENT

SAMPLE*	DIOXANE	MEK	DMF	MC	NB	TOL	THF	NMP
A	S	P.S	S	P.S	S	P.S	S	S
B	S	P.S	S	P.S	-	P.S	S	S
C	S	P.S	S	P.S	-	P.S	S	S
D	S	P.S	P.S	P.S	-	P.S	P.S	S
E	P.S	P.S	P.S	P.S	-	P.S	P.S	S
F	I.S	I.S	I.S	I.S	I.S	I.S	I.S	I.S
G	I.S	I.S	I.S	I.S	I.S	I.S	I.S	I.S

* 0.2 g polymer in 3 ml solvent at room temperature; S soluble; P.S partially soluble; I.S insoluble.

MEK methyl ethyl ketone; DMF dimethyl formamide;
MC methylene chloride; NB nitrobenzene;
TOL toluene; THF tetrahydrofuran;
NMP N-methyl pyrrolidinone.

Table 4-6: Solubility of 83:17 VDC-BMA copolymer latex films.

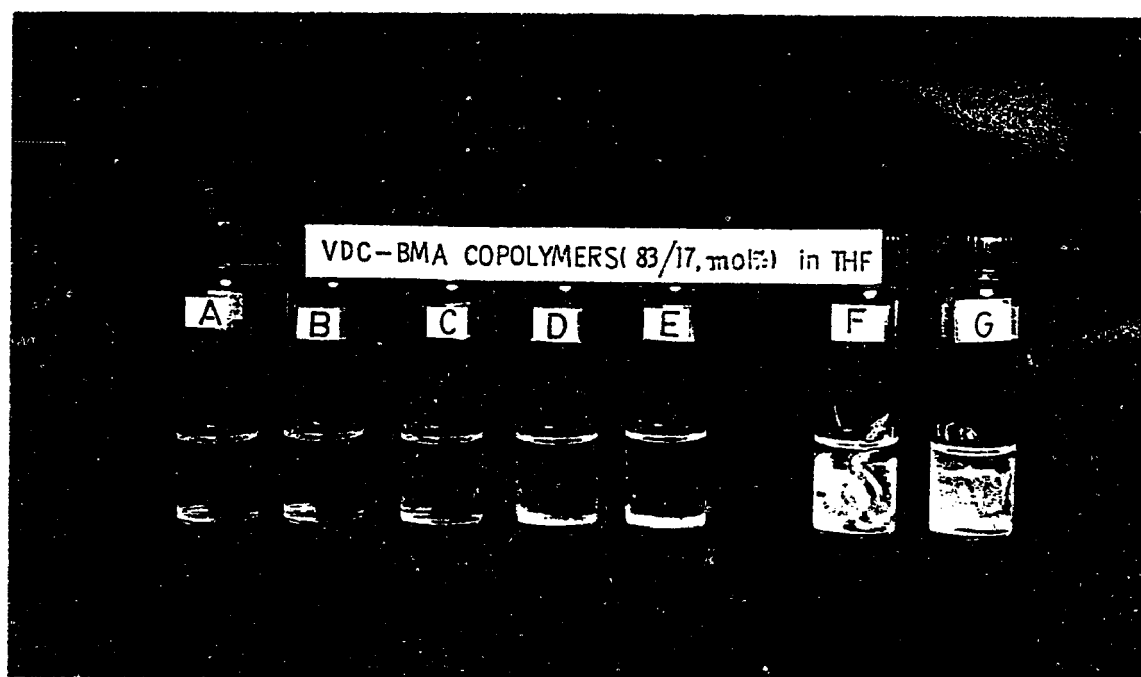


Figure 4-29: Solubility of 83:17 VDC-BMA copolymer latex films in tetrahydrofuran.

after heat-treatment, as shown in Table 4.6. The latex film A, prepared by semi-continuous polymerization with the slowest feed rate, was totally soluble in these solvents. Furthermore, the latex films F and G, prepared by seeded batch and batch polymerization, were partially soluble or totally insoluble in these solvents. The results indicate that the freshly made latex films A to G tended to be more soluble or more amorphous in character, and became less soluble with time at room temperature. THF, DMF, toluene, NMP, and dioxane were found to be relatively good solvents for the latex films of 83:17 VDC-BMA copolymers prepared by semi-continuous polymerization at room temperature.

In summary, the solubility of the latex films varied inversely with their crystallinity. The results of the solubility behavior of these latex films in these solvents coincided well with those of other measurements previously described.

4.2.2.8 Water Vapor Transmission Rates (WVTR) of 83:17 VDC-BMA Copolymer Latex Films

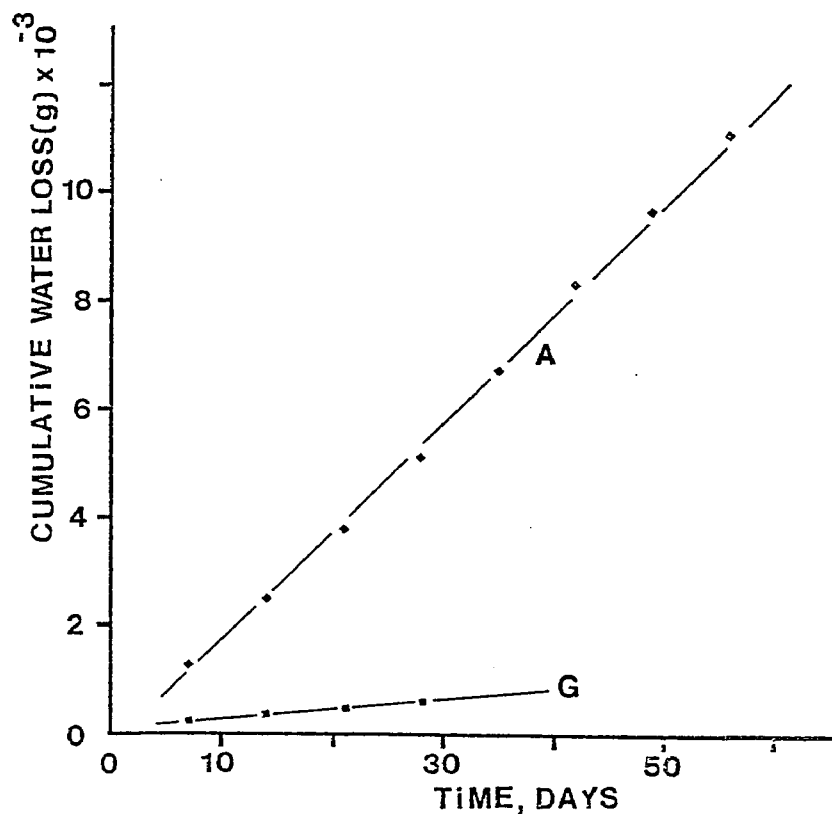


Figure 4-30: Water vapor transmission rates of 83:17 VDC-BMA latex films A and G.

One of the most valuable properties of vinylidene chloride copolymers is their good barrier properties against most gases and vapors. The barrier properties of polymers are in general related to the crystallinity and the molecular structure of the polymers (69).

A considerable difference was found in the water vapor transmission rates (WVTR) of the latex films A and G, prepared by semi-continuous polymerization with the slowest monomer feed rate and by batch polymerization,

respectively, as shown in Figure 4.30 and Table 4.12 in page 142. Latex film G had a WVTR about 12 times lower than latex film A. This result indicates that the presence of crystallites in latex film G improved the barrier properties by acting as a nonporous filler in the composite system (78).

4.2.2.9 Determination of the Aspect Ratio of the Crystallites, L/W

Assuming that the crystallites present in the VDC-BMA copolymer latex films act as a reinforcing filler, the aspect ratio of the crystallites present in 83:17 VDC-BMA copolymer latex film (G) prepared by the batch polymerization was determined the using modified Nielsen equation (79, 80).

$$P_c/P_p = V_p/[1+(L/2W)V_f] \quad (4.1)$$

where P_c/P_p is the ratio of permeability in the filled (P_c) to the unfilled system (P_p), V_f is the volume fraction of polymer, V_p the volume fraction of filler, and L/W the aspect ratio of the crystallites.

The value of V_f was replaced by the percent crystallinity of the latex film G, prepared by the batch polymerization, determined by the heat of fusion method using DSC, as described in section 3.4.5. The determined value was 13.7%. The values of P_c and P_p were replaced by the values of WVTR of the latex films G and A, respectively, prepared by the batch and semi-continuous polymerization with the slowest feed rate. The aspect ratio calculated using the modified Nielsen equation was about 140, indicating that the shape of the crystallites in the 83:17 VDC-BMA copolymer latex film G, prepared by the batch polymerization might be a fibrillar with a length-to-width ratio of 140.

4.3 Syntheses of 60:40 and 33:67 VDC-BMA Copolymer Latexes by Batch and Semi-continuous (R_a 0.27 wt%/minute) Polymerization, as well as Poly(vinylidene chloride) and Poly(butyl methacrylate) Latexes by Batch Polymerization

In addition to the syntheses of 83:17 VDC-BMA copolymer latexes described in section 4.2, 60:40 and 33:67 VDC-BMA copolymer latexes were prepared by batch and seeded semi-continuous (R_a 0.27 wt%/minute) polymerization. Vinylidene chloride and n-butyl methacrylate homopolymer latexes were also prepared by the conventional batch polymerization. The preparation of these latexes used the same recipe and polymerization conditions which were used as in the preparation of the 83:17 VDC-BMA copolymer latexes. The emulsion copolymerizations gave almost 100% conversion and the latexes were stable with negligible amounts of coagulum.

4.3.1 Particle Size and Particle Size Distribution

Table 4-7: Particle sizes of VDC-BMA latexes.

LATEX COMPOSITION VDC/BMA, mol%	BATCH (nm)			SEMI-CONT (nm)		
	D_n	D_w	D_w/D_n	D_n	D_w	D_w/D_n
1) 100/0	77	82	1.057	-	-	-
2) 83/17	113	116	1.020	121	124	1.024
3) 60/40	125	128	1.025	127	130	1.018
4) 33/67	162	164	1.010	136	139	1.022
5) 0/100	168	171	1.017	-	-	-

Table 4.7 shows the average particle diameters of the latexes prepared by both batch and semi-continuous polymerization, determined by transmission electron microscopy. The number-average particle diameter of the latexes

prepared by seeded semi-continuous polymerization increased with increasing amount of butyl methacrylate in the monomer composition, from 121 nm to 136 nm; all latexes had narrow particle size distributions, indicating that apparently no secondary nucleation took place after the seed formation. The use of 10 wt% monomer for seeding ensured that most of the emulsifier was adsorbed on the particle surface. Also, the number-average particle diameters of the latexes prepared by the batch polymerization increased with increasing amount of butyl methacrylate in the monomer composition, from 77 nm for poly(vinylidene chloride) to 168 nm for poly(butyl methacrylate), all with narrow particle size distributions. Transmission electron micrographs of the VDC-BMA copolymer latexes prepared by batch polymerization are shown in Figure 4.31. The number of particles increased with increasing amounts of vinylidene chloride in the VDC-BMA copolymerization. This might be explained by the higher water solubility of vinylidene chloride and the mechanism of homogeneous nucleation in the aqueous phase. Therefore, in VDC-BMA copolymerization, the number of nuclei generated would be proportional to the content of vinylidene chloride in the monomer mixture.

Figure 4.32 shows a transmission micrograph of poly(vinylidene chloride) latex particles. The particles are spheroidal in shape and their surfaces are rough. The same type of morphology for poly(vinylidene chloride) latex particles has been reported by Wessling et al. (42). They studied the morphology of poly(vinylidene chloride) latex particles using electron microscopy and X-ray diffraction and tried to determine whether the crystallization takes place during or after the polymerization. They concluded that this morphology was developed in the colloidal state by crystallization during polymerization.

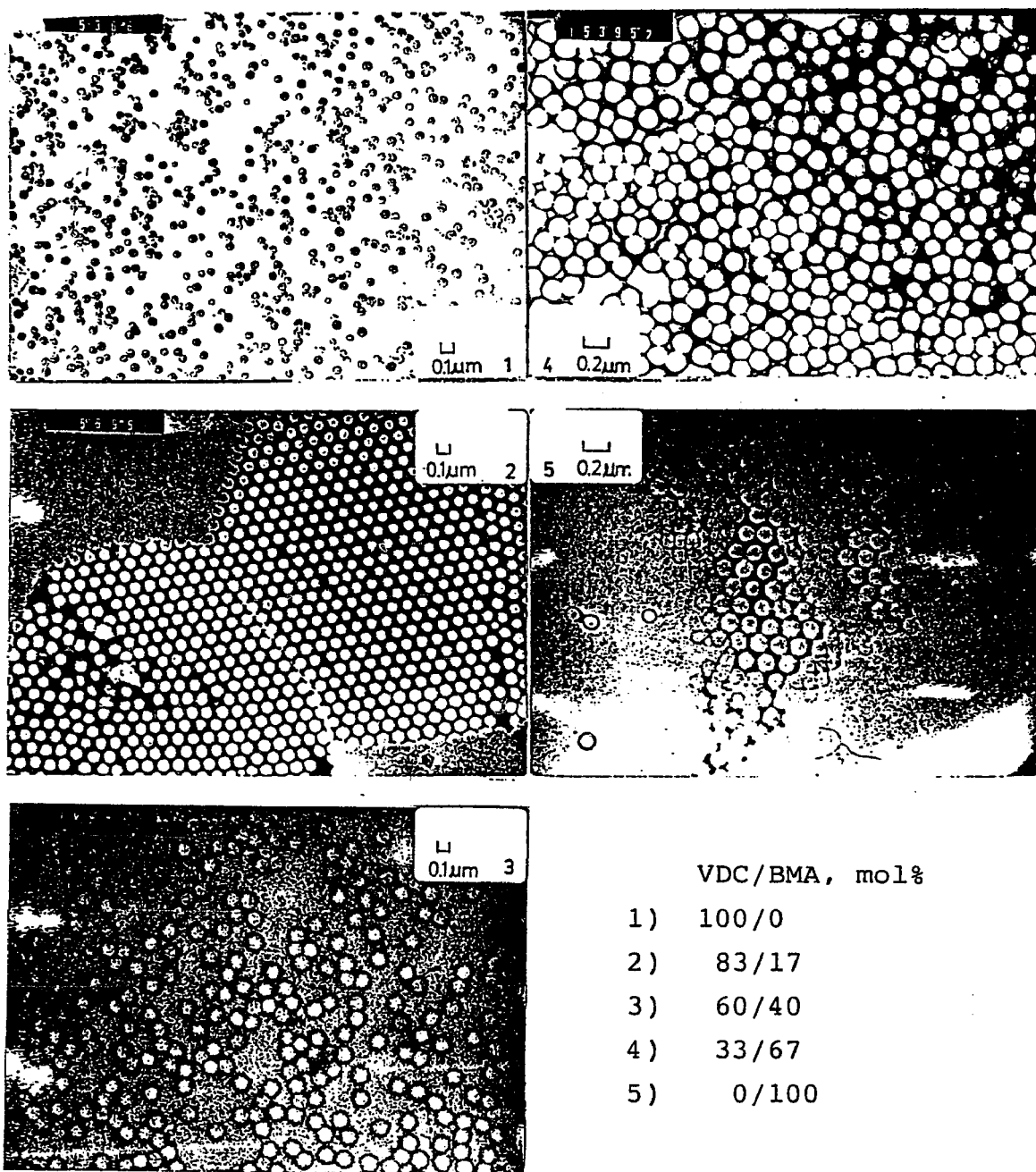


Figure 4-31: Transmission electron micrographs of VDC-BMA copolymer latexes prepared by batch polymerization.

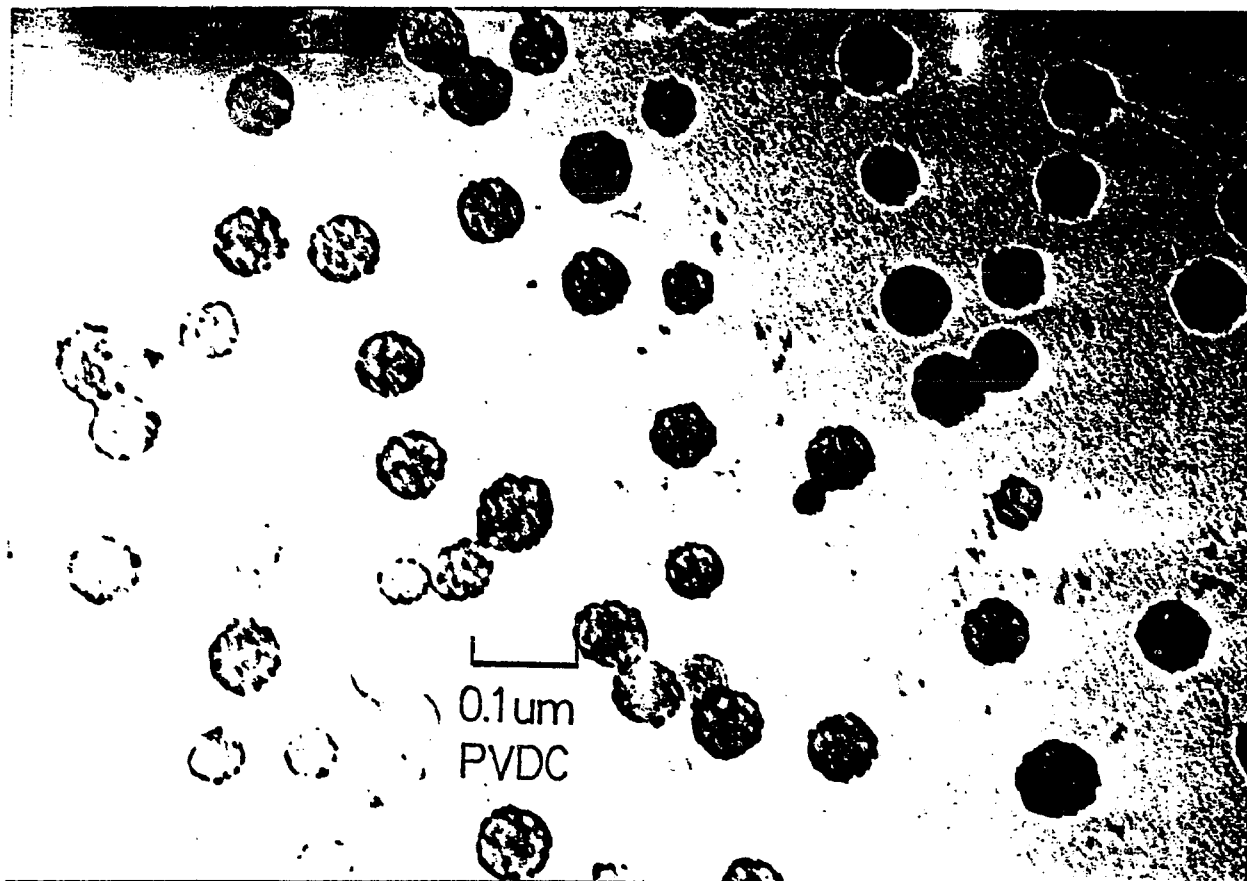


Figure 4-32: Transmission electron micrograph of poly(vinylidene chloride) latex particles.

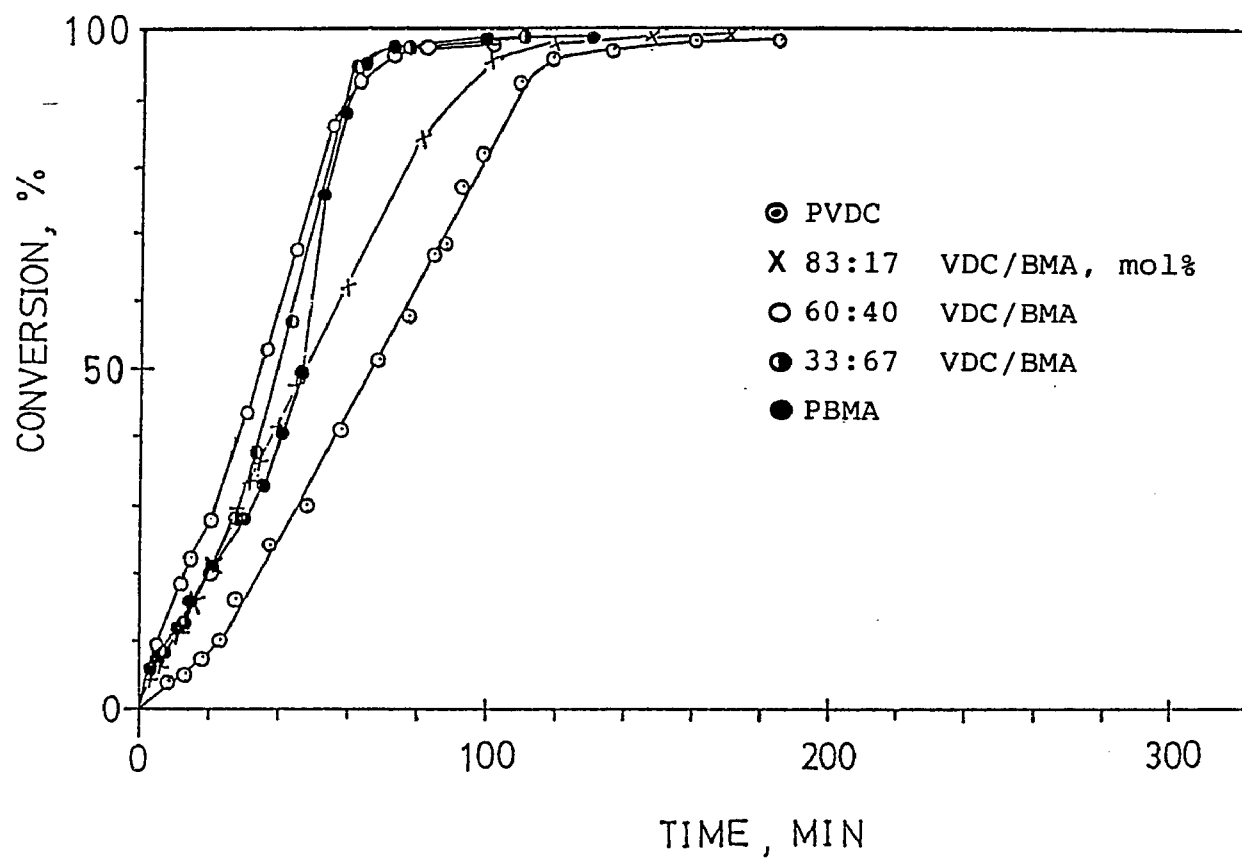


Figure 4-33: Conversion-time curves for VDC-BMA batch copolymerizations.

Table 4-8: Rates of polymerization in VDC-BMA batch copolymerizations.

RATES OF POLYMERIZATION AT THE BEGINNING OF SECOND STAGE OF BATCH POLYMERIZATION

VDC/BMA	$R_p \times 10^4 *$	$N_p / l \times 10^{-17}$	$R_{pp} \times 10^{21} **$
100/0	5.87	8.56	0.69
83/17	5.79	2.89	2.00
60/40	8.14	2.35	3.46
33/67	4.55	1.20	3.79
0/100	6.06	1.27	4.77

RATES OF POLYMERIZATION AT THE END OF SECOND STAGE OF BATCH POLYMERIZATION

VDC/BMA	$R_p \times 10^4 *$	$R_{pp} \times 10^{21} **$
100/0	5.87	0.69
83/17	6.08	2.10
60/40	9.33	3.97
33/67	9.34	7.78
0/100	16.05	12.64

R_p : overall rate of polymerization

* : $\text{mol} \cdot \text{l}^{-1} \cdot \text{sec}^{-1}$

R_{pp} : rate of polymerization per particle

** : $\text{mol} \cdot \text{particle}^{-1} \cdot \text{sec}^{-1}$

N_p : number of particles/unit volume

Figure 4.33 shows the conversion-time curves determined by gravimetry for the VDC-BMA batch copolymerizations. For the VDC and 83:17 VDC-BMA polymerizations, an oily flow appeared on the wall of the reaction flask during the polymerization, which resulted from the coalescence of monomer droplets owing to the shortage of emulsifier (23-27). However, the slowdown in polymerization rate at the beginning of the second stage in these conversion-time curves was not observed in the present study. That might be due to the experimental error.

In general, emulsion polymerization consists of three stages based on the particle number and the existence of a separate monomer phase. By the end of stage I, all of the micelles have disappeared, and the particle nucleation is completed. In VDC-BMA polymerizations, homogeneous nucleation was favored for VDC emulsion homopolymerization, both homogeneous and micellar nucleation in VDC-BMA emulsion copolymerizations, and micellar nucleation in BMA emulsion homopolymerization. In stage II, polymerization proceeds in a fixed number of latex particles with constant overall rate of polymerization as the monomer concentration in the particle is maintained at the saturation level by diffusion of monomer from the monomer droplet. This stage ends when all monomer droplets disappear. In VDC-BMA polymerizations, the transition from stage II to stage III occurred at progressively lower conversions, and the length of stage II was also progressively shorter, as the amount of BMA in monomer mixture was increased, indicating that the extent of swelling of the polymer particles by monomer plays an important role in stage II of VDC-BMA copolymerizations. In stage III, the monomer droplets are no longer present, and the monomer concentration in latex particles decreases with time. Therefore, the

overall rate of polymerization begins to deviate from linearity. This effect is partially obscured by the gel (Trommsdorff) effect, which becomes more prevalent with increasing BMA concentration. Table 4.8 shows the rate of polymerization R_p and rate of polymerization per particle R_{pp} at the beginning and end of stage II of the polymerizations. The rate of polymerization was determined from the slope of the conversion-time curves, and the rate of polymerization per particle was obtained from the ratio of the overall rate of polymerization to the number of latex particles. The rate of polymerization per particle increased with increasing butyl methacrylate concentration in the monomer mixture, and the particle number density was the dominant factor for the overall rate of polymerization. The extent of the autoacceleration increased with increasing concentration of butyl methacrylate.

4.3.2 Characterization of VDC-BMA Latex Copolymers

4.3.2.1 Molecular Weight and Molecular Weight Distribution

Table 4-9: Average molecular weight and molecular weight distribution.

VDC/BMA mol%	BATCH $\times 10^{-5}$			SEMI-CONT $\times 10^{-5}$		
	M_n	M_w	M_w/M_n	M_n	M_w	M_w/M_n
100/0	-	-	-	-	-	-
83/17	-	-	-	0.10	0.40	4.04
60/40	0.30	5.60	18.79	0.11	0.41	3.71
33/67	0.28	5.80	20.71	0.24	2.00	8.37
0/100	0.67	9.40	14.13	-	-	-

Table 4.9 shows the average molecular weights of the vinylidene chloride-butyl methacrylate copolymers prepared by batch and semi-continuous polymerization, determined by gel permeation chromatography. The determination of the molecular weights of the poly(vinylidene chloride) and the 83:17 VDC-BMA copolymer prepared by batch polymerization was impossible because of their insolubility at room temperature. Both the number-average and weight-average molecular weights of the copolymers prepared by seeded semi-continuous polymerization were lower than those of their batch counterparts, which can be explained by the lower monomer concentration during the semi-continuous polymerizations. The VDC-BMA latex copolymers prepared by batch polymerization were also found to have broader molecular weight distributions than their semi-continuous counterparts. This phenomenon might be due to the occurrence of the composition drift in the batch polymerization, resulting in BMA-rich copolymers of high molecular weight at the beginning and VDC-rich

copolymers of lower molecular weight at the end of polymerization.

4.3.2.2 Infrared Spectra of VDC-BMA Latex Films

Figure 4.34 shows the infrared spectra of VDC-BMA copolymer latex films prepared by both batch and semi-continuous polymerization, heated for 30 minutes at 70°C. Poly(vinylidene chloride) and the 83:17 VDC-BMA latex copolymers F and G (see Figure 4.9) prepared by batch polymerization showed the characteristic crystalline peaks, whereas none of the other spectra in Figure 4.34 showed these peaks, indicating that all of the VDC-BMA copolymers were amorphous except for the 83:17 VDC-BMA copolymers F and G.

4.3.2.3 X-ray Powder Diffraction of VDC-BMA Copolymer Latex Films

Figures 4.35 and 4.36 show the X-ray diffraction patterns and Debye-Scherrer ring patterns of VDC-BMA copolymer latex films prepared by both batch and semi-continuous polymerization and heated for 30 minutes at 70°C. Poly(vinylidene chloride) and the 83:17 VDC-BMA copolymers F and G, prepared by batch polymerization, showed diffraction peaks and regular ring patterns characteristic of crystallinity. However, none of the other copolymers showed peaks or regular ring patterns, indicating that these copolymers were amorphous in character. These results are consistent with the results of the infrared spectroscopy.

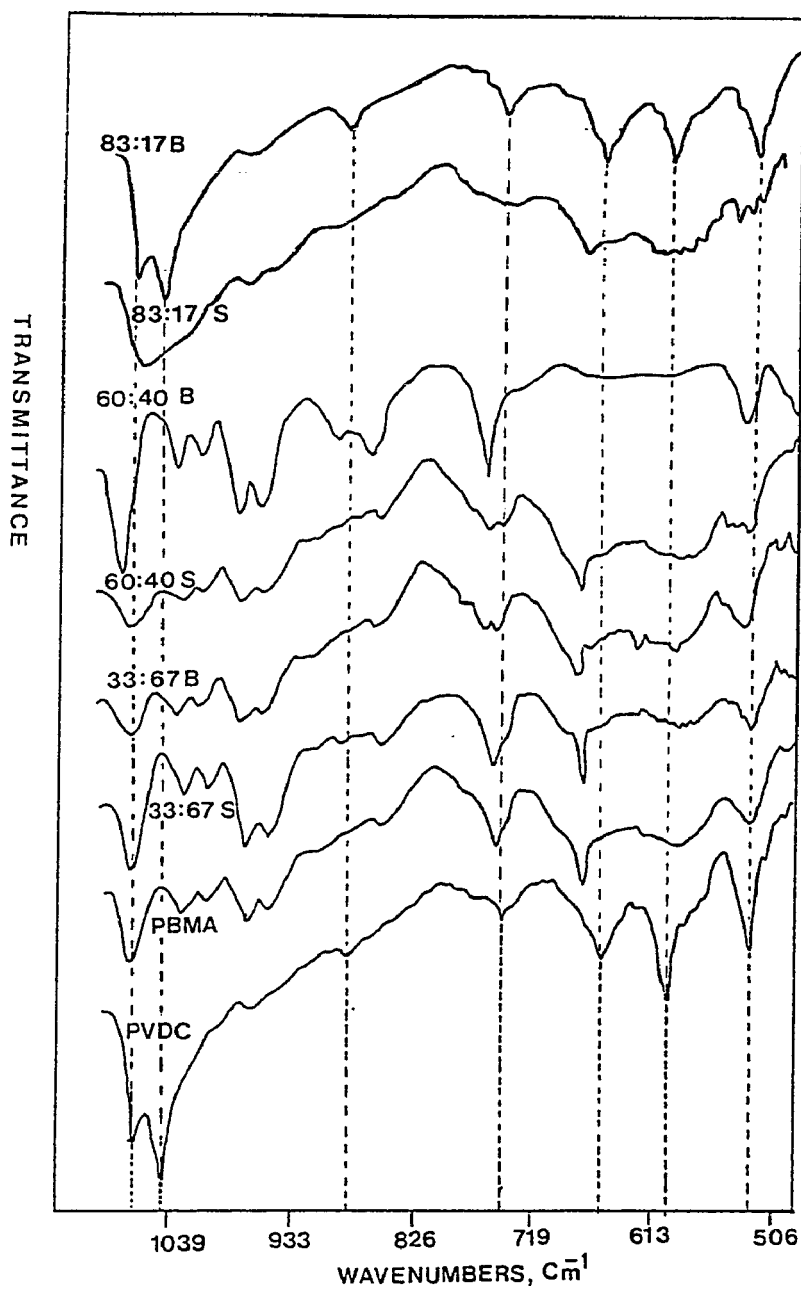


Figure 4-34: Infrared spectra of VDC-BMA copolymer latex films:
(B) batch; (S) semi-continuous polymerization.

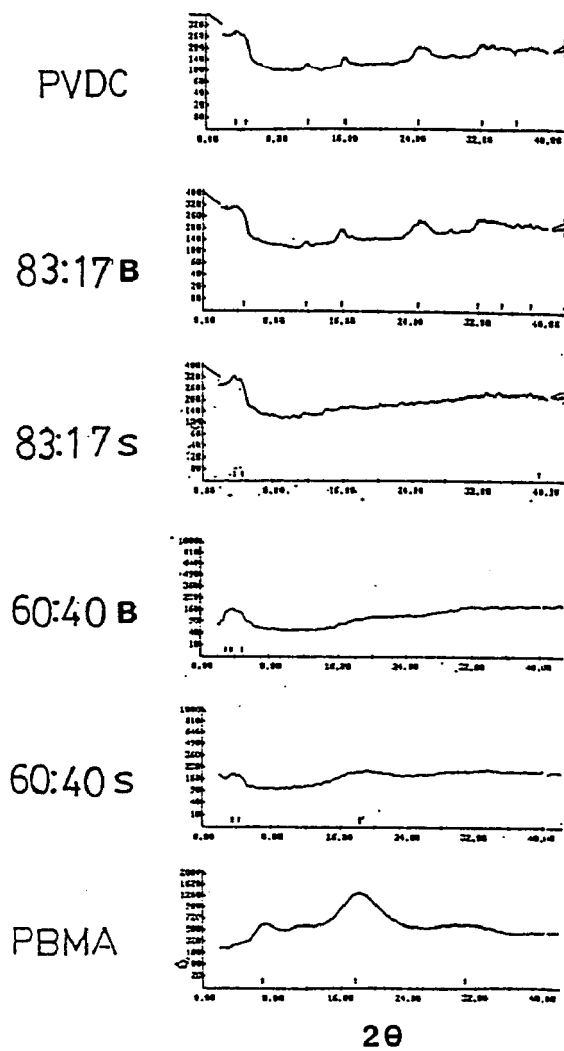


Figure 4-35: X-ray diffraction patterns of VDC-BMA copolymer latex films: (B) batch; (S) semi-continuous polymerization.

PVDC



83:17 B



60:40 B



33:67 B



PBMA



Figure 4-36: Debye-Scherrer ring patterns of VDC-BMA copolymer latex films.

4.3.2.4 T_g , T_m , and MFFT Values

Table 4-10: T_g , T_m , and MFFT of VDC-BMA copolymer latex films.

(°C)	PVDC	83:17		60:40		33:67		PBMA
		S	B	S	B	S	B	
T_g^*	5.9	16.3	24.2	33.0	32.0	39.2	38.8	38.1
T_g^{**}	-	30.9	41.3	46.0	44.3	54.4	54.9	47.5
MFFT	-	+	+	23.9	24.9	33.6	33.3	34.1
T_m^*	199.0	=	187.0	=	=	=	=	=

* determined by DSC; heating rate 20°C/min

** determined by Rheovibron at 110 Hz

+ lower than 5°C

= no T_m observed

S semi-continuous process

B batch process

Table 4.10 shows the glass transition temperature (T_g) and crystalline melting temperature (T_m) of VDC-BMA copolymer latex films prepared by both batch and semi-continuous polymerization, heated for 30 minutes at 70°C, as determined by DSC and dynamic mechanical spectroscopy. Also, the MFFT values for these latexes are presented. The differences in T_g between copolymers prepared by batch and semi-continuous polymerization decreased with increasing amount of butyl methacrylate, i.e., 8-9°C for the 83:17, 1-2°C for the 60:40, and 0-1°C for the 33:67 VDC-BMA copolymers, indicating differences in their sequence distributions.

None of the VDC-BMA copolymers showed a crystalline melting temperature, except the 83:17 VDC-BMA copolymers F and G, prepared by seeded batch and batch polymerization. The values of T_m were 184°C for

copolymer F and 187°C for copolymer G. The T_m value of the 83:17 VDC-BMA copolymer G was lower than the 199°C value for poly(vinylidene chloride). The difference in T_m between these polymers might be due to the difference in crystallite size resulting from different vinylidene chloride sequence lengths in the polymer chains. The percents crystallinity of PVDC and the 83:17 VDC-BMA copolymers, prepared by batch and seeded batch polymerization, determined by DSC as described in section 3.4.5. were 45, 13.7, and 12 %, respectively.

It is interesting to note that these VDC-BMA copolymers prepared by batch polymerization have a T_g maximum at around 39.0°C for the 30:70 VDC-BMA copolymer, as shown in Figure 4.37. The T_g of the VDC-BMA copolymers increased with increasing butyl methacrylate content and reached a T_g maximum and leveled off. Many investigators (81-86) reported a pronounced T_g maximum and T_g minimum in vinylidene chloride copolymer systems. The cause of the T_g maximum in vinylidene chloride-acrylates copolymer systems has been also the subject of some discussion (83-86). Wessling (83) considered the possibility that the increase in T_g at low comonomer level results from a loss of chain symmetry. Wood (85) proposed that the acrylate groups interfere sterically with the free rotation of the poly(vinylidene chloride) chain. Both Barton (86) and Ellerstein (84) suggested that chain stiffening results from polar interactions between chlorine and oxygen substituents. Therefore, the T_g maximum observed in Figure 4.37 can be explained as the result of these effects. The introduction of butyl methacrylate units into a poly(vinylidene chloride) chain increases stiffness and destroys symmetry. Therefore, the T_g rises with butyl methacrylate content. But, finally the symmetry of the polymer chain is destroyed completely, all possible polar interactions are satisfied, and at this monomer

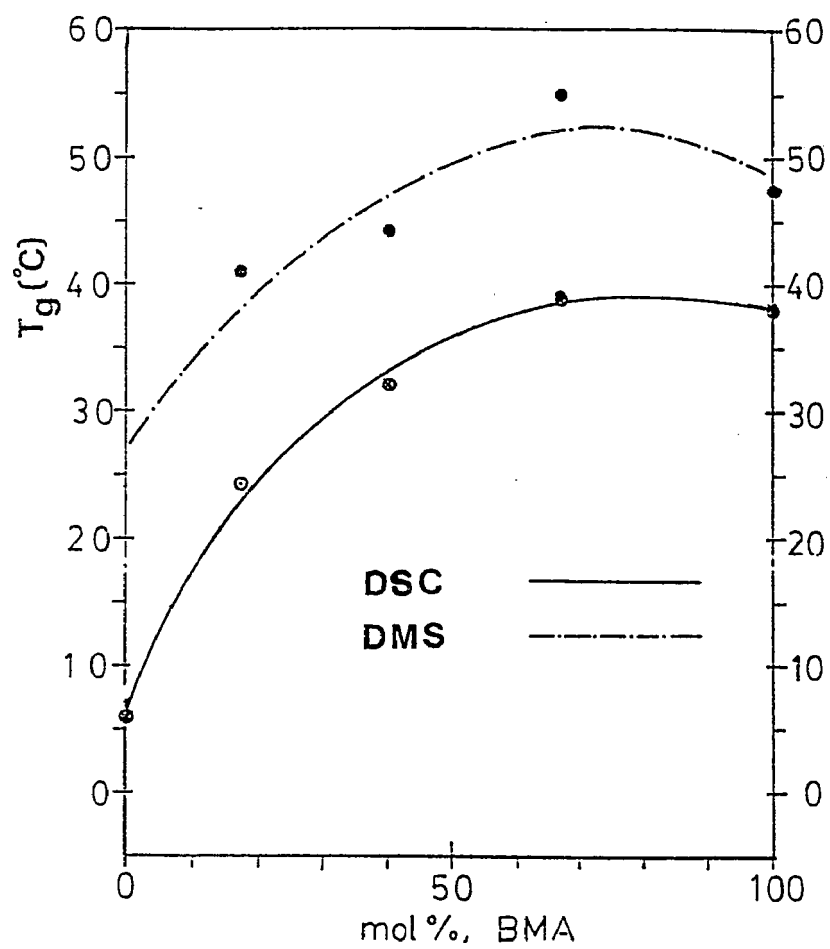


Figure 4-37: Variation of T_g with composition for VDC-BMA batch copolymers.

composition, the copolymer shows a maximum T_g . Further increase in methacrylate content reduces the possibilities for dipole interactions, and T_g falls toward the value of the butyl methacrylate homopolymer.

4.3.2.5 Tensile Properties of VDC-BMA Copolymer Latex Films

Table 4-11: Tensile properties of VDC-BMA copolymer latex films.

SAMPLES	83:17		60:40		33:67		PBMA
	S*	B	S	B	S	B	
Young's modulus, $E^{a,b}$ (MPa)	3.4	296.3	274.2	294.2	314.2	359.0	370.7
ultimate strength, $\sigma^{b,u}$ (MPa)	1.3	8.4	19.3	20.2	24.5	24.1	13.7
elongation to break, ϵ (%)	588	87	228	234	91	42	6
energy to break, τ^b (MJ/m ³)	15.6	6.1	32.8	34.4	11.5	3.1	0.4

a : determined from the initial slope of the stress-strain curve

b : based on the initial cross-sectional area

S : semi-continuous process

B : batch process

* monomer feed rate: 0.27 wt%/minute (sample A)

Table 4.11 shows measurements of tensile strength for the VDC-BMA copolymer latex films. As previously described in section 4.2.2.6., a significant difference was found for the 83:17 VDC-BMA latex films, depending on the method of monomer addition. The latex films prepared by semi-continuous polymerization were flexible and tough, while the latex films prepared by batch and seeded batch polymerization were strong and brittle. For the 60:40 VDC-BMA copolymer latex films prepared by both batch and semi-continuous polymerization, the tensile properties were found to be similar, irrespective of the polymerization process. However, for the 33:67 VDC-BMA copolymer latex

films, those prepared by batch polymerization showed higher moduli, lower percents elongation and lower energies to break, resembling poly(butyl methacrylate).

4.3.2.6 Solubility of Latex Films in THF

The solubility behavior of the VDC-BMA copolymer latex films in tetrahydrofuran (THF) also showed the existence of significant differences depending on the polymerization methods and comonomer composition, as shown in Figures 4.38 and 4.39. All of the latex films prepared by seeded semi-continuous polymerization were found to be completely soluble in THF, irrespective of the monomer composition, indicating that the copolymers were amorphous and the copolymer composition homogeneous. In contrast, the latex films prepared by batch polymerization showed different behavior depending on the monomer composition. The amount of insoluble polymer increased with increasing VDC content, indicating an increase in the degree of crystallinity and a more heterogeneous copolymer composition.

4.3.2.7 WVTR Values of VDC-BMA Copolymer Latex Films

Table 4.12 shows the values of the WVTR of VDC-BMA copolymer latex films prepared by both batch and semi-continuous polymerization, heated for 30 minutes at 70°C. In general, the value of the WVTR decreased with increasing amount of vinylidene chloride in the copolymer, and the values of the WVTR of the latex films prepared by batch polymerization were smaller than those of their semi-continuous counterparts. The values of the WVTR determined in the present study are in good agreement with those reported elsewhere as shown in Table 4.12 (70). The reported values for VDC copolymers containing 60-90 mol% VDC in the monomer mixture are in the range 1.5×10^{-8} to 7.2×10^{-7}

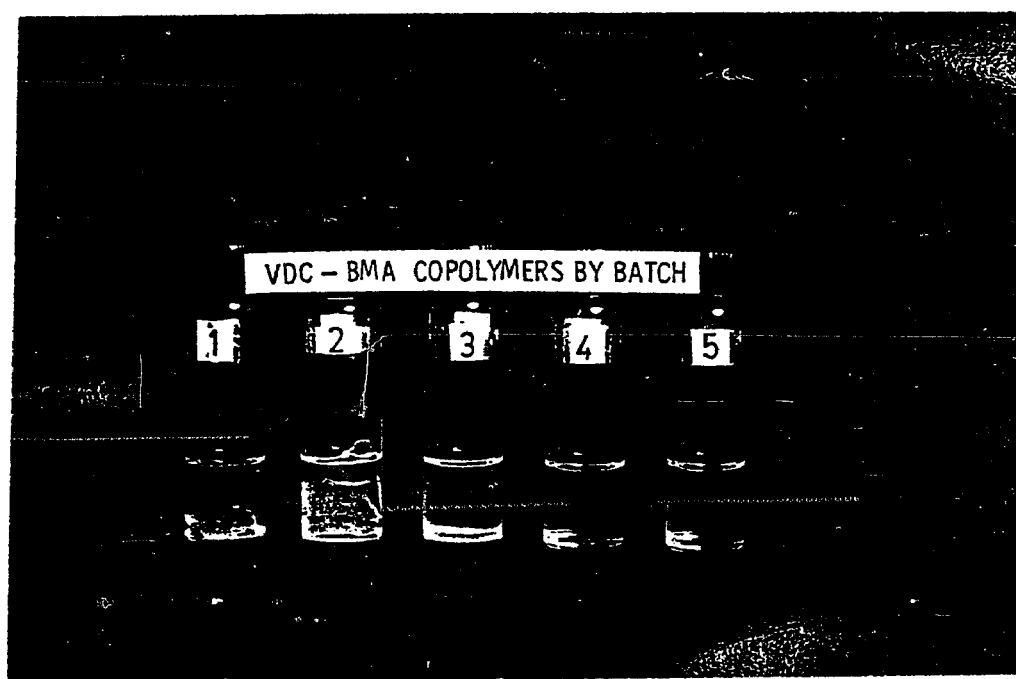


Figure 4-38: Solubility in THF of VDC-BMA copolymer latex films prepared by batch polymerization:
(1) PVDC; (2) 83:17; (3) 60:40; (4) 33:67; (5) PBMA.

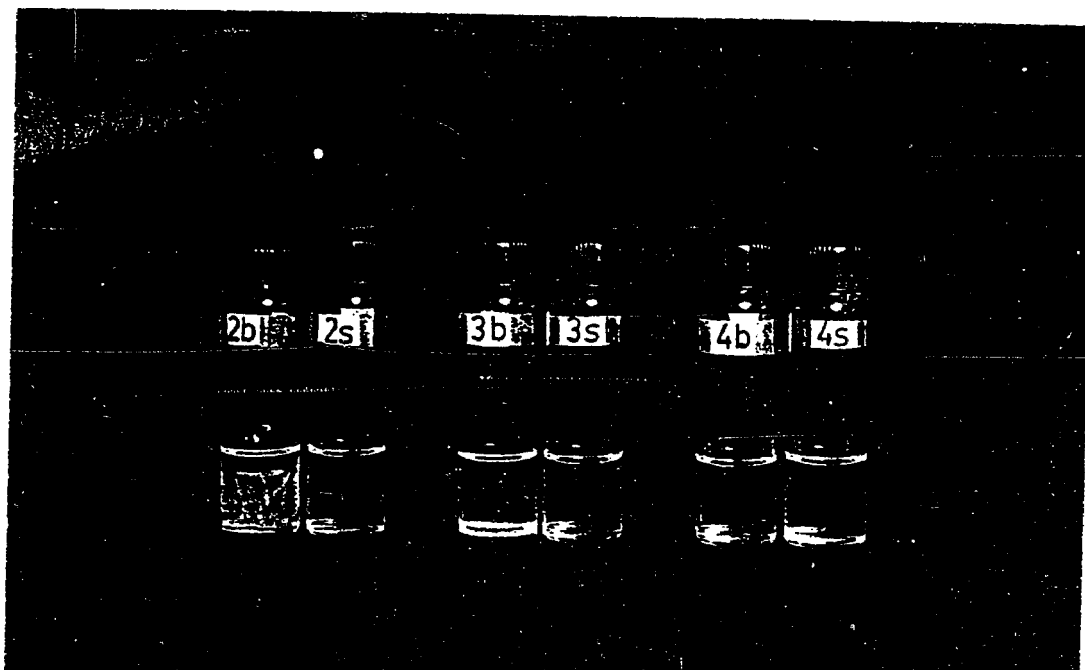


Figure 4-39: Solubility in THF of VDC-BMA copolymer latex films prepared by (b) batch and (s) semi-continuous polymerization : (2) 83:17; (3) 60:40; (4) 33:67 VDC-BMA.

Table 4-12: WVTR values of VDC-BMA copolymer latex films.

$\times 10^8 (\text{gm} \cdot \text{mil} / \text{cm}^2 \cdot \text{min})$						
83:17		60:40		33:67		PBMA
S	B	S	B	S	B	
19.6	1.6	143.0	91.9	335.0	177.0	350.0

g-mil/cm²-min, in good agreement with the 1.6×10^{-8} and 9.2×10^{-7} g-mil/cm²-min obtained in the 83:17 and 60:40 mol% VDC-BMA latex films prepared by batch polymerization in this study.

4.3.2.8 Surface Characterization of VDC-BMA Copolymer Latexes

The surface groups of the VDC-BMA copolymer latexes are derived from two main sources: (1) the initiator fragments and their hydrolysis and oxidation products (sulfonate, sulfate, hydroxyl, and carboxyl groups); and (2) the hydrolysis of the methacrylate ester in the polymer chains (carboxyl groups).

It is well known (2, 74) that the surface concentration of acid endgroups is dependent on (1) the average molecular weight and the molecular weight distribution of the polymer; (2) the degree of hydrolysis of the sulfate endgroups and their oxidation to carboxyl groups during the polymerization; and (3) the extent to which the endgroups have become buried beneath the surface.

Table 4-13: Surface characterization of cleaned VDC-BMA copolymer latexes.

LATEX COMPOSITION VDC/BMA (mol%)	CONCENTRATION OF END GROUPS ($\mu\text{eq/g polymer}$)		TOTAL	SURFACE CHARGE DENSITY ($\mu\text{C/cm}^2$)	
	STRONG	WEAK		STRONG	WEAK
	ACID	ACID		ACID	ACID
<u>BATCH PROCESS</u>					
100/0	11.98	11.06	23.04	2.61	2.41
83/17	10.50	8.10	18.60	3.11	2.40
60/40	10.01	7.87	17.88	2.95	2.32
33/67	10.20	6.49	16.69	3.40	2.17
0/100	16.00	5.20	21.20	4.55	1.48
<u>SEMI-CONTINUOUS PROCESS</u>					
83/17	10.00	12.00	22.00	3.17	3.80
60/40	10.50	7.76	18.26	3.15	2.33
33/67	11.20	6.49	17.69	3.14	1.82

Table 4.13 shows the results of the surface characterization of cleaned VDC-BMA copolymer latexes prepared by both batch and semi-continuous polymerization. These latexes were cleaned with distilled-deionized-water (DDI) using the serum replacement technique described in section 3.4.12. For latexes

prepared by batch polymerization, the surface charge density derived from the strong-acid groups decreased, and the surface charge density derived from the weak-acid groups increased, with increasing vinylidene chloride content in the copolymer. This phenomenon might be due to the catalytic effect of hydrochloric acid (generated by the degradation of the vinylidene chloride units) and of sulfuric acid (generated from the hydrolysis of the sulfate end groups) on the hydrolysis of strong-acid groups and probably the oxidation reaction of the hydroxyl groups. The determination of the number- and weight-average molecular weights of VDC-BMA copolymers by gel permeation chromatography, described in section 4.3.2.1, showed that the semi-continuous copolymers have lower number- and weight-average molecular weights than the batch copolymers, suggesting that the semi-continuous copolymers should, on the average, have a larger number of acid endgroups per unit weight of the polymer.

For latexes prepared by semi-continuous polymerization, the concentration of both strong- and weak-acid groups was found to be similar to those in the batch latexes. However, taking into consideration the possibility of a high degree of burial of acid endgroups inside the particles and the longer reaction times, it is likely that the semi-continuous copolymer latexes have higher concentrations ($\mu\text{eq/g polymer}$) of surface acid endgroups than the batch copolymer latexes.

Table 4.14 shows the results of the surface characterization of cleaned VDC-BMA latexes after heat treatment for 24 hours at 85°C. The reason for choosing 85°C for the experiment is that, after 24 hours at this temperature, the poly(vinylidene chloride) latex became discolored, changing from blue-white to yellow. This indicates that some degradation took place with the evolution of hydrochloric acid and the formation of conjugated double bonds by vinylidene

Table 4-14: Surface characterization of cleaned VDC-BMA copolymer latexes heated for 24 hours at 85°C.

LATEX COMPOSITION VDC/BMA (mol%)	CONCENTRATION OF END GROUPS ($\mu\text{eq/g polymer}$)		TOTAL	SURFACE CHARGE DENSITY ($\mu\text{C/cm}^2$)	
	STRONG ACID	WEAK ACID		STRONG ACID	WEAK ACID
<u>BATCH PROCESS</u>					
100/0	5.65	22.44	28.09	1.23	4.89
83/17	6.75	17.74	24.49	2.00	5.26
60/40	7.27	16.30	23.57	2.14	4.80
33/67	9.26	13.07	22.33	3.09	4.57
0/100	10.27	15.24	25.52	2.92	4.32
<u>SEMI-CONTINUOUS PROCESS</u>					
83/17	8.25	14.77	23.02	2.61	4.68
60/40	8.58	13.75	22.33	2.58	4.12
33/67	8.12	14.73	22.85	2.28	4.14

chloride sequences in the copolymers. For the latexes prepared by batch polymerization, the surface charge density derived from the strong-acid endgroups decreased with increasing content of vinylidene chloride in the copolymer, and the surface charge density derived from the weak-acid endgroups did seem to increase with increasing content of vinylidene chloride in the copolymer. These results indicate that heat treatment for 24 hours at 85°C and H^+ generation resulted in the hydrolysis of both strong-acid endgroups and methacrylate ester groups, and probably the oxidation of the hydroxyl endgroups. The trends are consistent with the occurrence of a core-shell morphology in VDC-BMA copolymer latexes prepared by batch polymerization. On the other hand, for the latexes prepared by semi-continuous polymerization, the surface charge density derived from both strong- and weak-acid groups was virtually independent of the composition of the copolymers, indicating that the

semi-continuous copolymers have a more homogeneous composition on the surface of particles.

Table 4-15: Surface characterization of cleaned VDC-BMA copolymer latexes aged for four months.

LATEX COMPOSITION VDC/BMA (mol%)	CONCENTRATION OF END GROUPS ($\mu\text{eq/g polymer}$)		TOTAL	SURFACE CHARGE DENSITY ($\mu\text{C/cm}^2$)	
	STRONG ACID	WEAK ACID		STRONG ACID	WEAK ACID
	<u>BATCH PROCESS</u>				
100/0	6.92	11.95	18.87	1.51	2.60
83/17	8.13	10.60	18.73	2.41	3.14
60/40	7.52	9.74	17.26	2.22	2.87
33/67	9.01	11.54	20.55	3.00	3.85
0/100	8.45	9.60	18.05	2.40	2.72
<u>SEMI-CONTINUOUS PROCESS</u>					
83/17	8.53	14.77	23.30	2.70	4.68
60/40	9.21	12.90	22.11	2.77	3.87
33/67	9.14	11.30	20.44	2.57	3.17

Table 4.15 shows the results of the surface characterization of cleaned VDC-BMA copolymer latexes aged for four months at room temperature. For the latexes prepared by batch polymerization, the surface charge density derived from the strong-acid groups decreased with increasing amount of vinylidene chloride in the copolymer, and the surface charge density derived from the weak-acid groups was virtually independent of the composition of the copolymer. These results indicate that aging of the latexes at room temperature also resulted in the hydrolysis of both strong-acid endgroups and methacrylate ester groups, and probably the oxidation of the hydroxyl endgroups. On the other hand, for the latexes prepared by semi-continuous polymerization, the surface charge density derived from the strong-acid groups was virtually independent of the composition of the copolymer. The trends found are consistent with those

obtained in unaged latexes and the heat-treated latexes, as shown in Tables 4.13 and 4.14.

4.3.2.9 Determination of Copolymer Composition

Table 4-16: Composition of VDC-BMA copolymers.

EXPECTED COMPOSITION	Chlorine% in COPOLYMERS	ACTUAL COMPOSITION
VDC/BMA (mol%)	(Wt %)	VDC/BMA (mol%)
83/17		
(B)	53.46	79.8/20.2
(S)	52.89	79.3/20.7
60/40		
(B)	32.80	54.3/45.7
(S)	34.19	56.2/43.8
33/67		
(B)	15.67	28.5/71.5
(S)	15.82	28.8/71.2

(B) : Batch process

(S) : Semi-continuous process

Table 4.16 shows the average copolymer compositions determined by elemental chlorine analysis of the VDC-BMA copolymers. The copolymer compositions calculated from the percents chlorine are in relatively good agreement with the values expected for 100% conversion, and the copolymer compositions prepared by both processes are relatively close to each other.

4.3.2.10 Nuclear Magnetic Resonance Spectroscopy

It is well known that the microstructure and sequence distributions of copolymers are the most important factors to determine the physical and mechanical properties. ^{13}C NMR is usually the method for characterizing the monomer composition, sequence distributions, and microstructure of copolymers. In the present studies, ^{13}C NMR spectroscopy was used to determine the sequence distributions of VDC-BMA copolymers, prepared by batch and semi-continuous emulsion polymerization.

The 83:17 VDC-BMA copolymer prepared by batch polymerization did not dissolve in any of the solvents at room temperature. At temperatures above 130°C, however, it did dissolve in nitrobenzene, with serious degradation and discoloration, and the evolution of hydrochloric acid.

Figure 4.40 shows the ^{13}C solid-state NMR spectra of poly(vinylidene chloride) and 83:17 VDC-BMA copolymers prepared by batch and semi-continuous polymerization, respectively, using the cross-polarization (CP) technique (87), which allows the detection of the immobile regions of the sample (i.e., the crystallites and their surroundings), in which the strong dipolar interaction remains. The resolution of these spectra was much poorer than that determined by ^{13}C liquid NMR for the 83:17 VDC-BMA copolymer prepared by semi-continuous polymerization, as shown in Figure 4.41. This poor resolution gave unreliable measurements of the sequence distribution from solid-state NMR spectra. Figures 4.42 and 4.43 show the ^{13}C liquid NMR spectra of 50 wt% deuterated benzene-swollen or dissolved 83:17 and 60:40 VDC-BMA copolymers prepared by batch and semi-continuous polymerization, respectively. These spectra were obtained in a liquid one-pulse NMR experiment with magic angle spinning (high power proton-decoupling). It should be noted that the resolution of the spectra of these samples was much improved by using solvent-swollen samples, indicating that this technique yields much enhanced motion of the polymer molecules. It was also found that, for the 83:17 VDC-BMA copolymers, the semi-continuous sample gave a better signal-to-noise ratio than its batch counterpart, as shown in Figure 4.42, suggesting that the batch sample showed less molecular motion than the semi-continuous sample owing to the presence of crystallites in the batch sample. Table 4.17 shows the

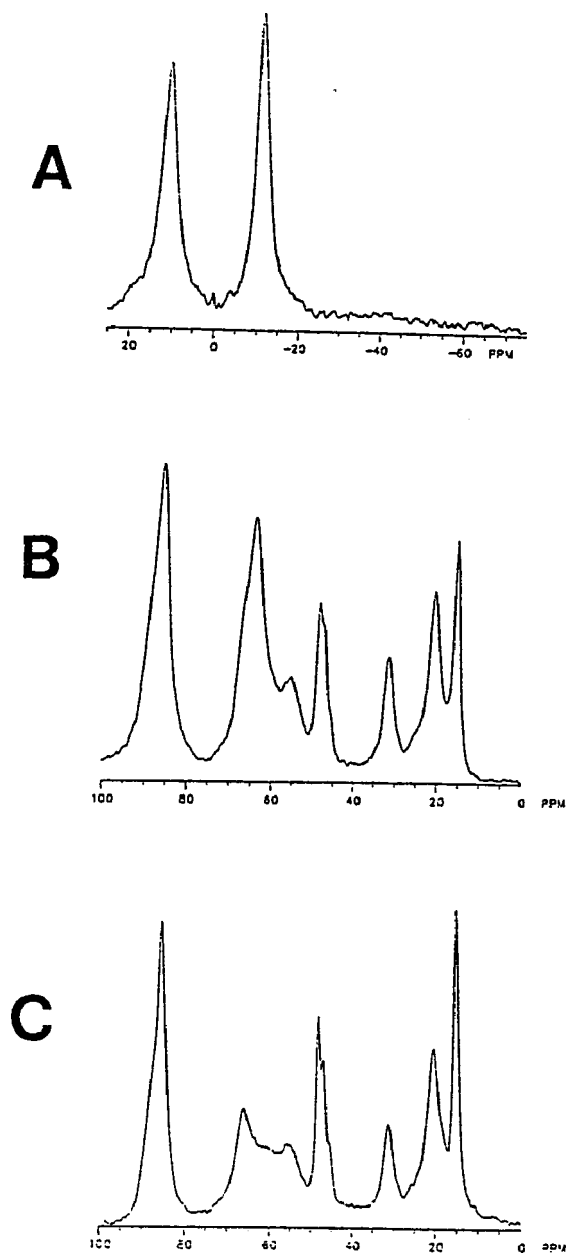


Figure 4-40: ^{13}C solid-state NMR spectra: (A) PVDC; 83:17 VDC-BMA copolymers prepared by (B) batch and (C) semi-continuous polymerization.

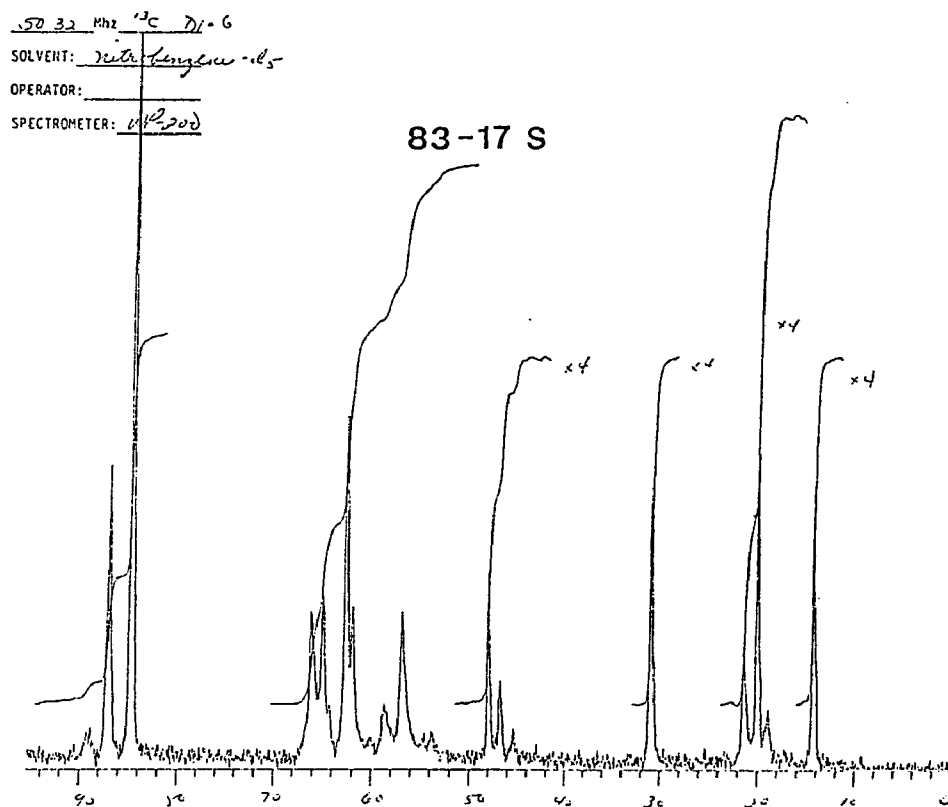


Figure 4-41: ^{13}C liquid NMR spectrum of the 83:17 VDC-BMA copolymer prepared by semi-continuous polymerization.

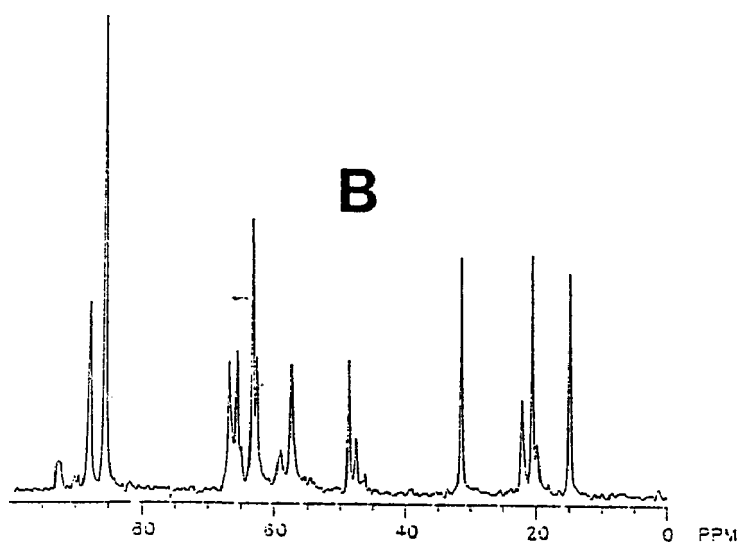
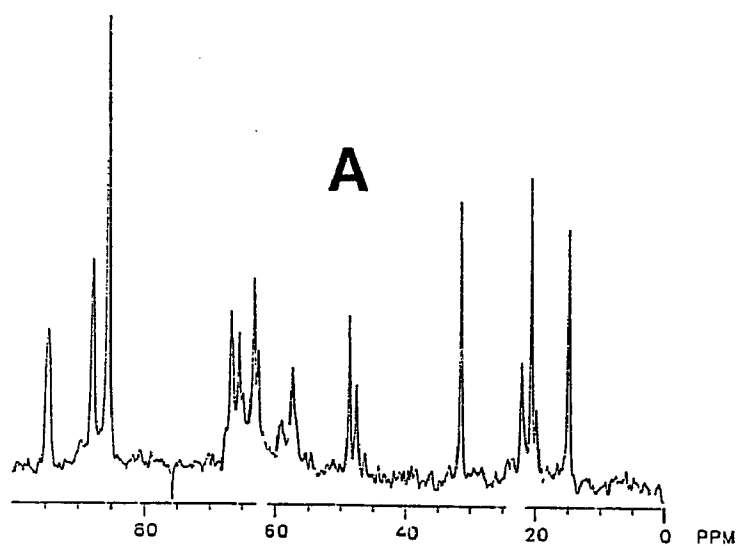


Figure 4-42: ^{13}C Liquid NMR spectra of the 83:17 VDC-BMA copolymers prepared by (A) batch and (B) semi-continuous polymerization, obtained using solid-state NMR parameters.

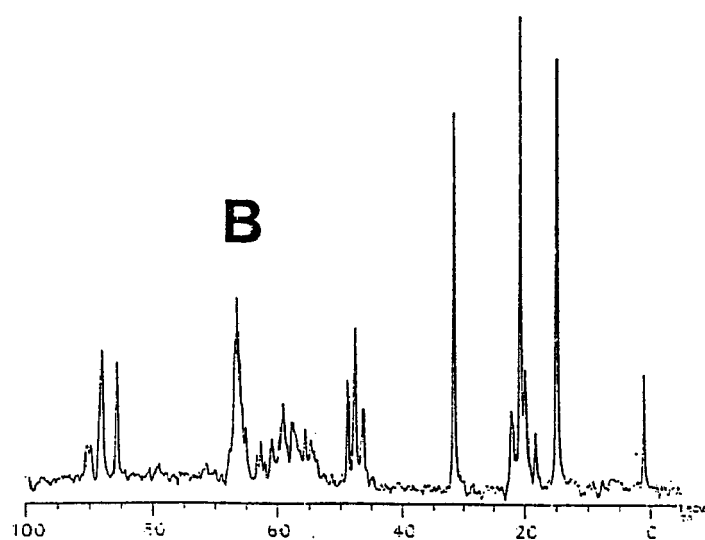
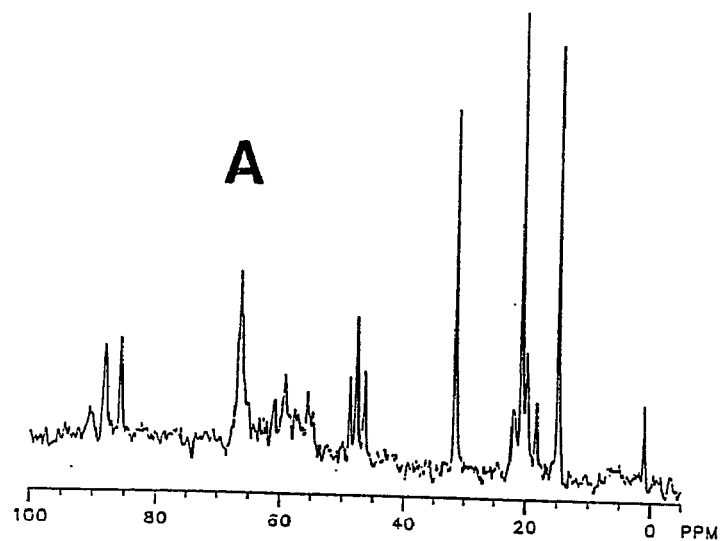


Figure 4-43: ^{13}C liquid NMR spectra of the 60:40 VDC-BMA copolymers prepared by (A) batch and (B) semi-continuous polymerization, obtained using solid-state NMR parameters.

Table 4-17: Concentrations of VDC- and BMA-centered triads in the VDC-BMA copolymers.

POLYMER COMPOSITION	VDC-Centered Triads			BMA-Centered Triads		
	BVB	BVV	VVV	VBV	VBB	BBB
<u>VDC/BMA (mol %)</u>						
83/17						
(B)	7.3	36.3	56.4	58.4	35.7	5.7
(S)	3.6	30.5	65.9	55.0	30.5	14.5
60/40						
(B)	20.3	45.7	34.0	25.3	48.8	25.9
(S)	20.5	48.0	31.5	27.0	49.0	24.0

B : butyl methacrylate; V : vinylidene chloride
(B) batch process; (S) semi-continuous process

concentrations of both VDC- and BMA-centered triads (88) determined from Figures 4.42 and 4.43. Theoretically, the copolymers prepared by batch polymerization should have higher concentrations of VVV and BBB triads than their semi-continuous counterparts. For the 83:17 VDC-BMA copolymers, however, the concentrations of both VDC- and BMA-centered triads were quite different from those expected, indicating that the spectra might not be representative of the whole polymer. Probably, the crystallites present in the batch polymer did not contribute to the quantitative spectrum.

Figure 4.44 show the ^{13}C solid-state NMR spectra of deuterated benzene-swollen or dissolved 83:17 VDC-BMA copolymers prepared by batch and semi-continuous polymerization, respectively, using the cross-polarization (CP) technique. The batch sample showed two strong peaks at 64 and 87 ppm, which represent poly(vinylidene chloride), as shown in Figure 4.40, and four small peaks at 15, 21.5, 31.3, and 48.6 ppm, which arise from poly(butyl

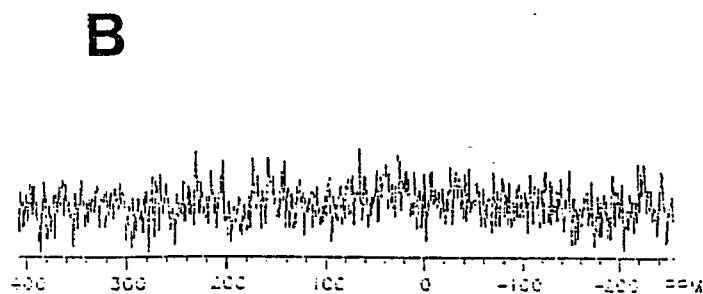
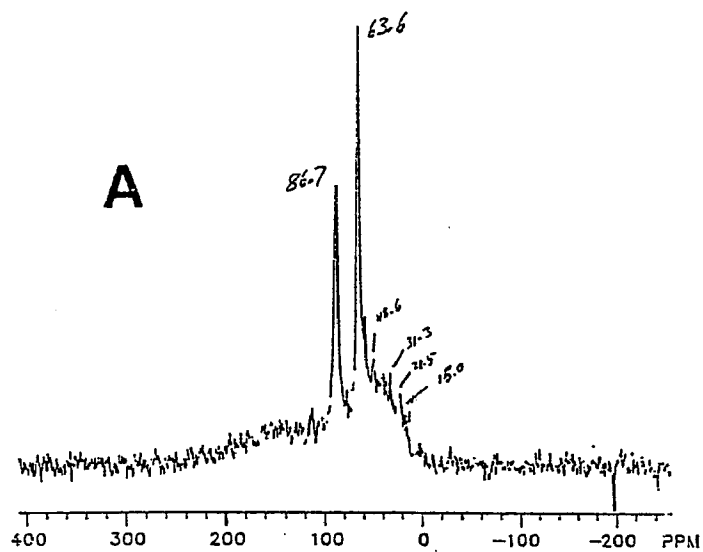


Figure 4-44: ^{13}C solid-state NMR spectra of deuterated benzene-swollen or dissolved 83:17 VDC-BMA copolymers prepared by (A) batch and (B) semi-continuous polymerization, using the cross-polarization technique

methacrylate) units adjacent to extended VDC sequences. These poly(butyl methacrylate) molecules have relatively small motions compared to butyl methacrylate molecules in the amorphous regions. In contrast, the semi-continuous sample did not show any significant peaks under the same cross-polarization technique, indicating the sample was amorphous. It is intrinsically difficult to obtain quantitative information from cross polarization NMR spectra of systems with significant motion. However, the differences between the spectra of the batch and semi-continuous samples suggest that the batch sample had much less molecular motion due to the presence of the crystallites.

In summary, the ^{13}C solid-state NMR spectra of the VDC-BMA copolymers using the cross-polarization (CP) technique were too poor in resolution to calculate the sequence distributions. The solvent-swollen technique in ^{13}C NMR spectra for the VDC-BMA copolymers gave much improved resolution, but not quantitative information for the entire sample. The CP technique for the solvent-swollen 83:17 VDC-BMA copolymers showed that the batch sample gave two strong peaks which represent poly(vinylidene chloride). However, the semi-continuous sample did not have any significant peaks, as predicted, indicating that the batch sample is crystalline in character (swollen in benzene) with long VDC sequences, and the semi-continuous sample is amorphous in character (totally soluble in benzene) with short VDC sequences. The CP technique for the solvent-swollen or dissolved samples, however, does not give reliable quantitative information.

Chapter 5

CONCLUSIONS

1. The reactivity ratios of VDC-BMA in emulsion copolymerization were determined to be $r_1 = 0.22$ and $r_2 = 2.41$, similar to those reported in bulk polymerization in the literature ($r_1 = 0.35$ and $r_2 = 2.20$), indicating that VDC-BMA emulsion copolymerizations take place mostly in the monomer-polymer particles rather than in the aqueous phase, and that, in batch polymerization, the copolymer composition drifts with conversion, yielding BMA-rich copolymers at the beginning and VDC-rich copolymers at the end of the copolymerization.

2. All of the emulsion polymerizations carried out by both batch and semi-continuous polymerization gave stable latexes of almost 100% conversion with negligible coagulum.

3. For 83:17 VDC-BMA emulsion copolymerizations A to E carried out by seeded semi-continuous polymerization, the rates of polymerizations (R_p) increased with increasing monomer feed rate, i.e., the rate of polymerization was controlled by the monomer feed rate. Specifically, the monomer feed rates in the polymerizations A to D were less than the observed maximum rate of batch polymerization, indicating that the monomer concentration in latex particles in the polymerization A to D are much lower than those of the batch and seeded batch polymerization G and F, respectively. In other words, the polymerizations A to D occurred under monomer-starved condition. However, for the polymerization E, which used the highest monomer feed rate, the corresponding conversion versus time curve was nearly the same as those obtained in the batch copolymerization G and the seeded batch polymerization F, indicating that the polymerization E is in near-flooded condition.

4. Significant differences were found in the physical and mechanical properties of the 83:17 VDC-BMA copolymer latex films, depending on the mode of monomer addition. Infrared spectroscopy, ^{13}C solid-state NMR spectroscopy, X-ray diffraction, solubility in various solvents, the T_g and T_m values by DSC, dynamic mechanical spectroscopy, tensile strength measurements, and water vapor transmission rates (WVTR) of the latex films post-heat-treated for 30 minutes at 70°C or aged for several months at room temperature demonstrated that, in batch polymerizations F and G, the copolymer composition drifted with conversion, resulting in copolymers of heterogeneous composition and a crystalline character. In contrast, in semi-continuous polymerizations A to E, the polymerizing particles were monomer-starved during the polymerizations, resulting in copolymers of more uniform composition and an amorphous character.

5. The conversion-time curves for the polymerizations of 0:100 to 100:0 VDC-BMA mixtures showed that the rate of polymerization (R_p) was a function of the particle number density, and the rate of polymerization per particle (R_{pp}) increased with increasing proportion of butyl methacrylate in the monomer mixture.

6. The number-average particle diameters of the latexes prepared by batch polymerization increased with increasing proportion of butyl methacrylate in the monomer mixture, from 77 nm for PVDC to 168 nm for PBMA; those of the latexes prepared by seeded semi-continuous polymerization were 121, 127, and 136 nm for the 83:17, 60:40, and 33:67 VDC-BMA copolymers, respectively. All of the latexes prepared by both batch and semi-continuous polymerization had narrow particle size distributions. The greater particle number density in the

VDC polymerization and the greater water solubility of VDC suggest that the homogeneous nucleation mechanism is operative for VDC-BMA emulsion copolymerizations.

7. The latex copolymers prepared by semi-continuous polymerizations had lower number-average and weight-average molecular weights than those of the corresponding batch copolymers, because of the lower monomer concentration of the semi-continuous polymerizations. The broader molecular distributions found in the batch copolymers might be explained by the occurrence of the composition drift, resulting in BMA-rich copolymers of high molecular weight at the beginning, and VDC-rich copolymers of low molecular weight at the end of the polymerization.

8. The differences in T_g between the copolymers prepared by the batch and semi-continuous polymerization were found to decrease with increasing butyl methacrylate content, i.e., 8-9°C for the 83:17, 1-2°C for the 60:40, and 0-1°C for the 33:67 VDC-BMA copolymers, indicating differences in sequence distributions. A maximum value for T_g was found at around 39°C for the 30:70 VDC-BMA monomer composition. Only PVDC, and 83:17 VDC-BMA copolymers prepared by batch (G) and seeded batch (F) polymerization showed crystalline melting temperatures, i.e., 199, 187, and 184°C, respectively; all other copolymers prepared by both processes showed no crystalline melting temperature. The percent crystallinity of PVDC and the 83:17 VDC-BMA copolymers prepared by batch and seeded batch polymerization, determined by DSC were 45, 13.7, and 12.0 %, respectively.

9. The solubility in THF, tensile properties, X-ray diffraction, water vapor transmission rates, and T_g and T_m values of the VDC-BMA latex films of 100:0

to 0:100 monomer composition demonstrated that all of the copolymers prepared by semi-continuous polymerization were amorphous, irrespective of the monomer composition. In contrast, the copolymers prepared by batch polymerization showed different degrees of crystallinity depending on VDC-BMA ratio in the monomer composition.

10. The surface characterization of the cleaned VDC-BMA latexes showed that, for the latexes prepared by batch polymerization, the surface charge density derived from strong-acid endgroups decreased with increasing amounts of VDC in the monomer mixture. This may be due to the catalytic effect of hydrochloric acid derived from the degradation reaction on the VDC sequence units of the copolymer and of sulfuric acid derived from the hydrolysis of the $-\text{SO}_4^- \cdot \text{H}^+$ groups, on the hydrolysis of the strong-acid groups. On the other hand, for the latexes prepared by semi-continuous polymerization, the surface charge density derived from strong-acid endgroups did not vary with monomer composition. These results indicate that the copolymer latexes prepared by batch polymerization may have a core-shell morphology, while the copolymer latexes prepared by semi-continuous polymerization may have a more homogeneous composition on the particle surface.

11. The ^{13}C solid-state NMR spectra of the VDC-BMA copolymers using the cross polarization (CP) technique were too poor in resolution to calculate the sequence distributions. The ^{13}C liquid NMR spectra of the VDC-BMA copolymers using magic angle spinning (high power proton decoupling) gave much improved resolution, but did not define the entire sample quantitatively. The cross-polarization technique for solvent-swollen or dissolved samples (83:17 VDC-BMA copolymer) demonstrated that the batch sample was crystalline in

character because of the low degree of molecular motion due to the presence of the crystallites; the semi-continuous sample, however, was amorphous in character with significant molecular motion.

Chapter 6

RECOMMENDATIONS FOR FUTURE WORK

Several studies are recommended for future work.

1. The homogeneity of the VDC-BMA copolymers is a strong function of the monomer feed rate. The correlation between the VDC copolymer sequence distribution, copolymer blockiness, monomer feed rate, and copolymer physical and mechanical properties should be investigated for practical as well as academic purposes. For this purpose, the microstructure of VDC-BMA copolymers prepared by both batch and semi-continuous polymerization should be investigated using ^{13}C liquid and solid-state NMR spectroscopy.

2. The morphology of the latex particles and latex films of the VDC-BMA copolymers prepared by both batch and semi-continuous polymerization should be studied using transmission electron microscopy and scanning electron microscopy, staining the sample if necessary, to see the effect of the mode of monomer addition on the morphology.

3. The development of crystallinity in the latex particles with time should be carried out using FTIR.

4. The amount of copolymers grafted on the copolymer backbone, as well as the distribution of homopolymers and copolymers, in the VDC-BMA copolymers prepared by both batch and semi-continuous polymerization should be determined using the thin layer chromatography-flame ionization detection.

5. Based on the recipe developed in this research, synthesis of high-solids latexes should be tried, so that latex paints and lacquers can be formulated with good barrier properties.

REFERENCES

1. T. Makgawinata, Ph.D. Dissertation (Chapter II), Lehigh University, Bethlehem, PA, 1981.
2. M. S. El-Aasser, T. Makgawinata, S. C. Misra, and J. W. Vanderhoff, "Emulsion Polymerization of Vinyl Acetate", M. S. El-Aasser and J. W. Vanderhoff, eds., Applied Science Publishers, 1981, p. 215.
3. M. S. El-Aasser, T. Makgawinata, and J. W. Vanderhoff, J. Polymer Sci. Part A., **21**, 2363 (1983).
4. S. C. Misra, C. Pichot, M. S. El-Aasser, and J. W. Vanderhoff, J. Polymer Sci. Part A., **21**, 2383 (1983).
5. C. Pichot, M. F. Llauro, and Q. T. Pham, J. Polymer Sci. Part A., **19**, 2619 (1981).
6. R. M. Jayasuriya, Ph.D. Dissertation, Lehigh University, 1985.
7. R. C. Reinhardt, Ind. Eng. Chem., **35**(4), 422 (April, 1943).
8. R. A. Wessling and V. L. Stevens, Mod. Paint Coatings., 148 (October, 1982).
9. R. A. Wessling, "Polyvinylidene Chloride", Gordon and Breach Science Publishers, New York, 1977.
10. J. C. Bax, Paint Technol., **29**(4), 14 (1964).
11. J. C. Bax, Mod. Paint Coatings., **32** (January, 1983).
12. M. L. Caine, Mod. Paint Coatings., **37** (September, 1983).
13. J. C. Bax, J. Oil Col. Chem. Assocn., **53**, 592 (1970).
14. A. J. Burgess, D. Caldwell, and J. C. Padget, J. Oil Col. Chem. Assocn., **64**, 175 (1981).
15. R. A. Wessling, "Vinylidene Chloride and PVDC", Kirk-Othmer Encycl. Chem. Technol., Third Ed., Vol. 23, New York, J. Wiley & Sons, 1983, p. 764.
16. L. S. Luskin, "Acrylic and Methacrylic Acids and Esters", F. D Snell and C. L. Hilton, eds, Encycl. Ind. Chem. Analysis, Vol. 4, John Wiley & Sons, Inc., New York, 1967, p. 181.

17. J. W. Vanderhoff, J. Polymer Sci. Polym. Symp., **72**, 161 (1985).
18. G. W. Poehlein, 17th Annual Short Course "Advances in Emulsion Polymer & Latex Technology", Emulsion Polymers Institute, Lehigh University, June 1986.
19. W. V. Smith and R. W. Ewart, J. Chem. Phys., **16**, 592 (1948).
20. W. V. Smith, J. Am. Chem. Soc., **70**, 3695 (1948).
21. J. Ugelstad and F.K. Hansen, Rubber Chem. Technol., **49**, 536 (1976).
22. H. Wiener, J. Polymer Sci., **7**, 1 (1951).
23. P. M. Hay, J. C. Light, L. Marker, R. W. Murray, A. T. Santonicola, O. J. Sweeting, and J. G. Wepsic, J. Appl. Polym. Sci., **5**, 23 (1961).
24. J. C. Light and A. T. Santonicola, J. Polym. Sci., **36**, 549 (1959).
25. J. C. Light, L. Marker, A. T. Santonicola, and O. J. Sweeting, J. Appl. Polym. Sci., **5**, 31 (1961).
26. C. P. Evans, P. M. Hay, L. Marker, R. W. Murray, and O. J. Sweeting, J. Appl. Polym. Sci., **5**, 39 (1961).
27. L. Marker, O. J. Sweeting, and J. G. Wepsic, J. Polym. Sci., **57**, 855 (1962).
28. A. Klein, "Latex Technology", Kirk-Othmer Encycl. of Chem. Technol., Third Ed., Vol. 14, New York, J. Wiley & Sons, 1981, p. 82.
29. J. W. Vanderhoff, "Semi-continuous Emulsion Polymerization", Future Directions in Polymer Science (Preliminary Manuscripts), NATO Advanced Research Workshop, Racine, Wis, June 1986.
30. H. Naidus, Ind. Eng. Chem., **45**, 712 (1953).
31. P. Fram, G. T. Stewart, and A. J. Szlachtun, Ind. Eng. Chem., **47**(5), 1000 (1955).
32. F. T. Wall, C. J. Delbee, and R. E. Florin, J. Polym. Sci., **9**, 177 (1952).
33. B. G. Elgood, E. V. Gulbekian, and D. Kinsler, J. Polym. Sci. Part

- B., **2**, 257 (1964).
34. J. E. Vandegaer, J. Appl. Polym. Sci., **9**, 2929 (1955).
 35. D. M. Woodford, Chem. Ind., 316 (1966).
 36. V. I. Eliseeva, V. F. Malofeyevskaya, A. S. Gerasimova, Yu. A. Makarov, I. S. Izmailova, and K. G. Orlova, Vysokomol. Soyed. A9, **4**, 730 (1967).
 37. V. I. Eliseeva, V. F. Malofeyevskaya, A. S. Gerasimova, Yu. A. Makarov, and I. P. Izmailova, Vysokomol. Soyed. A11, **5**, 1005 (1969).
 38. R. A. Wessling, J. Appl. Polym. Sci., **12**, 309 (1968).
 39. J. J. Krakeler and H. Naidus, J. Polym. Sci., Part C., **27**, 207 (1969).
 40. H. Gerrens, J. Polym. Sci., Part C., **27**, 77 (1969).
 41. K. Chujo, Y. Harada, S. Tokuhara, and T. Tanaka, J. Polym. Sci., Part C., **27**, 321 (1969).
 42. R. A. Wessling and D. S. Gibbs, J. Macromol. Sci.-Chem., A7(3), 647 (1973).
 43. J. Snuparek, Jr., Angew. Makromol. Chem., **25**, 105 (1972).
 44. J. Snuparek, Jr., Angew. Makromol. Chem., **25**, 113 (1972).
 45. J. Snuparek, Jr., Angew. Makromol. Chem., **37**, 1 (1974).
 46. J. Snuparek, Jr., and F. Krska, J. Appl. Polym. Sci., **20**, 1753 (1976).
 47. J. Snuparek, Jr. and F. Krska, J. Appl. Polym. Sci., **21**, 2253 (1977).
 48. J. Snuparek, Jr., J. Appl. Polym. Sci., **24**, 909 (1979).
 49. J. Snuparek, Jr., J. Appl. Polym. Sci., **24**, 915 (1979).
 50. P. Bataille, B. T. Van, and Q. B. Pham, J. Appl. Polym. Sci., **22**, 3145 (1978).
 51. K. W. Min and H. I. Gostin, Ind. Eng. Chem., Prod. Res. Dev., **18**

- (4), 272 (1979).
52. K. L. Hoy, J. Coat. Technol., **53** (651), 27 (1979).
53. I. Xue, Grad. Res. Prog. Report, Emulsion Polymers Institute: Lehigh university, **26**, July 1986, p. 109.
54. S. Krimm and C. Y. Liang, J. Polym. Sci., **22**, 95 (1956).
55. S. Narita, S. Ichinohe, and S. Enomoto, J. Polym. Sci., **37**, 251 (1959).
56. S. Narita, S. Ichinohe, and S. Enomoto, J. Polym. Sci., **37**, 263 (1959).
57. S. Narita, S. Ichinohe, and S. Enomoto, J. Polym. Sci., **36**, 389 (1959).
58. J. G. Cobler, M. W. Lang, and E. G. Owens, "Polymer Thin Films", Ch. 15, Gordon and Breach, New York, 1972, p. 706.
59. J. Harris, Off. Dig., **30**, 30, January 1956.
60. M. Chainey, M. C. Wilkinson, and J. Hearn, J. Appl. Polym. Sci., **30**, 4273 (1985).
61. T. F. Protzman and G. L. Brown, J. Appl. Polym. Sci., **10**, 81 (1960).
62. D. W. Van Krevelen and P. J. Hoftyzer, "Properties of Polymers", Ch. 19, Elsevier Science Publishing Company, New York, 1976.
63. Perkin-Elmer DSC-1B, Manual, 1971, p. 46.
64. V. P. Lebedev, N. A. Okladnov, and M. N. Shlykova, Vysokomol. Soyed. A9, (3), 491 (1967).
65. K. Okuda, J. Polym. Sci., Part A., **2**, 1749 (1964).
66. R. A. Wessling, J. Polym. Sci., **14**, 2263 (1970).
67. R. A. Wessling, "Vinylidene Chloride Polymers", Encycl. Polym. Sci. Technol., Vol. 14, J. Wiley and Sons, New York, 1971, p. 540.
68. S. M. Webler, J. A. Manson, and R. W. Lang, "Polymer Characterizations", Ch. 6, Ad. Chem. Ser. **203**, 109 (1983).

69. P. W. Morgan, *Ind. Eng. Chem.*, **45**(10), 2296 (1953).
70. J. W. Vanderhoff, *J. Polym. Sci, Symp. Ser.* **41**, 155 (1973).
71. G. M. Yenwo, M. S. Thesis, Lehigh University, 1974.
72. S. M. Ahmed, M. S. El-Aasser, G. H. Pauli, G. W. Poehlein, and J. W. Vanderhoff, *J. Colloid. & Interface Sci.*, **73**, 388 (1980).
73. W. C. Wu, Ph.D. Dissertation, Lehigh University, 1977.
74. A. A. Kamel, Ph.D. Dissertation, Lehigh University, 1981.
75. P. Agron, T. Alfrey, Jr., J. Bohrer, H. Haas, and H. Wechsler, *J. Polym. Sci.*, **3** (2), 157 (1948).
76. B. G. Elgood, and B. J. Sauntson, *Chem. Ind.*, 1558 (September, 1965).
77. F. R. Mayo and F. M. Lewis, *J. Am. Chem. Soc.*, **66**, 1594 (1944).
78. J. A. Manson and L. H. Sperling, "Polymer Blends and Composites", Plenum Press, New York, 1976, p. 412.
79. R. M. Barrer, J. A. Barrie, M. G. Rogers, *J. Polym. Sci.*, **A1**, 2565 (1963).
80. L. E. Nielsen, *J. Macromol. Sci.*, **A1**, 929 (1967).
81. R. A. Wessling, F. L. Dicken, S. R. Kurowsky, and D. S. Gibbs, *J. Appl. Polym. Symp.*, **25**, 83 (1974).
82. J. D. Flowers, A. F. Burmester, M. D. Marks, and R. A. Wessling, *Am. Paint Coat*, **41** (September 15, 1986).
83. R. A. Wessling, "Polyvinylidene Chloride", Ch. 8, Gordon and Breach Science Publishers, New York, 1977, p. 105.
84. S. M. Ellerstein, *Polym. Preprints*, **1**, 223 (1963).
85. L. A. Wood, *J. Polym. Sci.*, **28**, 319 (1958).
86. J. M. Barton, *J. Polym. Sci., Part C.*, **30**, 573 (1970).
87. A. Pines, M. G. Gibby, and J. S. Waugh, *J. Chem. Physics.*, **59**, 569 (1973).

88. C. J. Carman, ACS Symp. Ser., **142**, 81 (1980).

VITA

Ki-Chang Lee was born in Geju-Do, Korea on August 11, 1954, son between Young-sup and Ung-sup Lee.

He attended Dae-Kwang high school, Seoul, and graduated in 1973. The same year he entered INHA university, Incheon, and graduated with a B.Sc, and M.S. degrees in polymer science and engineering in 1977 and 1979, respectively. He joined the Korea Institute of Science and Technology (KIST) as a research scientist in polymer processing laboratory from 1979 to 1982. He got married to Hee-Soo Shin in 1982.

He came to the united states in Jan. 1983 to continue his studies at Lehigh university, and joined Emulsion Polymers Institute as a research assistant in 1984, and followed graduate studies in Polymer Science and Engineering Curriculum.

He is a father of Suk-Jin and Doo-Jin.